Role of Sprouty2 in Prostate Carcinogenesis

Meiling Gao

Thesis submitted to the University of Glasgow towards

the degree of Doctor of Philosophy

The faculty of Medicine

University of Glasgow

The Beaston Institute for Cancer Research

Cancer Research UK

Glasgow

November 2011

Abstract

Prostate cancer (PC) is the most common cancer in men. In the UK alone, there are over 30,000 men diagnosed with PC every year. Loss of SPRY2 and activation of receptor tyrosine kinases are common events in PC. However, the molecular basis of their interaction and clinical impact remains to be fully examined. SPRY2 loss may functionally synergise with aberrant cellular signalling to drive PC and to promote treatment resistant disease. Using a combination of *in vitro,* pre-clinical *in vivo* models and clinical PC, this thesis shows the impact of SPRY2 loss upon activation of the ErbB signalling system via a positive feedback regulation of the ErbB-PI3K/AKT cascade. Loss of SPRY2 resulted in hyper-activation of PI3K/AKT signalling to drive proliferation and invasion by enhanced internalisation of EGFR/HER2 and their sustained localisation and signalling at the early endosome in a PTEN-dependent manner. This involves activation of p38 MAPK by PI3K to facilitate clathrin-mediated ErbB receptor endocytosis. Furthermore, this thesis suggests a critical role of PI3K/AKT in PC whereby *in vitro* and *in vivo* inhibition of PI3K suppresses proliferation and invasion, supporting PI3K/AKT as a target for therapy particularly in patients with PTEN-haploinsufficiency, low SPRY2 and ErbB expressing tumours. In conclusion, SPRY2 is an important tumour suppressor in PC; its loss drives the PI3K/AKT pathway via functional interaction with the ErbB system.

Table of Contents

List of Figures

List of tables

Accompanying material

Part of this work has contributed to the publication, which is enclosed at the back of the thesis:

SPRY2 loss enhances ErbB trafficking and PI3K/AKT signalling in human and mouse prostate carcinogenesis

Meiling Gao, Rachana Patel, Imran Ahmad, Janis Fleming, Joanne Edwards, Stuart McCracken, Kanagasabai Sahadevan, Morag Seywright, Jim Norman, Owen Sansom, Hing Leung

Abbreviation

AR	*Androgen receptor*
ATCC	*American type culture collection*
BSA	*Bovine serum albumin*
C-CBL	*Mammalian homologue of Casitas B-lineage lymphoma proto-oncogene product*
CARN	*Castration resistant Nkx3-1-expressing cells*
CSC	*Cancer stem cell*
ECL	*Enhanced chemiluminescence*
EDTA	*Ethylene diamine triacetic acid*
EGF	*Epidermal growth factor*
EGFR	*Epidermal growth factor receptor*
ELISA	*Enzyme-linked immunosorbent assay*
ERK	*Extracellular signal-regulated kinase*
FBS	*Foetal bovine serum*
FGFR	*Fibroblast growth factor receptor*
GAPDH	*Glyceraldehyde-3-phosphate Dehydrogenase*
GFP	*green fluorescent protein*
H&E	*hematoxylin and eosin*
HRP	*Horseradish peroxidase*
JNK	*C-jun NH2-terminal kinase*
KD	*Knock down*
MAPK	*Mitogen activated protein kinase*
PBS	*Phosphate buffered saline*
PC	*Prostate cancer*
PFA	*Paraformaldehyde*

PIN	*Prostatic intraepithelial neoplasia*
PI3K	*Phosphatidylinositiol-3-kinase*
PIP2	*Phosphatidylinositiol-4,5-bisphosphate*
PIP3	*Phosphatidylinositiol-3,4,5-trisphosphate*
PKC	*Protein kinase C*
PLCγ	*phospholipase C gamma*
PMSF	*Phenylmethylsulphonyl fluoride*
PSA	*Prostate specific antigen*
PTEN	*Phosphatase and tensin homolog located on chromosome10*
ROS	*Reactive oxygen species*
RPMI	*Roswell Park Memorial Institute medium*
RTK	*Receptor tyrosine kinase*
SDS	*Sodium dodecyl sulphate*
SILAC	*Stable isotope labelling with amino acids in cell culture*
siRNA	*Short interfering RNA*
SPRED	*SPRY-related enabled/vasodilator stimulated phosphoprotein homology 1 domain containing*
SPRY	*Sprouty*
TE	*Tris-EDTA buffer*
TRAMP	*Transgenic adenocarcinoma of the prostate*
TUNEL	*Terminal deoxynucleotidyl transferase-mediated dUTP nick end-labelling*
VEGF	*Vascular endothelial growth factor*

Acknowledgement

Frist of all, I would like to thank my supervisor Hing Leung for his supervision and encouragement during the course of my PhD studies, and my advisor Mike Olson for his helpful advice and useful discussions. I also would like to thank all members of Hing's group for their support and help, especially Janis Fleming for her patience and sharing her invaluable experience and ideas with me.

This thesis would not have been possible without the help, support and patience of my dear friend and colleague Rachana. Her genius ideas and wicked sense of humour kept me more positive throughout my PhD. Even in those disheartening moments of my PhD, I was able to laugh and share the stories and memories we had together. I promised that I would adore those fine lines around my eyes, which was added by laughing with her. I am also grateful to my dear friend Imran for letting me stay in his house and focus on the publications during my PhD.

I would like to acknowledge the financial, academic and technical support of the Beatson Institute for Cancer Research and University of Glasgow.

Finally with all my heart, I would like to thank my parents and family, especially Sinok and Eoin, who have loved and believed in me at all times.

Author's declaration

I hereby declare that all of the work presented in this thesis was performed personally unless otherwise stated. No part of this work has been submitted for consideration as part of any other degree or award.

Chapter 1. Introduction

1. Introduction

1.1 Prostate Cancer

1.1.1 Natural history of prostate cancer

In 2007, there were around 36,100 men diagnosed with prostate cancer (PC) in the UK alone, and around 913,000 men were diagnosed with PC worldwide (CRUK 2010). Although the cancer death rate has decreased steadily since 1990s, prostate cancer remains the second most common cause of cancer death in UK men, after lung cancer. Such improvement in survival may be attributed to the increased use of prostate-specific antigen (PSA) testing. PSA, as a biomarker, revolutionised the diagnosis of prostate cancer. It allows the detection of prostate tumours at early stage, and the test procedure is easy and straightforward. Despite a vast increase in the diagnosis of PC, PSA testing is not able to differentiate between latent and life-threatening tumours reliably at the time of diagnosis. Patients with raised PSA levels typically undergo biopsy to assess the potential presence of cancerous disease. The biopsy samples are analysed according to the histopathological grading system called Gleason scoring, which classifies cancer from 1 to 5 based on histological appearance and tissue architecture (Mellinger et al., 1967, Epstein, 2010). In addition, patients are diagnosed with various stages based on the status of the primary tumours, including invasive disease (T1-4), lymph node involvement (N0-1), and metastatic PC (M0 and 1a-c) (Ohori et al., 1994, Falzarano and Magi-Galluzzi, 2011). Once early prostate cancer is diagnosed, the conventional treatment in UK includes external beam radiation therapy, brachytherapy, surgery and active surveillance with intent for deferred intervention. In addition castration for the treatment of advanced prostate cancer was such an important advance in the clinic that earned Charles Huggins a Nobel Prize in 1966 (Huggins, 1967). Historically ancient Egyptians first described PC as a clinical disease, and surgical castration reduces initial tumour burden by depleting androgen level, but eventually results castration-resistant disease. Unfortunately, to date such advanced PC remains incurable; current docetaxel-based chemotherapy or PC vaccine only extends patient survival up to 3-4 months (Petrylak, 2005, Jathal et al., 2011). This highlights the critical need for improved molecular markers and

other approaches by basic scientific research and preclinical models to complement the existing assessments of PC for more effective prognosis and treatment.

1.1.2 Prostatic intraepithelial neoplasia (PIN) and metastatic prostate cancer

Prostate cancer is widely considered as a progressive disease often involving sequential deregulation of molecular processes and pathways (Figure 1.1.1). The progression was described as from normal epithelium to PIN, then more aggressive adenocarcinoma and metatstasis. In 1987 Bostwick and Brawer first proposed the term PIN to describe low grade PC (Bostwick and Brawer, 1987). PIN is defined as a histological interpretation of cellular enhancement of the normal glandular architecture with cytological abnormality including enlargement of nuclei and nucleoli, and cytoplasmic hyperchromasia. PC is generally considered as a multifocal disease with formation of heterogenous foci and advanced metastasis to secondary organs. The heterogeneity is also observed in PIN with involvement of multiple clusters of glandular structures. In addition, the exhibition of increased cell proliferation markers in prostate is considered as high grade PIN (Bostwick, 1989, Shappell et al., 2004).

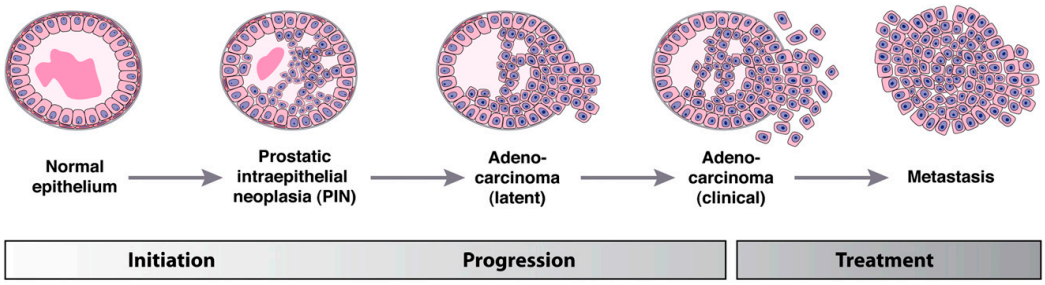

Figure 1.1.1 Stages of human prostate cancer progerssion. Adopted from Abate-Shen and Shen (2000)

Advanced PC often metastasises to distant organs including lung, liver and pleura. Interestingly, bone metastasis occurs inevitably with unknown reason in advanced PC patients, where it leads to osteoblastic lesions (Bubendorf et al., 2000, Logothetis and Lin, 2005). Such complication in bones is incurable and a major cause of morbidity for advanced PC patients, which creates another level of clinical challenge. Recent studies detected circulating prostate tumour cells

in the bone marrow and peripheral blood (Pantel and Alix-Panabieres, 2010). However, disseminated tumour cells were also found in patients with localised disease, which suggests the limited capability to metastasise at the early stage of the disease. Yet, the circulating tumour cells within metastatic disease consisted of multiple chromosomal rearrangements comparable with typical advanced PC (Attard et al., 2009, Holcomb et al., 2008, Leversha et al., 2009). Despite the clinical importance of tumour metastasis, the molecular mechanisms involved in promoting this process remains to be resolved. Furthermore, recent genomic analysis (Taylor et al., 2010) have provided a great deal of insight into the molecular signature of PC, which allows us to distinguish subtypes of PC and stratification of patients according to gene expression and copy number alteration.

1.1.3 Mouse model of prostate cancer

Mouse models have provided an extremely useful research platform to study PC including, xenograft, tissue reconstitution and genetically engineered models. *In vivo* PC studies are often carried out by implanting human PC cell lines in immunodeficient mice orthotopically or transplanting into the flank. The xenograft models provided a great insight into the molecular mechanisms involved in carcinogenesis and chemotherapeutic strategies. However there are major limitations to the xenograft models, notably the absence of a heterologous microenvironment associated with PC; inability to analyse the effect of the immune system and the restriction to using clonal cell lines. In order to manipulate specific genes in both mouse and human prostate tissue, tissue reconstitution models are employed to investigate not only prostate organogenesis but also prostate tumorigenesis *in vivo*. This procedure often uses immortalised human or mouse prostate cells, which can reconstitute relatively normal (histology) prostate tissue. The gene of interest can be overexpressed or knocked down *in vitro*, and the subsequent phenotypes *in vivo* analysed. Such methods also allow us to study stromal compartments using cancer associated fibroblasts, and assess genes that give lethal embryonic phenotypes.

Development of transgenic mouse models for prostate cancer has provided another useful approach to investigate prostate tumorigenesis and to recapitulate human disease. To date, there are a handful of genetically

engineered mouse models for PC. The first transgenic PC mouse model was generated by Greenberg using potent viral oncogenes (Greenberg et al., 1995). The TRAMP (transgenic adenocarcinoma of the prostate) mouse model developed an aggressive disease with neuroendocrine differentiation, which however is rarely observed in human PC (Shappell et al., 2004). Nonetheless, the first-generation of transgenic mouse model provided important insight into the disease progression and investigation of castration resistant disease. In order to target specifically prostate tissue, probasin and PSA promoters were used to drive candidate gene expression. The application of such approach to loss-of-function mutations in the genes of interest has led to the second-generation of mouse models. There are few popular choices of models including *Nkx3.1, Pten, Pb-Cre4,* and *Nkx3.1-Cre* transgenes.

Nkx 3.1 is a homeobox gene, which is shown to be involved in prostatic epithelial development and differentiation. Loss of *Nkx3.1* gene leads to hyperplastic lesions in anterior, dorsolateral prostate and stroma regions, but the ventral prostate appears to be normal in 1-2 year old mouse model. Also in prostate cell lines including PC3 and AT6 was observed decreased cell proliferation when *Nkx3.1* was overexpressed (Sciavolino et al., 1997, Kim et al., 2002a, Kim et al., 2002b). This suggested that the Nkx3.1 gene has a potential tumour suppressive role. Both loss of *Nkx 3.1* gene and epigenetic silencing of the gene have been detected in human prostate cancer (Emmert-Buck et al., 1995, Voeller et al., 1997). However, the homozygous deletion of *Nkx3.1* seems to only develop PIN phenotype with few layered epithelium and enlarged nucleoli but not extreme pleomorphism, and never progress into adenocarcinoma or metastatic disease. Given PC is a multistep process, combination of candidate tumour suppressor genes and oncogenes in mouse models have provided great insight into the molecular mechanisms involved in prostate carcinogenesis. *Pten* is one of the most commonly mutated tumour suppressor genes in human cancer, and *Pten* heterozygous mutant mice develop high grade PIN with incomplete penetrance, and the phenotype is closely related to the subtle *Pten* dosage in the mouse model (Carracedo et al., 2011b). Kim and his colleagues further investigated the cooperation of Nkx3.1 and *Pten* in mouse prostate. The double homozygous mutants displayed localised severe dysplastic lesions with higher penetrance in comparison with single mutant *Pten* or *Nkx3.1*

heterozygous mice. However, there was no difference in survival profile between double and single mutants. High-grade PIN was observed with *Nkx3.1*$^{-/-}$; *Pten*$^{+/-}$ prostates. This suggests the cooperation of tissue specific genes and common tumour suppressor genes can contribute to the tissue specific cancer progression. Furthermore, Tomlins and his colleagues discovered for the first time recurrent chromosomal rearrangement in human prostate cancer, which involves two ETS transcription factors (ERG and ETV1) and 5' untranslated region of TMPRSS2 (Tomlins et al., 2005). This study led to the generation of the TMPRSS2-ERG fusion mouse model, and the transgene positive mice developed dysplasia in prostate (King et al., 2009a). It suggested that such simple mutation might not sufficient for the initiation and progression of the PC. However, combination of Pten$^{+/-}$ and the TMPRSS2-ERG fusion mice developed PIN at 6 months with invasive phenotype, suggesting the cooperation between PI3K signalling pathway and ERG in the PIN development. Interestingly, the combination of different gene sets have demonstrated the development of PIN in mouse model, but these events alone could not progress into aggressive malignancies observed in human prostate. Recent intergrated genomic analysis of human PC suggests that additional mutational events are required for the development of prostate carcinoma in preclinical mouse model. Yet, as the complexity of mutations increase in mouse model, the accurate analysis and interpretation of mechanisms involved in the progression of the diseases become a great challenge.

1.1.4 Molecular mechanisms of prostate cancer initiation and progression

Recent progress in the genetically engineered mouse models and *in vitro* studies have significantly advanced our understanding of molecular mechanisms involved in prostate carcinogenesis. Patients with advanced PC are often treated with androgen deprivation therapy, which is performed either with the administration of drug using anti-androgens including bicalutamide, or surgical castration. AR plays a critical role in normal prostate development as well as prostate carcinogenesis. The Leydig cells within the testis synthesise the ligand testosterone acting as androgen, which is converted into its more active form dihydrotestosterone in prostatic cells. AR is a member of steroid nucleus

receptor, and acts as a transcription factor upon ligand binding. The best characterised and clinically implicated AR target gene is KLK3, which encodes PSA protein. The androgen depletion therapy initially leads to rapid regression of androgen-dependent prostate tissue via apoptosis, which is also induced by stromal tissue. The function of stroma was evident in tissue reconstitution experiments with androgen dependent cell lines, which undergo apoptosis following withdrawal of androgen. These cell lines showed reduced proliferation when androgen was not present, but not apoptosis when grown without stromal components (Gao et al., 2001, Kurita et al., 2001). Due to the selection pressure, PC eventually develops into a castration resistant state, which may involve AR mutation or increase in androgen synthesis. Castration resistant tumour cells employ various interesting ways to adapt and survive in AR withdrawn environment. The most common AR reactivation mechanisms are amplication/overexpression of AR, constitutively activating mutation, aberrant post-translational modification, and alternative splicing. For instance, approximately over 30% patients with castration-resistant disease show amplification of AR genes (Linja et al., 2001). Another common mechanism found in PC patients consists of gain of function mutation leading to more stable, greater sensitivity to the ligands or constitutive activation of the receptor with alternative splicing variant (Guo et al., 2009, Steinkamp et al., 2009, Brooke et al., 2008).

Another receptor family including ErbB is shown to interact with AR signalling cascade and stimulate prostate cancer cell survival. ErbB family members consist of ErbB1 (EGFR), ErbB2 (HER2), ErbB3 (HER3) and ErbB4 (HER4), which are essential for developmental process and tumour progression. Although there are no mutations of ErbB receptors identified in prostate cancer, crosstalk between AR and ErbB signalling and contribution to castration resistant PC progression was reported in recent years. EGFR and ErB2 expression was controlled by AR c-terminal domain and RTK are essential for cell proliferation in PC cell lines (Pignon et al., 2009). ErbB2 is also implicated in castration resistant PC through AR dependent DNA binding and its stablisation (Mellinghoff et al., 2004). Given the important role of ErbB signalling in PC progression and the successful outcome in targeting ErbB as treatment for breast cancer, various chemotherapies against EGFR and HER2 were tested in preclinical models and PC

patients. Currently, there are several tyrosine kinase inhibitors (TKI) and monoclonal antibodies developed for clinical trials, these include HER2-directed antibody trastuzumab, EGFR inhibitors (erlotinib and gefitinib) and EGFR-directed monoclonal antibodies (cetuximab and panitumumab). Despite report of these TKI and monoclonal antibodies inhibiting cell proliferation *in vitro* and in xenograft models (Tomlins et al., 2005), phase II clinical trials on patients with advanced PC indicated no significant effect neither in PSA levels nor survival benefit (Gross et al., 2007, Morris et al., 2002, Salzberg et al., 2007). These disappointing results can be explained by the effect of the redundant ErbB family members and their complex signalling network. Also RTK amplication does not occur as often as in breast and lung cancer.

PTEN (phosphatase and tensin homolog located on chromosome10) is among the most frequently mutated or deleted tumour suppressor genes in human cancers, and was first identified in breast and PC (Li et al., 1997, Steck et al., 1997). PTEN is encoded on chromosome 10q23, and consists of a phosphatase domain, C2 or lipid membrane-binding domain, C-terminal region and PDZ-binding domain (Figure 1.1.2). PTEN is well known for its negative regulatory role in PI3K/AKT signalling pathways via dephosphorlation of the 3-phosphoinositide. The PI3K/AKT pathway is an important regulator of cell growth and survival. The exact status of PTEN deregulation in PC was unclear until recent multiple research approaches. The main questions were whether PTEN alleles were both deleted or only one allele is lost and the other one is mutated, or the expression is affected. After a long-standing debate, it is accepted that PTEN undergoes copy number loss at the early stage of carcinogenesis, and complete loss of PTEN occurs at a relatively late stage of PC progression, including aggressive, and castration-resistant disease (Taylor et al., 2010). Pandolfi and colleagues asked an intriguing question regarding the relationship between subtle PTEN expression level and cancer susceptibility (Carracedo et al., 2011a). It is well known that a complete loss of PTEN bypass cellular senescence in prostate mouse model, and becomes a hallmark of advanced human PC. The PC genomic cBio portal showed that only 7% of PC patients harboured complete loss of PTEN, which means the majority of cases still retain normal or low PTEN expression level (Taylor et al., 2010).

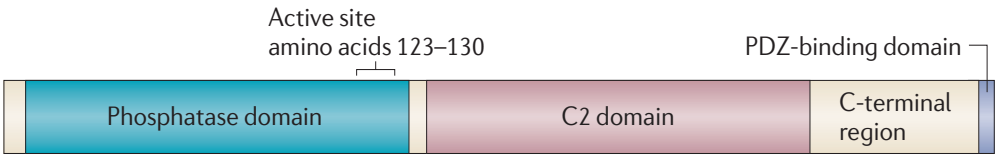

Figure 1.1.2 Schematic of the PTEN protein. Adopted from Hollander, Blumenthal and Dennis (2011)

Indeed, it is important to address the importance of subtle reduction of PTEN in prostate carcinogenesis and other tumours. Interestingly, hypomorphic PTEN mouse model with PTEN expression level between heterozygous and knockout resulted in a full penetrance PC with invasive phenotype (Trotman et al., 2003b). Furthermore, there are also other tumour suppressor genes, which exert their inhibitory function through PTEN, including Sprouty family members (Edwin et al., 2006). This suggests an interesting idea that subtle PTEN reduction can have a dramatic impact in carcinogenesis. In addition to the membrane PTEN tumour suppressor role, recent reports suggest an interesting function of nuclear PTEN in cell cycle arrest, genomic instability, differentiation, and gene expression. In the nucleus, the phosphatase domain seems to not play a crucial role regarding nucleus PTEN enzymatic activities (Lindsay et al., 2006). On the basis of these studies, the membrane PTEN is merely one aspect of PTEN function in various cellular compartments.

PTEN deficient PC results in abnormal activation of PI3K/AKT signalling pathway (Thomas et al., 2004). The canonical PTEN/PI3K/AKT pathway is initiated from the activation of receptor tyrosine kinases (RTK), such as EGFR, and ERBB2. When PTEN expression is decreased or absent, products of PI3K activates AKT via its upstream kinase PDK1 in an uncontrolled manner. There are many downstream targets for AKT including GSK3, p27, p21, mTOR and FOXO, which are responsible for cell cycle progression, invasion and proliferation. mTOR also activates AKT in reciprocal feedback loop in PTEN deficient cancer cells. Given the importance of PTEN/PI3K/AKT signalling pathway, there are many candidate drugs developed to target mTOR or PI3K or as dual inhibitors. However, tumour cells evolve to adopt other kinase signalling pathways, including MAPK cascades, and consequently resulting in more aggressive drug resistant disease. Using combinatory therapy to target such parallel networks

seemed more effective in a preclinical model with PTEN depletion and castration resistant PC (Gumerlock et al., 1997).

Initially recurrent chromosomal rearrangements were discovered in haematological and mesenchymal neoplasm but rarely in solid tumours. However, recent studies identified that such events also occur in many epithelial cancers including PC. For instance, Tomlins (Tomlins et al., 2005) identified chromosomal rearrangement between the ETS family of transcription factors and TMPRSS2 gene, which creates TMPRSS2-ERG or TMPRSS2-ETV1 fusion genes in the majority (79%) of prostate cancer. TMPRSS2 is an androgen responsive gene loacated on the chromosome 21q, which activates the ETS family transcription in the case of the fusion gene. The mechanisms for chromosomal rearrangement at these loci were suggested as either an interstitial deletion or unbalanced interchromosomal translocation (Iljin et al., 2006, Perner et al., 2006). In addition, AR signalling cascade was shown to be involved in DNA damage by recruiting topoisomerase, which may be associated with chromosomal rearrangement at this site (Haffner et al., 2010). Recent genomic profiling and mouse model studies suggest that the functional effect of ETS family alone is moderate which lead to the development of a weak PIN phenotype (Tomlins et al., 2007). Addition of the PTEN deletion synergises with ETS to result in high grade PIN and carcinoma in mice (Carver et al., 2009, King et al., 2009b). Thus despite the identification of the chromosomal arrangement, the functional effect remains to be fully elucidated. The fusion genes may cooperate with other oncogenic events to promote prostate carcinogenesis.

The first proposal of cancer stem cell (CSC) model in myeloid leukemia by John Dicks and colleagues became a paradigm for later studies in solid tumour CSC nearly a decade ago (Lapidot et al., 1994). The CSC was firstly identified in breast cancer as a solid tumour model, and represents a distinct population within the tumour (Visvader, 2009). CSC is generally defined as subsets of cells with self-renewal ability, which can produce many different types of cancer cells with more differentiated phenotype. Such ability may explain the heterogeneity of solid tumours particularly in PC. The origin of CSC is unclear may derive from the normal stem cells which accumulate mutations. For prostate cancer CSC field, there are still many questions to be answered. It is believed that the

localisation of prostate stem cells in the tissue is highly relevant to the origin of the CSC (Lawson and Witte, 2007). A glandular organ, the prostate consists of anatomically distinct epithelial cells including basal cells forming the basement of each prostatic duct, neuroendocrine cells in the basement layer along with the basal cells, and luminal cells lining the ductal lumens above the basal cells. Wang and his colleagues first characterised a rare population of prostate CSC called CARNs (castration resistant Nkx3-1-expressing cells) in an elegantly designed transgenic mouse model. CARNs represent a luminal stem cell population with bipotential and self-renewal *in vivo*, which generates high grade PIN with targeted PTEN loss (Wang et al., 2009). Yet, identification of prostate cancer cell-of-origin was reported with isolation of normal human prostate with basal cell characteristics, which is transplanted to induce adenocarcinoma formation with luminal phenotype in a reconstitution mouse model (Goldstein et al., 2010). Altogether, prostate cancer may involve distinct subtypes of CSC, and recent CSC models required PTEN deletion to progress into aggressive tumour. However the different molecular pathways involved in lineage progression to prostate cancer initiation remains to be elucidated.

1.2 Sprouty and cancer: history of discovery

Over a decade ago, the Sprouty (SPRY) family was discovered in a genetic screen while investigating genes involved in tracheal branching in *Drosophila*, owing its name to the ability to prevent excessive airway branching (Hacohen et al., 1998). The *Drosophila* SPRY protein was shown to be a general antagonist of several different receptor tyrosine kinases (RTK) (Casci et al., 1999, Kramer et al., 1999, Reich et al., 1999). Subsequently, multiple orthologues of SPRY proteins have been identified in zebrafish, Xenopus, mouse, chicken and human (Chambers and Mason, 2000, Furthauer et al., 2001, Minowada et al., 1999). There are four unique *spry* genes identified in mammals to date. The mouse and human SPRY (SPRY 1-4) genes encode 32-34 kDa proteins that are considerably smaller in size than *Drosophila* SPRY (63 kDa) (Figure 1.2.1). The mammalian SPRY family members consist of divergent sequence at their amino termini, which may dictate their differential functions. The conserved cysteine-rich domain is located at the carboxyl terminus of all SPRY proteins, and outside of this region there is conserved tyrosine residues. SPRY proteins interact with

other signalling molecules containing Src-homology-2 (SH2) domains via the conserved tyrosine residues region. SPRED (SPRY-related enabled/vasodilator-stimulated phosphoprotein homology 1 domain containing) proteins are related to SPRY proteins structurally and functionally. So far three human, three mouse, two Xenopus and one *Drosophila* SPRED members have been described (DeMille et al., 1996, Kato et al., 2003, Sivak et al., 2005). SPRED family members consist of the C-terminal cysteine-rich Sprouty-related domain (SPR) shared with SPRY proteins, and an N-terminal Enabled/VASP homology 1 domain (EVH1) (Wakioka et al., 2001, Kato et al., 2003).

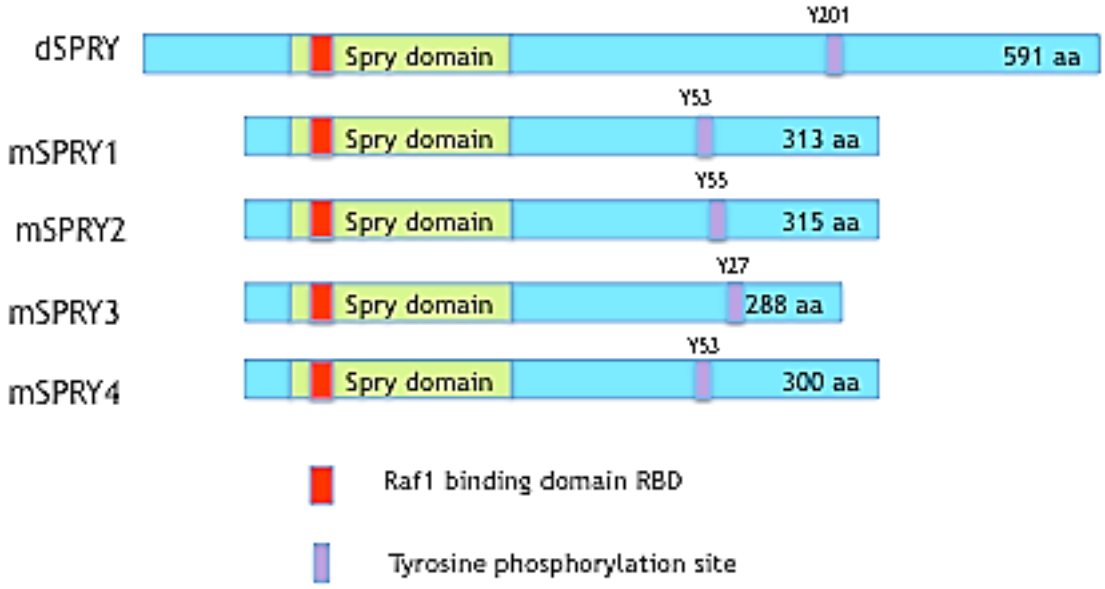

Figure 1.2.1 Schematic of SPRY family members, indicating Drosophila and 4 mammalian SPRY

Mammalian SPRY proteins are widely expressed in the developing embryo as well as in adult tissues. Some initial studies showed that expression of SPRY proteins were regulated by growth factors (Minowada et al., 1999, Tefft et al., 1999, Chambers and Mason, 2000, Chambers et al., 2000, Su et al., 2002). Large-scale gene analysis of both human and mouse transcriptomes, showed SPRY2 to be ubiquitously expressed, but the other isoforms are more limited to certain organs and tissues. For instance, SPRY3 is distributed only in brain and testis (Minowada et al., 1999). Given the prototype member of SPRY family is an antagonist of RTKs in Drosophila, many reports suggested the involvement of SPRY members in various cancer types. SPRY1 and SPRY2 are consistently

downregulated at mRNA and protein expression level in more than 90% breast cancer patient samples, acting as an inhibitory regulator of Ras/MAPK signalling pathway (Lo et al., 2004). In liver cancer, there is evidence for silencing of SPRY2 but not SPRY1, but the percentage of patients with low expression of SPRY2 is not as great as in breast cancer (Fong et al., 2006). This may due to the fact that abnormal RTK signalling plays a pivotal role in breast cancer, and emphasises the importance of SPRY in RTK signalling regulation network and tumorigenesis. In addition, ectopically expressed SPRY2 in a non-small lung cancer cell line and *in vivo* model reduced cell migration and proliferation via inhibition of Ras/MAPK cascade, suggesting a tumour suppressive role in lung cancer (Sutterluty et al., 2007). However, there are a few tumour types including colon cancer and melanoma, where a controversial role for SPRY is suggested. For instance, Spry is shown to be upregulated in global gene expression analysis of melanoma cell lines (Bloethner et al., 2005) (Table 1.1). Nonetheless, SPRY2 knockdown in melanocytes with wild type BRAF inhibited MAPK signalling cascade, but did not affect mutant BRAF containing cells (Tsavachidou et al., 2004). Interestingly, human colon adenocarcinoma consists of high expression level of SPRY2 compared with normal tissue, and overexpression of SPRY2 even exacerbated cell proliferation and invasiveness in the xenografts and orthotopic models respectively, suggesting oncogenic function of SPRY2 in colon cancer (Holgren et al., 2010). Collectively, these evidences suggest the complexity of SPRY2 function in various types of carcinogenesis, and emphasise the context dependent nature of SPRY2 action.

Table 1.1 Expression of SPRY2 in a number of cancer types

Type of Cancer	SPRY2 level	Reference
Breast Cancer	↓	(Lo et al., 2004)
Colon Cancer	↑	(Holgren et al., 2010)
Hepatocellular Carcinoma	↓	(Fong et al., 2006, Lee et al., 2008)
Prostate Cancer	↓	(McKie et al., 2005)
Non-small Cell Lung Cancer	↓	(Sutterluty et al., 2007)
Melanoma	↑	(Bloethner et al., 2005)

1.3 Function of SPRY2

1.3.1 SPRY2 and growth factor signalling

The precise mode of SPRY action is difficult to pinpoint, as the functional role of the SPRY isoforms in different growth factor pathways varies in a distinct cell and tissue dependent manner. Mammalian SPRY proteins are referred to as master of modulators of growth factor signalling, and for most RTK signalling cascades. For FGF signalling, all of the SPRY isoforms inhibit FGF-induced MAPK activation to varying degrees (Lao et al., 2006, Ozaki et al., 2005). Yet, in response to EGF stimulation, SPRY2 acts as a positive enhancer and potentiates MAPK activation in some cell types (Egan et al., 2002, Fong et al., 2003, Rubin et al., 2003).

Given SPRY2 is the most highly conserved isoforms across vertebrates; most research has been heavily focused on SPRY2 in order to elucidate SPRY mediated functions. The inhibitory role of SPRY2 was first studied in the FGFR signalling cascade. In response to FGF, activation of FGFR recruits downstream molecule Shp2, which binds to phosphorylated tyrosines on FRS2. Activation of the SOS-Grb2 complex facilitates the activation of membrane-located Ras and downstream ERK signalling (Hadari et al., 1998). It is reported that SPRY2 physically interacts with Grb2 adaptor protein, and results in disruption in the formation of adaptor complexes including FRS2 and SOS1, consequently inhibiting Ras-Raf-MAPK signalling pathways as shown in the figure 1.3.1 (Lao et al., 2006, Martinez et al., 2007). The interaction between Grb2 and SPRY2 was attributed to the stronger inhibitory role of SPRY2 compared to its other family members SPRY1 and SPRY4, which are due to the weak binding of Grb2-SPRY1 and SPRY4 only binds to SOS1 and not Grb2 (Ozaki et al., 2005). Interestingly, Martinez's work showed that the mutation at the Grb2 binding sites did not affect the inhibitory role of SPRY2 in FGFR signalling, contradicting Lao and colleagues' findings (Lao et al., 2006). The major differences in these two studies are the duration of FGFR mediated MAPK activation (transient and stable ectopic FGFR transfection) and cell types, hence the inhibitory effect of SPRY2 in FGF signalling may be considered as temporal and cell context dependent.

The impact of SPRY family members in VEGF signalling cascades are often implicated in aberrant angiogenesis during carcinogenesis. Upon stimulation of VEGFR, PLCγ (phospholipase C gamma) and PKC (protein kinase C) phosphorylate Raf1 which in turn activates MAPK signalling molecules in a Ras independent manner (Takahashi et al., 2001) (Figure 1.3.1). Consequently, the inhibitory action of SPRY is different from other RTK pathways. It is reported that SPRY4 strongly interacts with Raf1 via its RBD (Raf1 binding domain) and subsequently disrupts Raf1 mediated MAPK signalling. Given all SPRY members consists of a RBD in their highly conserved C-terminus, it is expected that other SPRY isoforms may have similar inhibitory effects in VEGFR signalling pathways.

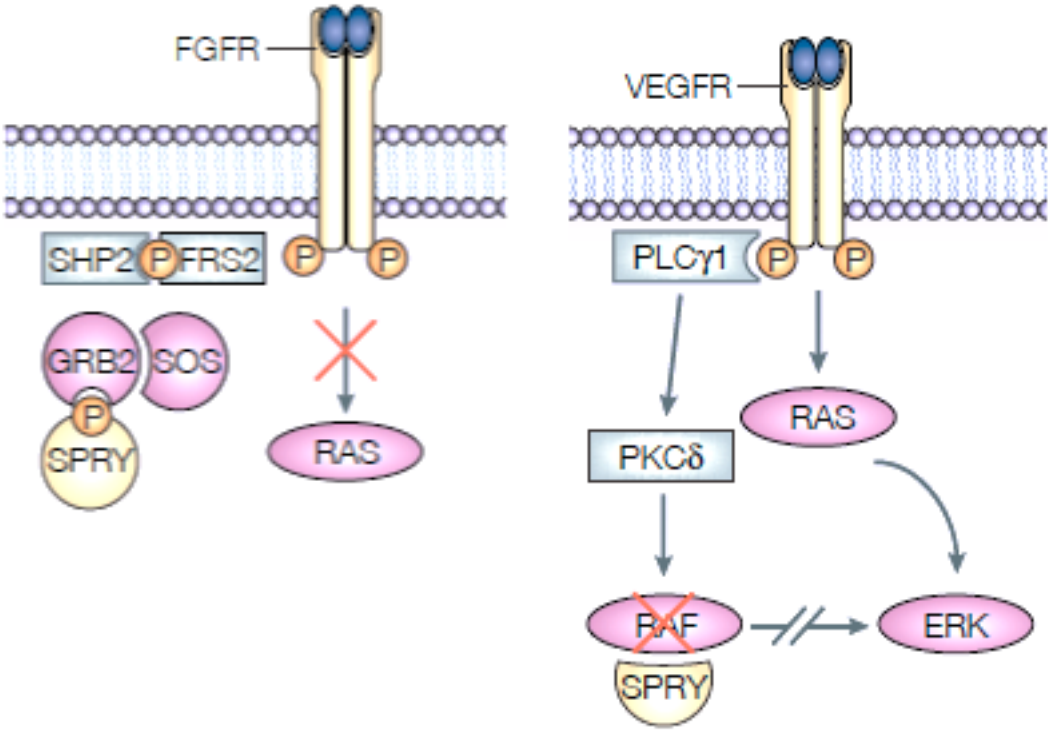

Figure 1.3.1 Schematic presentation of FGFR and VEGFR signalling pathways and inhibitory effect of SPRY2. Adopted from Kim and Bar-Sagi (2004).

1.3.2 SPRY2 and EGF signalling

For many years, SPRY2 was generally considered as a Ras-MAPK inhibitor in the RTK signalling cascade. However, recent studies challenged the traditional view of the SPRY function particularly in EGFR signalling network. The controversial view is that SPRY can potentiate MAPK signalling in EGF stimulated cells with cell type dependent manner. This is due to the fact that EGFR signalling involves a more complex mechanism involved in the balance between trafficking and degradation of the receptor. Upon ligand stimulation, EGFR can be rapidly degraded in order to control the magnitude of the signalling via interaction with the E3 ubiquitin ligase c-Cbl. It is reported that SPRY2 competes with EGFR for the c-Cbl binding sites, which in turn prevents the degradation of the receptor and enhances EGFR mediated signalling (Haglund et al., 2005). Other RTK including FGFR is also degraded by c-Cbl, but SPRY2 does not interfere with the interaction between FGFR and c-Cbl. How SPRY2 distinguishes between EGFR and FGFR remains to be investigated. Kim and his colleagues described that overexpression of SPRY2 delays EGFR trafficking to late endosomes, consequently rather potentiating EGFR mediated ERK activation (Kim et al., 2007). In summary, SPRY2 exerts tight spatial and temporal regulation in order to achieve signalling specificity.

1.4 Regulation of SPRY gene expression and localisation

Drosophila *Spry* gene expression is generally controlled by RTK mediated transcription. It was first reported that overexpression of Drosophila FGFR otholog (*Branchless*) induced expression of SPRY (Hacohen et al., 1998). In mammalian cells, *Spry2* and *Spry4* expression are induced via activation of EGF, FGF and PDGF mediated MAPK function, but FGF and PDGF showed downregulation of *Spry1* transcription (Gross et al., 2001, Impagnatiello et al., 2001, Sasaki et al., 2001). Gene array analysis revealed Spry2 gene promoter contained FOXO binding elements, and SPRY2 expression level is associated with FOXO deletion in endothelial cells (Dejana et al., 2007b).

The regulation of SPRY2 protein is achieved by a balance between its degradation and synthesis. Growth factors including FGF, EGF and VEGF stimulation leads to the induction of Spry gene transcription (Impagnatiello et al., 2001, Sasaki et al., 2001, Ozaki et al., 2001), which initiates the negative feedback in RTK signalling network. Many reports suggested the phosphorylation of serine or tyrosine residues of SPRY2 allows interaction with other regulatory molecules, and in turn affects its stability. For instance, upon EGF/FGF stimulation, MAPK-interacting kinase 1 (Mnk1) phosphorylates SPRY2 at serine 112 and 121 residues, which competes with tyrosine phosphorylation at the conserved N-terminal. This protects SPRY2 from binding C-cbl, and enhances its stability (DaSilva et al., 2006). In addition to C-cbl mediated degradation, a yeast two-hybrid screen revealed another E3 ubiquitin ligase interaction partner SIAH2, which binds to SPRY2 regardless of RTK mediated tyrosine phosphorylation (Nadeau et al., 2007). All together, SPRY2 as a key regulator of RTK is tightly regulated in a temporal manner both in transcription and post-translational level.

1.5 SPRY2 in prostate carcinogenesis

As mentioned before, loss of SPRY2 appears to be a common event in many tumour types, particularly in prostate cancer. First report from Kwabi-Addo showed an involvement of SPRY family member SPRY1 in prostate carcinogenesis (Kwabi-Addo et al., 2004). The prostate cancer TMA (tissue microarray) analysis revealed over a third of patients showed SPRY1 downregulation compared to normal tissue. However, the result was debatable, as some prostate tumours showed upregulation of SPRY1. Also it is reported that SPRY2 expression is controlled by genomic methylation, particularly in prostate cancer. Patient TMA analysis showed that high-grade tumours (gleason score 3-5) had less SPRY2 mRNA level compared to benign prostatic hyperplasia (BPH), indicating a potential tumour suppressor role of SPRY in prostate carcinogenesis (McKie et al., 2005). There is evidence of loss of heterozygosity (LOH), but with lower incidence than epigenetic silencing. In addition, recent cBio Cancer Genomic Portal analysis showed 26% of cases (n=103) with down-regulation of

SPRY2, with no case of mutation or copy number changes in Spry2 gene. In metastatic PC cases (n=37), there were 14 cases that reduced SPRY2 expression. Furthermore, patients with low level of SPRY2 expression showed significantly poorer survival outcome compared with unaltered SPRY2 expression level (Figure 1.5.1). In summary, loss of SPRY2 is an important event in prostate carcinogenesis. However, at what stage SPRY2 loss occurs and what its functional impact is remain to be elucidated.

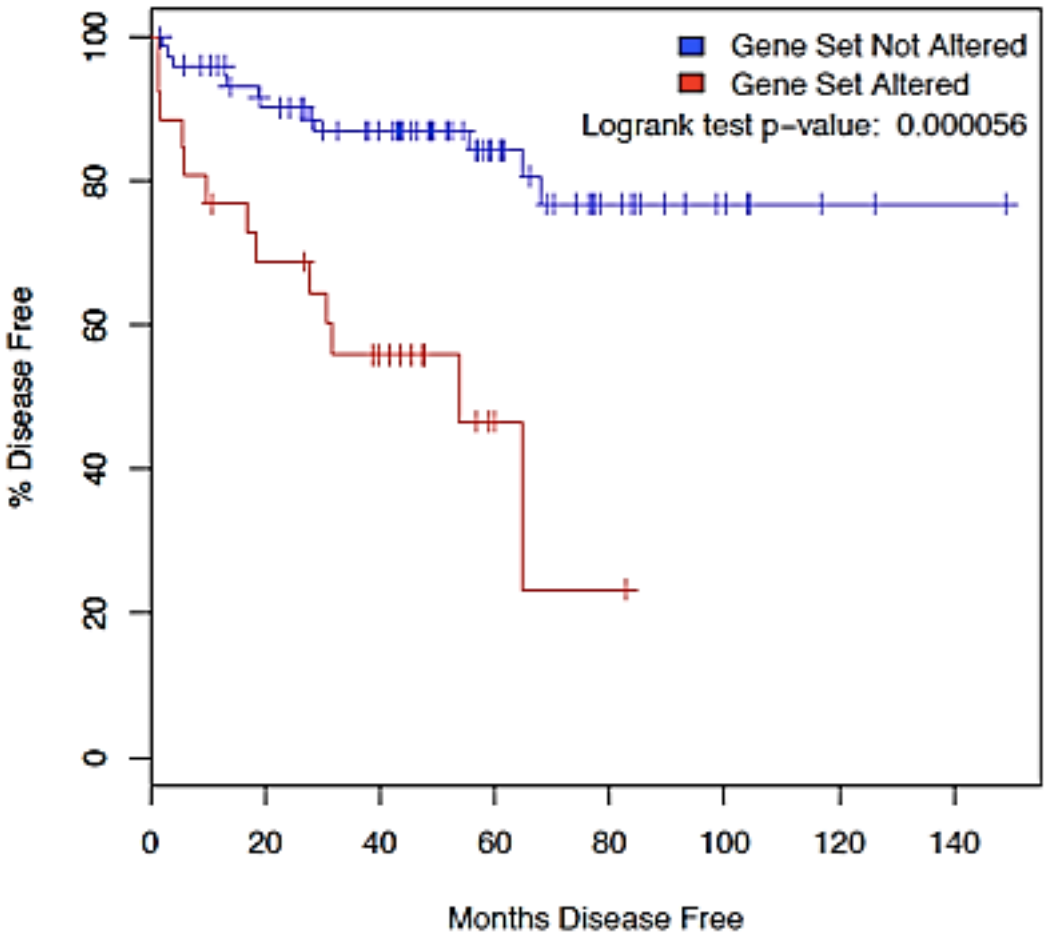

Figure 1.5.1 Poor survival outcome in patients with low SPRY2 expression
cBio Cancer Genomic Profile data was used to plot survival curve, patient with downregulated SPRY2 showed significantly poorer survival outcome with median 53.8 months.

1.6 Aims of the project

The aim of this study is to investigate the impact of SPRY2 loss in prostate carcinogenesis, particularly the controversial mechanism involved in the crosstalk between SPRY2, EGFR and PTEN/PI3K/AKT signalling networks in advanced prostate cancer including the use of preclinical models. The functional impact of SPRY2 loss is described in prostate cancer cell lines and *in vivo* in a preclinical mouse model. The involvement of SPRY2 reduction in RTK signalling pathway was investigated including EGFR/HER2 trafficking and downstream signalling cascades. Given the important function of SPRY2 loss in prostate cancer, we assessed targeted chemotherapeutic strategies in a *Spry*$^{+/-}$ *Pten*$^{+/fl}$ preclinical model. Finally the potential interaction partners of SPRY2 in prostate cancer cell lines are examined using SILAC proteomic technology

Chapter 2. Materials and Methods

2. Materials and Methods

2.1 Materials

All general laboratory reagents used in this study are listed in Table 2.1 below.

Table 2.1 General reagents

Reagent	Source
Ampicillin	Sigma
BSA (bovine serum albumin)	Sigma
DAPI (4',6-diamidino-2-phenylindole)	Vector
DMEM (Dulbecco's Modified Eagle's Medium)	GIBCO
DMSO (dimethyl sulfoxide)	Fisher Scientific
ECL (enhanced chemiluminescence)	GE healthcare
Ethanol	Sigma
F12	GIBCO
FBS (fetal bovine serum)	PAA
kanamycin	Sigma
L-glutamine	GIBCO
Lipofectamine 2000	Invitrogen
Matrigel	Invitrogen
Methanol	Sigma
MOPS SDS running buffer (20x)	Invitrogen
NaCl	Sigma
Nitrolcellulose membranes	Fisher Scientific
Penicillin Streptomycin	GIBCO
PFA (paraformaldehyde)	Science Services
Phosphatase inhibitors cocktail	Thermo Scientific
Protease inhibitors cocktail	Thermo Scientific
RPMI-1640	GIBCO
SimplyBlue Safestain	Invitrogen
Tris-HCl	Sigma
Triton X-100	Sigma
Trypsin	GIBCO
Tween-20	Sigma
ß-Mercaptoethanol	Sigma

All buffers and solutions used in the study are listed in Table 2.2.

Table 2.2 Solutions and buffers

Solution	Composition
Phosphate Buffered Saline (PBS)	170 mM NaCl 3.3 mM KCl 1.8 mM Na2HPO4 10.6 mM KH2PO4 PH 7.4
Tris-buffered saline - Tween (TBST)	25 mM Tris - HCl pH 7.4 137 mM NaCl 5 mM KCl 0.1% Tween - 20
Immunoblotting buffer	192 mM glycine 25 mM Tris 20% methanol
Lysis buffer	50 mM Tris - HCl pH7.5 150 mM NaCl 1% Triton 1 mM EDTA
Fixing solution	4% PFA 96% PBS
Blocking buffer (Immunoblotting)	5% w/v milk powder in TBS-T
Blocking buffer (immunofluorescence)	10% FBS 1% w/v BSA 90% PBS
Permeabilizing solution (immunofluorescence)	0.1% Triton X-100 in PBS
Lysogeny broth (LB)	1% Bacto-tryptone 86 mM NaCl 0.5% yeast extract
LB agar	1.5% agar
Tris-EDTA (TE)	10 mM Tris-HCl pH 8.0 1 mM EDTA
3x SDS-PAGE sample buffer	125 mM Tris pH 6.8 4% SDS 15% β-Mercaptoethanol 15% glycerol 0.01% bromophenol blue
Citrate buffer PH6	10 mM sodium citrate 0.05% Tween 20
Tris-buffered Saline (TBS)	25 mM Tris - HCl pH 7.4 137 mM NaCl 5 mM KCl

2.2 Methods

2.2.1 Cells and Growth Condition

Human prostate cancer cell lines DU145, PC3, LNCaP and CWR-22 were authenticated by LCG standards and purchased from ATCC. These cells were grown in RPMI (Gibco) containing 10% fetal bovine serum (FBS) and 2mM L-Glutamine (GIBCO) at sub-confluent conditions. Cells were maintained as described previously (Masters and Stacey, 2007). Briefly, cells were grown in a humidified incubator at 37°C in 5% CO_2 and passaged every 3-4 days. Medium was aspirated and cells were washed with PBS once, followed by incubation with Trypsin (Invitrogen). Cells were collected and counted with CASY® cell counter (Innovatis) and seeded for maintenance.

For long-term storage cell lines were cryo-frozen. Cells were trypsinised and resuspended in 50% FBS, 40% full medium and 10% DMSO, then froze in cryotubes (Nunc) at -80°C overnight and stored in liquid nitrogen.

2.2.2 Cell Proliferation Assay

Cells were seeded at a concentration of 5 x 10^3cells/well in 100 μl culture medium into microplates (tissue culture grade, 96-wells, flat bottom) (Becton Dickinson). After various treatments for 48 h at 37°C and 5% CO_2 condition, 10μl Cell Proliferation Reagent WST-1 (Roche) was added and incubated for 30 mins. The absorbance of the samples against a background control as blank was measured using a microplate (ELISA) reader. The wavelength for measuring the absorbance was 450nm and the reference wavelength was set at 650nm.

2.2.3 Matrigel Invasion Assay

For the invasion assay, the 24-well configuration of the BioCoat™ Matrigel™ Invasion chambers (BD Sciences) was used. The matrigel was rehydrated with warm serum free medium for 2h in a humidified tissue culture incubator. After incubation, 40,000 cells/well were seeded in triplicate and

allowed to invade through transwell chambers with 8 mm pore membranes coated with matrigel for 8 h with 10% serum or 20 ng/ml EGF (Invitrogen) as chemo-attractant. The chemo-attractant was added in the wells of a companion plate. After incubation, the non-invading cells were removed from the upper surface of the membrane using cotton buds. Cells that had invaded to the lower surface of the membrane were fixed in 100% methanol and the membrane was mounted onto slides. Invaded cells were stained with DAPI and visualised under microscope (Nikon).

2.2.4 Receptor Internalisation Assay

EGFR internalisation assays were performed after overnight serum starvation followed by EGF (Invitrogen) treatment (20 ng/ml) as described previously (Sarto et al., 2007). Cells were coated with NHS-S-S-biotin (Sigma) before EGF treatment for 30 mins at 4°C with rocking, then cells were washed 2 times with cold PBS. The cell surface biotin was reduced with cell impermeable MesNa (sodium 2-mercapto-ethanesulfonate) (Sigma) for 1 h with rocking at 4°C. The reaction was stopped with reducing agent iodoacetamide (Sigma). Cells were washed with PBS 2 times, and WCL (whole cell lysate) were collected for either ELISA or IP (Immunoprecipitation) experiments. For ELISA detection, 96 well plates were coated with EGFR antibody overnight and washed with PBST (5% BSA). Internalisation assays were performed in the presence of 0.6 mM of primaquine (Sigma). For IP, the internalisation was performed and whole cell lysates were used to IP the biotin labelled EGFR with Dynabeads® (Invitrogen) or NeutrAvidin (Thermo Scientific) instead of ELISA plates. Dynabeads® were incubated with EGFR antibody (BD bioscience) for 1h at 4°C, and the beads were washed with lysis buffer 3 times before added to the WCL for IP. Proteins bound to the beads were eluted by boiling, and western blot analysis was performed.

2.2.5 Immunoblotting

Cells were lysed with lysis buffer containing Halt protease inhibitor cocktail (Thermo Scientific) and Halt phosphatase inhibitor cocktail (Thermo Scientific) as described by the manufactures instruction. Briefly, the whole cell lysate were centrifuged for 15 mins at 13200 rpm, and the supernatant was collected for measurement of protein concentration. Bio-RAD Protein Assay (Bio-

RAD) and spectrophotometer (595 nm) was used for determining protein concentration. All the protein samples were adjusted to be at equal concentration with lysis buffer. Subsequently the samples were boiled in 3x sample buffer for 10 min at 100°C and loaded in NuPAGE® 4-12% Bis-Tris Gel (Invitrogen). The gels were electrophoresed in XCell SureLock™ Mini-Cell tank (Invitrogen) at 120mA and 200V in 1x MOPS SDS running buffer (Invitrogen).

The separated proteins were transferred from the gel to nitrocellulose membrane using semi-dry western transfer in 1x transfer buffer. Each gel was transferred at 20 V and 200 mA for 1h. The membranes were blocked in 5% milk (Marvel)/TBST for 60 mins incubated with primary antibodies solution overnight at 4°C. After washing with 3x TBS-T for 5 mins, secondary antibodies were added in the blocking solution for 1h at room temperature. The antibodies used in this study are listed in Table 2.4. The proteins on the membrane were visualised by ECL detection kit (GE Healthcare).

2.2.6 Transfection

For generation of stable SPRY2 knock down cell lines, a 19mer sprouty2 target sequenc (5'-AACACCAATGAGTACACAGAG-3') (Qiagen) was used, and non-silencing control sequence was obtained from Qiagen. Plasmid pTER+ were used to insert the sequence of interest, and stably expressed in DU145 and PC3 cell lines. The stable SPRY2 KD cell lines were generated by Dr Rachana Patel. For transient SPRY2 siRNA transfection, two different siRNA sequences were purchased from Dharmacon, and PTEN siRNA was obtained from Cell Signalling. Transfection was carried out with Amaxa Cell Line Nucleofactor Kit (Lonza) as manufactors instruction.

For IP and IF, plasmids were transfected into cells with Lipofectamine™ 2000 (Invitrogen) following the manufacturer's instructions. For 150 mm plate, 3 μg of appropriate DNA plasmids were mixed with 1 ml serum free medium and 20μl Lipofectamine™ 2000, and incubated at room temperature for 20 mins to allow DNA-Lipofectamine™ 2000 complexes to form. After incubation, the mixture was added to the cells drop wise. Cells were incubated in humidified tissue culture incubator until ready to assay (24-48 h post transfection).

2.2.7 Immunofluorescence (IF)

Cells were transfected with GFP-EEA1 vector (Addgene) for 24 h and fixed in 4% paraformaldehyde for 15 mins. Cells were permeabilised with 0.1% Triton X-100 (Sigma). Non-specific binding was blocked with a mixture of 10% FBS, 1% BSA and PBS. Then the blocking solution was removed and cells were incubated with appropriate primary antibodies for 1h at room temperature. Primary antibodies were diluted in 10% FBS, 1% BSA and PBS. Alexa Fluor® 555 and 488 (Invitrogen) was used as secondary antibody, and the nucleus was stained with DAPI. Simultaneous dual fluorescence acquisitions were performed using confocal microscope (Nikon) with 488 and 568 nm laser lines to visualise GFP and Texas red dyes using 60x oil immersion (scale bar 20μm).

2.2.8 SILAC (stable isotope labelling with amino acids in cell culture) labelling

Cells were grown in the medium containing appropriate stable isotopic amino acids reagents listed below for at least 5 passages. The whole cell lysates were collected and tested for incorporation. When the incorporation rate reached above 90%, cells were used for IP experiments.

Table 2.3 Stable isotopic amino acids used in SILAC media

Stable isotopic amino acids	Concentration in RPMI	Mass difference	Source	Combination
L-lysine 2HCL	100mg/L	0Da	Sigma	Light
L-Arginine HCl	100mg/L	0Da	Sigma	Light
L-Lysine 2HCl (4,4,5,5-D4)	100mg/L	4Da	Cambridge Isotope	Medium
L-Arginine (13C6)	50mg/L	6Da	Cambridge Isotope	Medium
L-Lysine 2HCl (13C6, 15N2)	100mg/L	8Da	Cambridge Isotope	Heavy
L-Arginine HCl (13C6, 15N4)	50mg/L	10Da	Cambridge Isotope	Heavy

2.2.9 Immunoprecipitation (IP)

Prior to harvesting the cells, they were transfected with GFP (Addgene) or GFP tagged SPRY2 plasmids for 48 h. GFP tagged SPRY2 plasmid was constructed

with inserting SPRY2 sequence into GFP plasmid. Cells were stimulated with 100 ng/ml EGF after 24 h starvation. Cells were lysed in lysis buffer and the lysate was cleared by centrifugation at 13000 rpm for 15 min at 4°C. The whole cell lysates were incubated with GFP-Trap®_A beads (Chromotek) at 4°C for 1h with rotation. The beads were washed 3 times with lysis buffer and then boiled at 100°C in 1% SDS to elute IP proteins bound to the beads.

2.2.10 Animals

All animal experiments were carried out under the UK Home Office guidelines (project licence 60/3947, and personal licenced 12870). Mice were of a mixed background and littermates were used as control mice.

Nkx 3.1-Cre (Hsieh et al., 2010) mice were crossed to those harbouring *Spry2*$^{+/-}$ (Shim et al., 2005) *and Pten*$^{fl/+}$ (Lesche et al., 2002). The mice were genotyped by PCR by Transnetyx^{TM} (Shim et al., 2005, Lesche et al., 2002, Andrechek et al., 2000). Prostates were dissected out and placed in formalin for overnight fixation before paraffin embedding.

PI 103 treatment was commenced when the prostate tumour was palpable in the mouse model (10-11 months). PI 103 was injected daily 50 mg/kg intra-peritioneal (ip) for 4 weeks. Prostate tissues were collected and fixed in formalin or frozen in liquid nitrogen for western analysis.

2.2.11 Immunohistochemistry

Tissue samples were formalin-fixed, paraffin-embedded, and stained for at least 3 samples from 3 different mice. The tissue sections were prepared in the histology services. For Ki67 staining, Ki67 antibody (Vector Labs) was used at 1/100 dilution, and antigen unmasking was performed in citrate buffer (pH 6) and incubated for 50 mins at 99°C in a water bath. For p-AKT (ser473) (Cell Signaling, 1/50 dilution) and pERK1/2 (Cell Signaling, 1:100 dilution), citrate buffer or Tris/EDTA buffer (pH8) and microwave antigen retrieval method was used. The antibodies are listed in the Table 2.4.

2.2.12 Tissue microarray analysis of human prostate cancer

With ethical approval (MREC 01/0/36), formalin-fixed, paraffin-embedded (FFPE) sections from 239 patients were studied. These consisted of 209 primary prostate carcinomas (PC) and 30 benign prostatic hyperplasia (BPH) samples. Three 0.6mm cores of prostate cancer tissue from each case were identified by pathologists and removed from representative areas of the FFPE blocks. All cancer samples had been taken from prostate cancer patients at the time of trans-urethral resection of the prostate (TURP). These samples consisted of Gleason 3 (n=123), 4 (n=49) to 5 (n=37) cancers, as determined independently by two consultant pathologists (MS and RJB). These samples were processed by immunohistochemistry. Survival analysis was performed using Kaplan Meier plot and log rank test.

2.2.13 Statistics

All the statistical analysis was performed using Prism 5 software, and all graphs were generated using Microsoft Excel software. The error bars were calculated and represented in terms of mean ± SD.

Table 2.4 List of antibodies used in this study

Antigen	Supplier	Dilution
Actin	Sigma; A4700	1:1000
AKT	Cell Signaling; 9272	1:1000
ATF2	Cell Signaling; 9226	1:1000
BRaf	Cell Signaling; 9433	1:1000
CKB	Abcam; ab38212	1:1000
Clathrin	Cell Signaling; 4796	1:1000
EGFR	Cell Signaling (western)	1:1000

	Santa Cruz; sc103 (IHC) BD Bioscience (IP and IF)	1:100 1:!00
ERK1/2	Cell Signaling; 9102	1:1000
GAPDH	Sigma; G9295	1:12000
GFP	Cell Signaling; 2956	1:1000
HER2	Cell Signaling; 8339 (western) Cell signalling (IHC)	1:1000 1:100
HER3	Cell Signaling; 8339	1:1000
p-AKT	Cell Signaling; 4060 (western) Cell signalling (IHC)	1:1000 1:100
p-ATF2	Cell Signaling; 9221	1:1000
p-EGFR	Cell Signaling; 9922	1:1000
p-ERK1/2	Cell Signaling; 9101 (western) Cell signaling (IHC)	1:1000 1:100
p-HER2	Cell Signaling; 8339	1:1000
p-HER3	Cell Signaling; 8339	1:1000
p-p38	Cell Signaling; 9790	1:1000
P38	Cell Signaling; 9790	1:1000
PKM2	Cell Signaling; 3198	1:1000

PP2A	Cell Signaling; 2259	1:1000
PTEN	Cell Signaling; 9188 (western) Cell Signaling (IHC)	1:1000 1:50
SPRY2	Abcam; ab50317 (IHC) Sigma; s1444 (western)	1:50 1:1000
Tubulin	Sigma; T6557	1:2000
FLAG	Sigma; F3165	1:100
Anti-rabbit IgG, HRP-linked Antibody	Cell Sigmaling; 7074	1:5000
Anti-mouse IgG, HRP-linked Antibody	Cell Signaling; 7076	1:5000

Table 2.5 List of inhibitors used in this study

Inhibitors	Suppliers	Dilutions
Gefitinib	LC Laboratories; G4408	15 μM
Lapatinib	LC Laboratories; L4804	10 μM
SB203580	Sigma; s8307	10 μM
PI103	Tocris Bioscience; 2930	50 mg/kg
LY294002	Sigma; L9908	10 μM
Dynasore	Sigma; D7693	5 μM
PD098059	Sigma; p215	10 μM

Chapter 3. Functional contribution of SPRY2 in human PC cells and a preclinical mouse model

3 Functional contribution of SPRY2 in PC cell line and preclinical mouse model

In prostate cancer, work from our laboratory has previously showed that SPRY2, one of mammalian SPRY orthologues (SPRY 1-4), is epigenetically silenced in almost 70% of primary prostate cancer (McKie et al., 2005). SPRY2 physically interacts with several adaptor/regulator proteins downstream of RTKs, including PP2A, Grb2, Braf, Shp2, c-Cbl and GAP1 (Danese et al., 2007). The large number of binding partners for SPRY2 is consistent with its crucial yet complicated role in RTK signalling. Indeed, whether SPRY2 functions as a positive or negative regulator in EGFR signalling network remains an important question. In addition to its well-reported function as an inhibitor of RAS/RAF/MEK signalling cascade (Bordoni et al., 2007), Edwin and his colleagues reported that SPRY2 exerts its inhibitory role in PI3K/AKT signalling pathway through PTEN, by enhancing its activation and stability (Edwin et al., 2006). PTEN is among the most commonly mutated genes in human cancer, including prostate cancer. Progressive inactivation or loss of PTEN appears to be involved in development of invasive and metastatic PC. Transgenic mice with PTEN heterozygous deletion targeted to the prostate develop high-grade PIN, which fails to progress into invasive phenotype (Mellinghoff et al., 2004). Furthermore, complete loss of PTEN is thought to be a late event and can be considered a critical landmark for progression to aggressive and invasive disease. Indeed, the *Pten null* murine prostate cancer model developed invasive adenocarcinoma (Song et al., 2011). This is consistent with the cBio portal data, which revealed ~24% (25/104) of PC retains PTEN expression albeit at low levels and only ~7% (7/104) of PC showed evidence of homozygous *Pten* deletion (cBio Cancer Genomics Portal) (Taylor et al., 2010). It is worth noting that as many as 50% (17/37) of metastatic tumours harboured biallelic *Pten* loss.

To date, functional studies of SPRY2 have studied effects of transiently or stably over-expressed SPRY2 in *in vitro* cell models (Kawakami et al., 2009, Rubin et al., 2003). As SPRY2 expression tends to be suppressed in cancer, we set out to investigate the significance of SPRY2 loss using human prostate cancer cell models with knocked down SPRY2 expression and a preclinical mouse model.

3.1 Analysis of SPRY2 expression and effect of SPRY2 loss in prostate cancer cell lines

In order to understand the effect of SPRY2 in prostate cancer progression, the expression of SPRY2 was examined in various prostate cancer cell lines, including PC3, PC3M, LNCAP, DU145, CWR22 and PNT-2A. The classic prostate cancer cell lines including PC3 and DU145 were obtained from a patient with metastatic PC, and PC3 cell line is generally considered having more invasive ability compared to DU145. DU145 is derived from a distant metastatic organ (brain) in a PC patient. Among these cancer cell lines, except LNCAP cells expression of SPRY2 is detected by western blot analysis (Figure 3.1.1). Considering the important role of PTEN in the function of SPRY2, PC3 and DU145 cell lines were selected to further study the effect of SPRY2 loss, since they have PTEN null and positive background respectively.

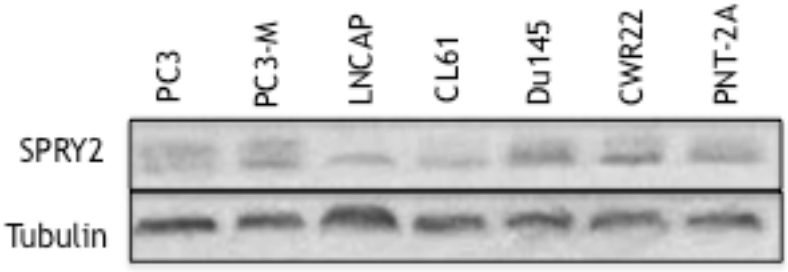

Figure 3.1.1 Expression level of SPRY2 in prostate cancer cell lines
Panel of prostate cancer cell lines were lysed and performed western bot analysis, the expression of SPRY2 was detected across different prostate cancer cell lines. Tubulin was used as a loading control.

Stable knockdown of SPRY2 clones of prostate cancer cell line DU145 (CL13 and CL61) and PC3 (CL1 and CL10) along with non-silencing control (Nsi) cells were generated. Western blot analysis confirmed reduction of SPRY2 expression in knockdown clones (Figure 3.1.2). Due to the difference in the shRNA sequence, the knockdown effect was expected to be different; consequently the impact of the two shRNA in SPRY2 KD clones may vary. The

effect of SPRY2 KD in DU145 and PC3 were examined in response to EGF stimulation. Upon the ligand binding, DU145 SPRY2 KD clones 13 and 61 showed significantly more EGF mediated proliferation compared to the Nsi control. However, PC3 cells did not show any difference in cell growth between SPRY2 KD clones and control cells (Figure 3.1.2). Such difference may be attributed to the PTEN status in these cells. It is reported that presence of PTEN is essential for SPRY2 to act as an inhibitory regulator in RTK signalling cascades, particularly in cell proliferation (Edwin et al., 2006). In addition, matrigel plug was used to test the invasiveness of SPRY2 KD cells. The PTEN positive DU145 cells with reduced SPRY2 expression showed over 40% more cells invading through the matrigel towards to the chemoattractant EGF when compared to Nsi control cells. The number of invading SPRY2 KD cells were visualised with DAPI staining and were more than 2 fold higher than that observed for Nsi control cells. Interestingly, loss of SPRY2 in PC3 cells decreased the invasiveness in response to EGF (Figure 3.1.3). We reasoned the difference in proliferation and invasiveness in PC3 and DU145 with loss of SPRY2 may be attributed to the level of PTEN expression.

In order to investigate the functional effects of PTEN in relation to SPRY2 expression status, we used siRNA to transiently KD PTEN in DU145 Nsi and SPRY2 KD cells. Western blot analysis showed the reduction of PTEN expression with the siRNA transfection but not with the control scramble siRNA treated cells (Figure 3.1.4). Consistent with my hypothesis, the concomitant loss of SPRY2 and PTEN expression in DU145 cells led to one-fifth reduction in invasion, and there was no alteration observed in cell growth. Furthermore, there were increases both in cell growth and invasion in Du Nsi cells with PTEN siRNA tranfection (Figure 3.1.4). Reduction in PTEN level may release the inhibition of PI3K/AKT signalling pathways, which leads to the increase in proliferation and invasion in Nsi cells. Overall, loss of SPRY2 cooperates with EGF stimulation, and enhances cell proliferation and invasion in PTEN-dependent manner.

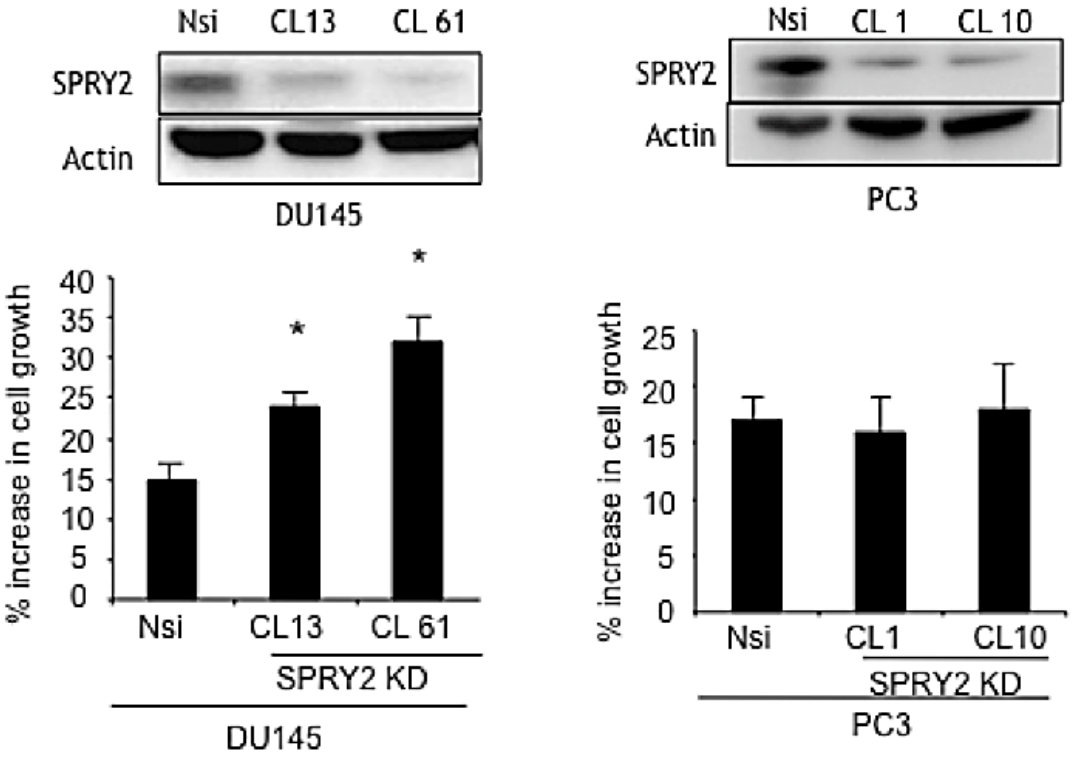

Figure 3.1.2 Stable SPRY2 KD and its effect on proliferation

SPRY2 KD Du145 and PC3 cells were lysed and analysed with western blot analysis. Actin was used as a loading control. Cells were treated with 20 ng/ml EGF for 48 hours and determined the percentage of cell growth using WST-1 assay (*$p<0.001$ n=3).

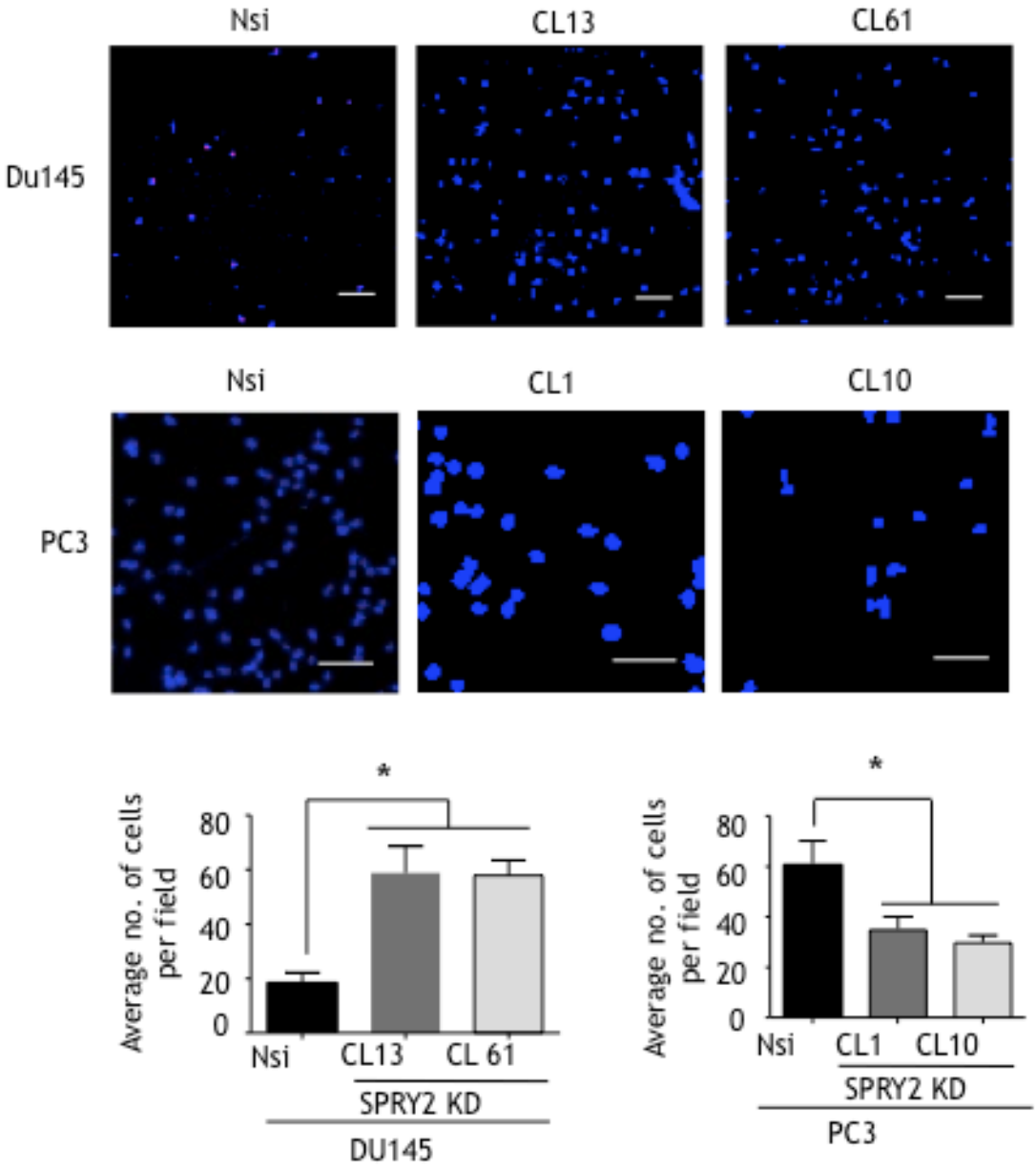

Figure 3.1.3 Loss of SPRY2 resulted more invasive phenotype in DU145 cells
Invasion assay was performed with Du145 and PC3 in the matrigel invasion chamber for 8 hours incubation, EGF was used as a chemoattactant. The number of cells which invade through the matrigel was quantified (*$p<0.001$ n=3), the scale bar = 100μm.

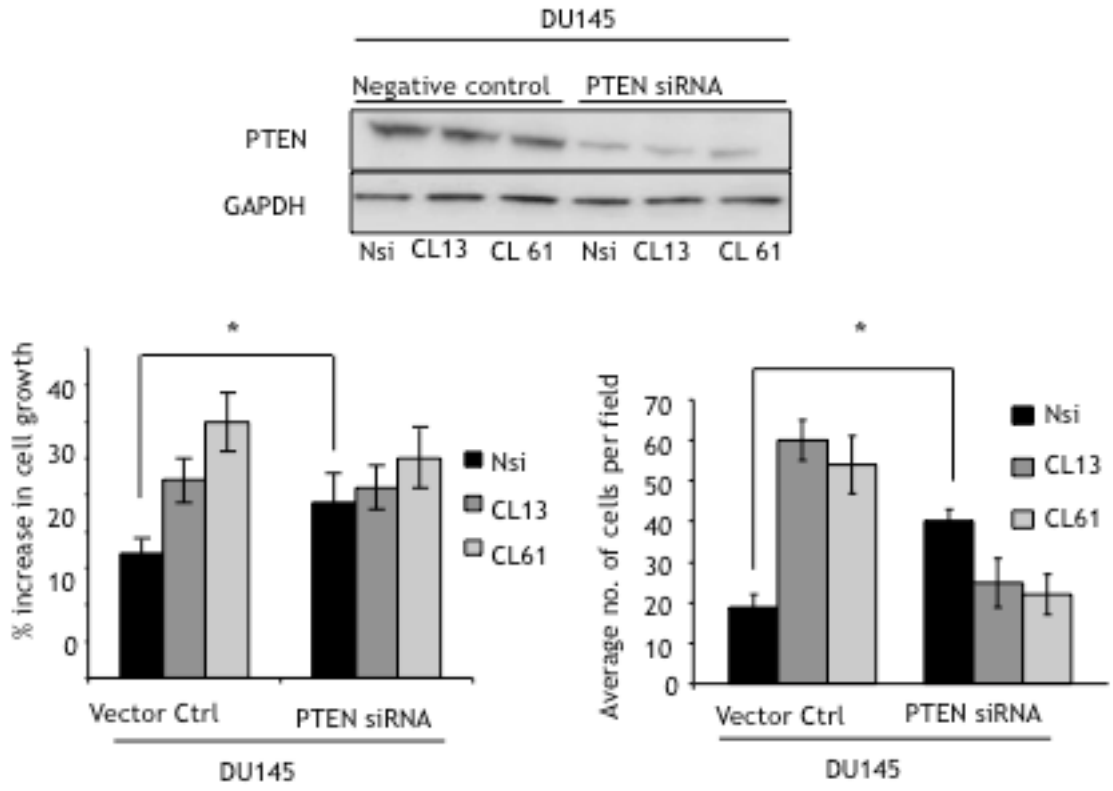

Figure 3.1.4 The effect of SPRY2 loss is PTEN dependent

Du145 control and SPRY2 KD clones are transfected with PTEN siRNA and analysed with western blot. GAPDH is used as a loading control. The percentage of proliferation was quantified with WST-1 assay (*p<0.001 n=3). The invasion assay was performed with a matrigel plug and quantified (*p<0.001 n=3).

3.2 Loss of SPRY2 enhances the activation of EGFR signalling pathways upon EGF stimulation

Downstream signalling following EGF stimulation in SPRY2 KD DU145 cells was examined using the Human Phospho-Kinase Array. Cells were serum starved overnight and stimulated with EGF for 15 minutes. Among the 46 phospho-kinase profile, PI3K/AKT and MAPK were key pathways activated upon EGF stimulation. Interestingly, we only observed a difference (20%) in AKT phosphorylation at serine 473, but not threonine 308. Activation of PI3K/AKT can lead to elevation of JNK phosphorylation, which contributes to prostate tumour cell proliferation and angiogenesis (Slack et al., 2005). Downstream signalling components of PI3K/AKT and MAPK such as JNK and c-Jun also showed higher level of phosphorylation in SPRY2 KD cells. Since DU145 cells have amplification of Ras, and an inhibitory effect of SPRY2 in Ras-MEK-ERK, both MEK1/2 and its downstream ERK1/2 are activated. We also observed enhanced activation of the stress MAP kinase p38 in SPRY2 KD cells by EGF (Figure 3.2.1). For p-P38 signal, the membrane was exposed slightly longer to detect the difference, it may be due to the sensitivity of p-P38 antibody in the assay kit or the amount of phosphorylated form of P38 is relatively less compared to other proteins (Figure 3.2.2). Some of the above findings were confirmed in Western blot following 15 and 30 minutes of EGF stimulation. As we expected, the PTEN null PC3 cells showed less activated level of p-AKT in SPRY2 KD cells compared to Nsi control cells (Figure 3.2.3). Thus there were no significant difference in increase of proliferation and invasiveness in SPRY2 KD PC3 cells compared to the Nsi control cells, which were observed in Chapter 3.1. Together, loss of SPRY2 activates PI3K/AKT signalling cascade, which is a key component for the EGF driven cell growth and invasion.

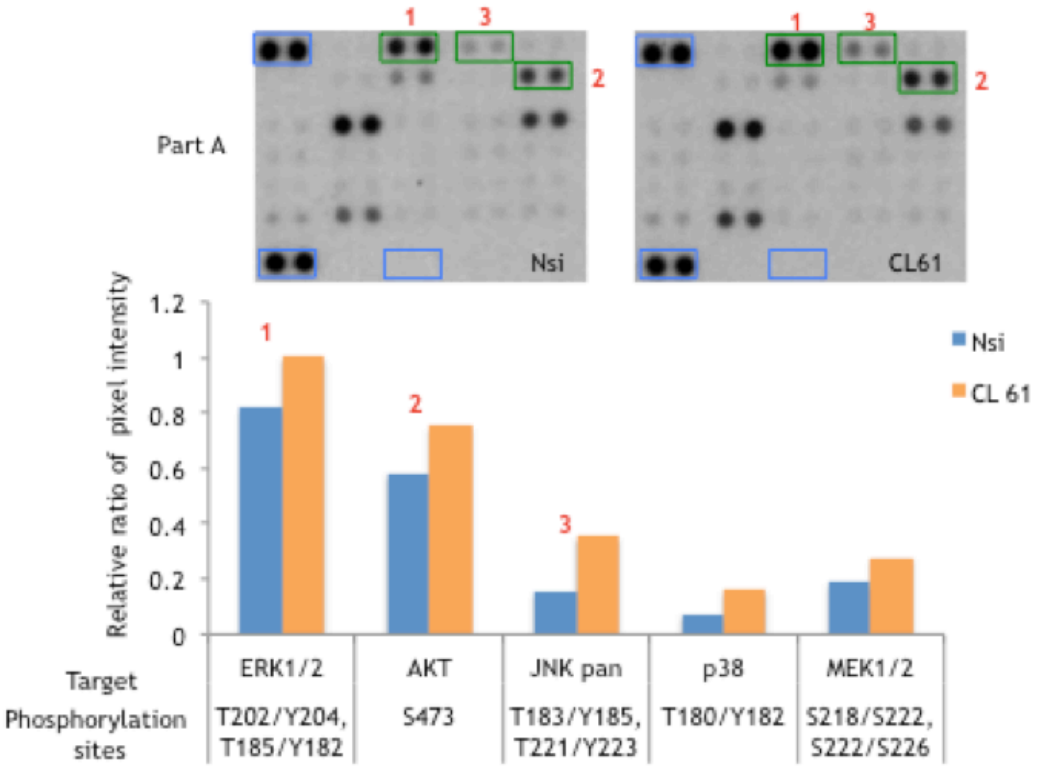

Figure 3.2.1 Human phospho-kinase array analysis

DU145 Nsi control and SPRY2 KD cells were serum starved overnight and stimulated with EGF (15 minutes). The whole cell lysates were collected and analysed with Human Phospho-Kinase Antibody Array Part A. The pixel intensity was quantified with image J software and relative ratio to the positive control were quantified and plotted. Positive and negative controls are labelled with blue boxes.

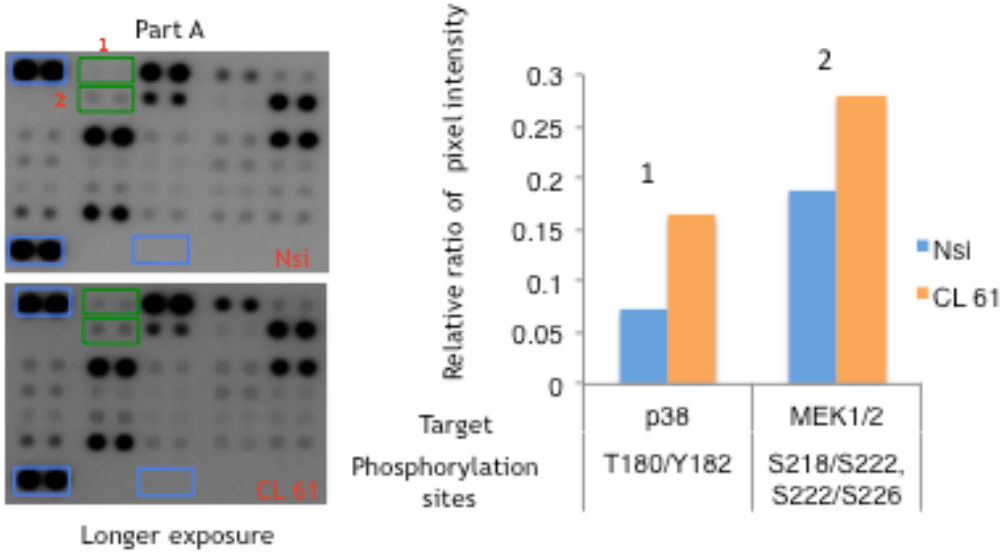

Figure 3.2.2 Human phospho-kinase array analysis

DU145 Nsi control and SPRY2 KD cells were serum starved overnight and stimulated with EGF (15 minutes). The whole cell lysates were subjected to Human Phospho-Kinase Antibody Array Part A. The pixel intensity was quantified with image J software and relative ratio to the positive control were quantified and plotted. Positive and negative controls are labelled with blue boxes. The blot was exposed for longer time due to the variation in antibody sensitivity.

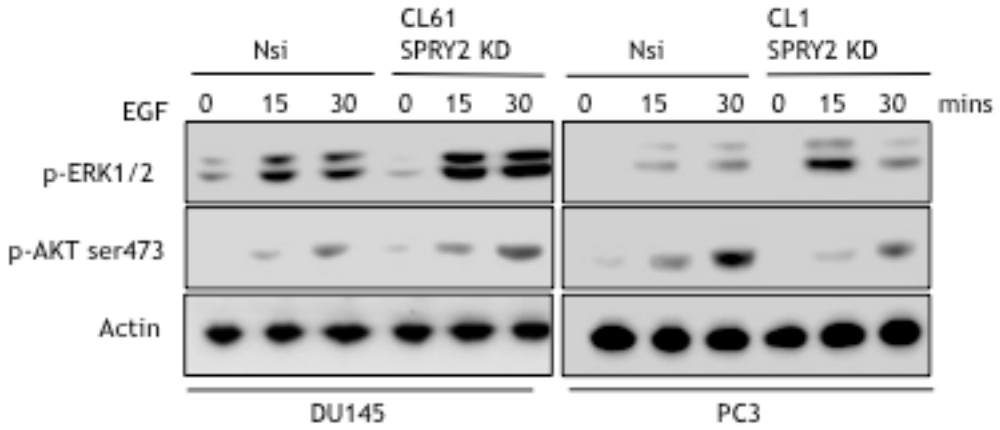

Figure 3.2.3 Validation of the human phospho-kinase array

Whole cell lysates were collected from EGF stimulated DU145 and PC3 cells, and analysed with western blotting to confirm the kinase array. Actin was used as a loading control.

3.3 Loss of SPRY2 and PTEN in a preclinical mouse model

The preclinical mouse model for prostate cancer is often studied using a conditional gene knockout (KO) method, which allows the functional analysis of the gene of interest. One of the common systems is the Cre loxP recombination system, which gives tissue specific gene alterations (Nagy, 2000). The technology works as follows: loxP sequence flanks the specific gene, and upon Cre recombinase expression the target gene is deleted through recombination between loxP sites. For the prostate, the organ specific deletion is often achieved with the Pb-Cre4 or Nkx3.1-Cre mediated strategies (Trotman et al., 2003a). Nkx Cre driven recombination occurs in the prostate epithelium, and also affects other organs during development (Thomsen et al., 2008, Zhang et al., 2008). Given the critical tumour suppressor role of PTEN, there are several reports on PTEN deletion in PC mouse model. Germline deletion of one Pten allele developed PIN and high grade PIN, but no adenocarcinoma or invasive prostate cancer was observed (Podsypanina et al., 1999, Di Cristofano et al., 1998). In addition more aggressive adenocarcinoma of prostate was observed when combinations of other oncogenic genes were engineered to cooperate with PTEN including c-Myc, p53, TMPRSS-ERG fusion (Carver et al., 2009, King et al., 2009b, Chen et al., 2005, Kim et al., 2009).

Considering the *in vitro* data shown in Chapter 3.1 and published human genomic data, the Spry2 and Pten heterozygous mouse model was generated to investigate the effect of SPRY2 and PTEN in prostate carcinogenesis. Nkx $Pten^{fl/+}$ $Spry2^{+/-}$ mouse were generated and the prostate tissue was harvested from mice around 10-12 months old. The H&E staining showed $Pten^{fl/+}$ developed PIN lesions in the prostate gland. The epithelial cells contained enlarged nuclei, and part of the epithelium showed irregular appearance and abnormal growth next to the normal cells (Figure 3.3.1). In contrast, loss of SPRY2 and PTEN resulted in aggressive prostate tumour, the glandular structure is no longer visible, and cancer cells infiltrated into surrounding areas (Figure 3.3.1). As expected, there are more Ki67 staining positive cells in the prostate epithelium of $Pten^{fl/+}$ $Spry2^{+/-}$ mice compared to that in $Pten^{fl/+}$ mice, indicating uncontrolled proliferation in the adenocarcinoma. Evidence suggested that loss of PTEN leads to the activation of PI3K/AKt signalling, with both $Pten^{fl/+}$ $Spry2^{+/-}$ and $Pten^{fl/+}$ showing

enhanced AKT activation, but the former with more aggressive phenotype showed relatively higher levels of pAKT with predominantly plasma membrane staining. In addition to PI3K/AKT signalling, pERK1/2 activation was also assessed, immunohistochemistry (IHC) results suggested enhanced pERK1/2 expression is restricted to only focal areas within the prostate (Figure 3.3.2). Altogether, concomitant loss of tumour suppressor gene Pten and Spry2 leads to activation of PI3K/AKT and drives aggressive prostate carcinogenesis *in vivo*.

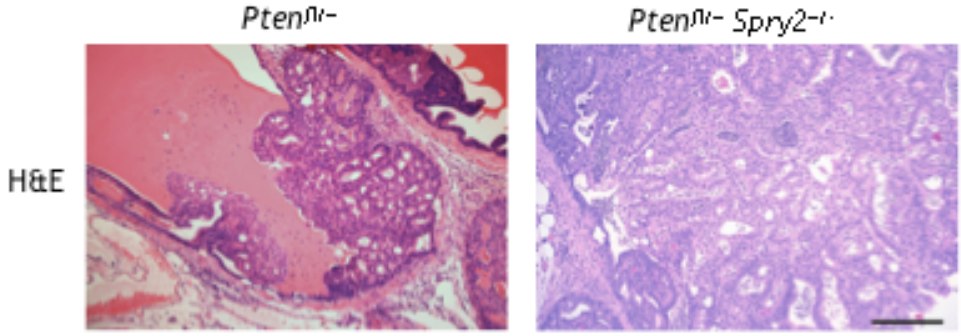

Figure 3.3.1 Nkx Pten$^{fl/+}$Spry2$^{+/-}$mouse model develop invasive prostate cancer
Prostate tissue was fixed and H&E staining shows PIN formation in Pten$^{fl/-}$ mouse (n=15), and Pten$^{fl/-}$ Spry2$^{-/-}$ mouse (n=12) developed aggressive adenocarcinoma within 10-12 months (scale bar = 200μm).

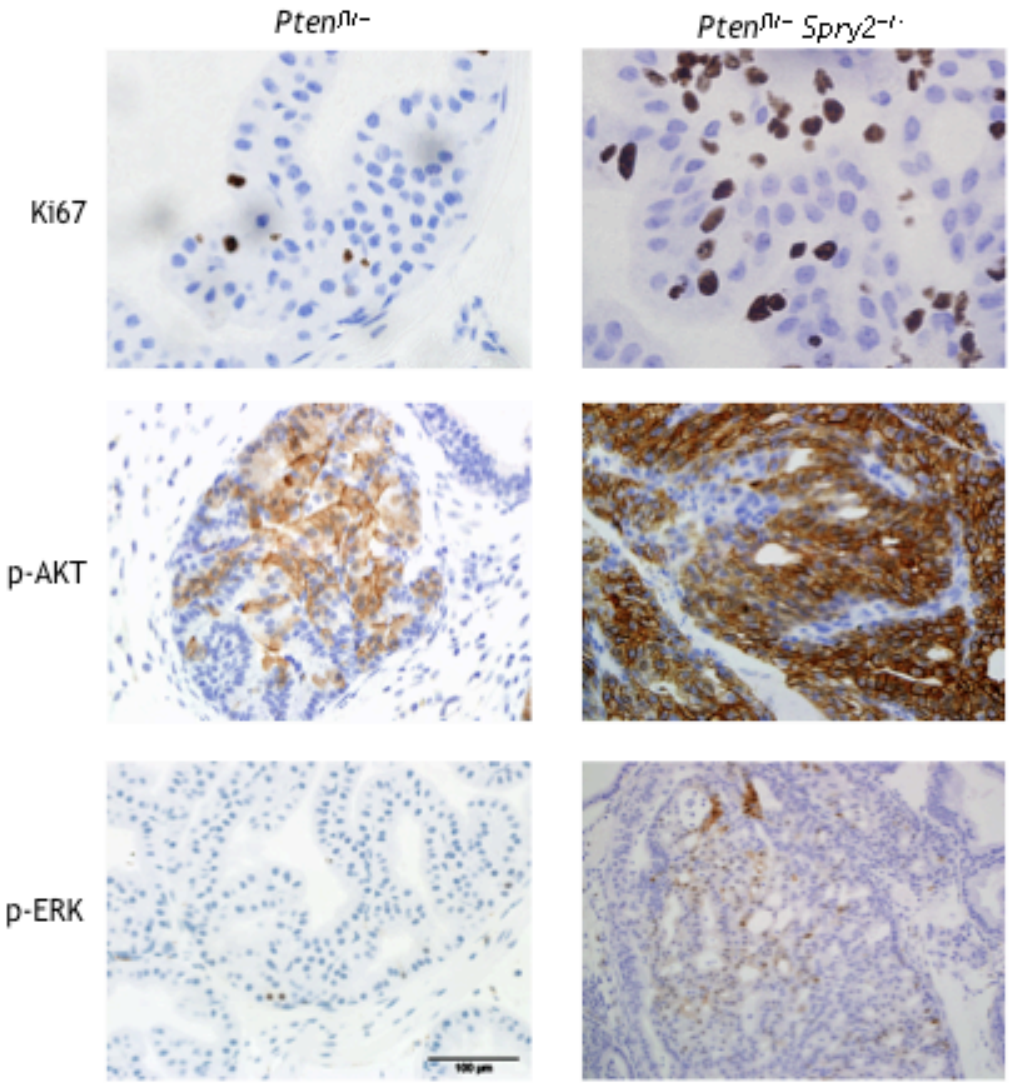

Figure 3.3.2 Nkx Pten$^{fl/+}$Spry2$^{+/-}$mouse model develop invasive prostate cancer
Prostate tissue was fixed and stained with ki67, p-AKT and p-ERk1/2. The tissue section from Pten$^{fl/-}$ Spry2$^{-/-}$ mouse showed higher number of ki67 positive nucleus and p-AKT staining, but pERK1/2 activation is moderate compare to Pten$^{fl/-}$ prostate tissue (n=3 each genotype).

3.4 Summary and discussion

SPRY2 was reported to be downregulated in several cancer types including PC. The function of SPRY2 was examined using human prostate cancer. The results suggested SPRY2 acts as a negative regulator, and reduced SPRY2 expression enhanced cell proliferation and invasiveness in response to EGF stimulation. These observations require the presence of PTEN, which is consistent with Edwin's report proposing PTEN's essential role for inhibitory effect of SPRY2 (Edwin et al., 2006). Human phospho-kinase array analysis revealed that loss of SPRY2 activates PI3K/AKT signalling cascades, which may be responsible for the aggressive phenotype observed in SPRY2 KD cells. Mutual exclusivity test using cBio Cancer Genomic Portal showed the odd ratio was 7.58 ($p=0.002095$), which is indicating a strong tendency toward co-occurrence. The murine model was used to examine whether PTEN and SPRY2 loss cooperate in prostate carcinogenesis. Nkx $Pten^{fl/+}$ $Spry2^{+/-}$ mouse model indeed progressed to an aggressive PC with lymph node metastasis by 10-12 months of age. The prostate tumours exhibited hyperactivation of p-AKT rather than MAPK activation. It is interesting that unlike lung cancer, there is very rare mutation/amplication of Ras/Raf in PC, which are often attributed to the abnormal activation of MAPK signalling. Concomitant low levels of two tumour suppressors SPRY2 and PTEN favour the activation of PI3K/AKT signalling cascades, which override normal checkpoints to result in tumour formation. Collectively, these results allow us to investigate PI3K/AKT as a potential target, and the mechanism of SPRY2 and PTEN cooperation in RTK needs to be elucidated.

Chapter 4. Modulation of EGFR and ErbB2 trafficking and signalling following SPRY2 KD

4 Modulation of EGFR and ErbB2 trafficking and signalling following SPRY2 KD

Prostate organogenesis and tumorigenesis are both critically dependent on androgen receptor (AR) signalling (Potente et al., 2007). Androgen depletion therapy is often used but will eventually result in progression to castrate resistant disease. Recent studies proposed that abnormal activity of receptor tyrosine kinases (RTK), particularly deregulated EGFR signalling is attributed to the acquisition of an androgen independent state in prostate cancer (Traish and Morgentaler, 2009). Despite an important role for the EGFR system, targeted therapies against the EGFR system in prostate cancer have been disappointing (Trotman et al., 2003a). Such discrepancies may be explained by complex regulatory mechanisms for the EGFR system and its downstream signalling cascade.

EGFR is a member of the ErbB family, which also consists of HER-2, 3 and 4. Epidermal growth factor (EGF) binding at cell surface induces receptor dimerization, activation of its tyrosine kinase domain and subsequent downstream signalling events, including both phosphatidylinositol 3-kinase (PI3K)/AKT and Ras/Raf/MEK pathways, which are pivotal in controlling proliferation and survival (Baluk et al., 2007, Dejana et al., 2007a). Concurrently, upon EGF binding, the receptor-ligand complexes internalise into endosomal compartments. Previously, the primary role of endocytosis was thought to terminate activation of RTKs. The attenuation of the receptors by endosomal degradation was even proposed to have a tumour suppressor role (Zhang et al., 1997, Kim et al., 2002a). However, several studies revealed that RTKs continuously recruit signalling molecules at the intracellular compartments, maintaining and amplifying its signalling outcome. EGFR signalling forms a complex signalling network with positive and negative regulators. SPRY protein was first described by Hacohen and colleagues (Hacohen et al., 1998), as an antagonist of fibroblast growth factor (FGF) signalling in *Drosophila*. Sprouty (SPRY) proteins are commonly deregulated in human cancers including melanoma and colon cancer (Weber et al., 2007, Woodfin et al., 2007). More recently, clathrin-mediated endocytosis upon EGFR

activation appeared to be particularly important for the activation of AKT and MAPK (Kim et al., 2002b). Zwang and Yarden (Zwang and Yarden, 2006) also proposed that the fate of EGFR was determined by the status of the stress kinase p38 MAPK, the activation of which allowed tumour cells to evade chemotherapeutic agents.

4.1 Loss of SPRY2 alters EGFR localisation and internalisation

Upon ligand binding, EGFR is involved in a series of trafficking events, which ultimately regulate its signal amplification and propagation. To determine how SPRY2 KD promotes EGF driven growth and invasion described in Chapter 3, we investigated the intracellular distribution of EGFR using fluorescence microscopy. Both Nsi control and SPRY2 KD DU145 cells were transiently transfected with GFP-tagged EEA1 plasmid transiently, which labels the endosomal compartment within the cells. In unstimulated cells, EGFR was predominantly localised to the cell surface. Following EGF stimulation, EGFR began to co-localise with EEA1 positive early endosomes in both Nsi control and SPRY2 KD cells at 20 and 30 minutes. Importantly, at 30 minutes following stimulation with EGF, SPRY2 KD DU145 cells showed enhanced and sustained localisation of EGFR at the early endosomes compared to the Nsi control cells (Figure 4.1.1).

To characterise the molecular basis of EGFR trafficking to the early endosomes, the internalisation kinetics of EGFR in SPRY2 KD DU145 cells was studied. Cell surface proteins were labelled with NHS-S-S-biotin, and then stimulation with EGF allows various surface protein to endocytose including EGFR at the indicated time. In order to capture internalised and biotin labelled EGFR, surface biotin was reduced with cell impermeable reducing agent. IP was carried out with EGFR antibody linked dynabeads after reducing surface biotin. This allowed us to pull down EGFR labelled with biotin at surface and trafficked into the endosomal compartments. As a control, surface biotin was not removed from the sample at 0 minutes. For subsequent time points only biotin-labelled EGFR (internalised EGFR) were detected with HRP-avidin among pulled down mixture of labelled and unlabelled EGFR pool. Western blot analysis showed similar total EGFR level in Nsi and SPRY2 KD cells. However, increased level of

intracellular EGFR in SPRY2 KD DU145 cells following EGF treatment for 15, 30 and 60 minutes in the presence of primaquine (a receptor recycling inhibitor). Increased internalisation and accumulation of EGFR in SPRY2 KD cells was also studied using the NHS-S-S-biotin internalisation assay in an ELISA format. 96-well plates were coated with EGFR antibody and incubated with whole cell lysates, which were collected after internalisation assay. There was significantly more (20%) intracellular EGFR detected in SPRY2 KD cells compared with Nsi control cells at 30 minutes of EGF stimulation (Figure 4.1.2).

EGFR trafficking employs mainly clathrin-dependent endocytic machinery, which recruits receptor clusters into clathrin-coated pits and the membrane invaginations followed by vesicle scission forming cargo-containing receptors. GTPase dynamins are involved in constriction and fissions of vesicle stalks, cooperating with Rab family proteins (Mosesson et al., 2008, Zerial and McBride, 2001). In order to assess if the discrepancy in AKT hyperactivation is due to EGFR trafficking, we used dynasore, a cell permeable inhibitor of dynamin to inhibit clathrin-mediated endocytosis. Indeed, dynasore inhibited EGFR endocytosis in both control and SPRY2 KD cells. Significantly, EGF induced activation of p-AKT in SPRY2 KD cells was abolished, confirming the importance of endosomal EGFR in promoting PI3K/AKT signalling (Figure 4.1.3). Altogether, loss of SPRY2 promotes rapid internalisation and sustained accumulation of intracellular EGFR in response to EGF stimulation to enhance AKT activation in SPRY2 KD cells.

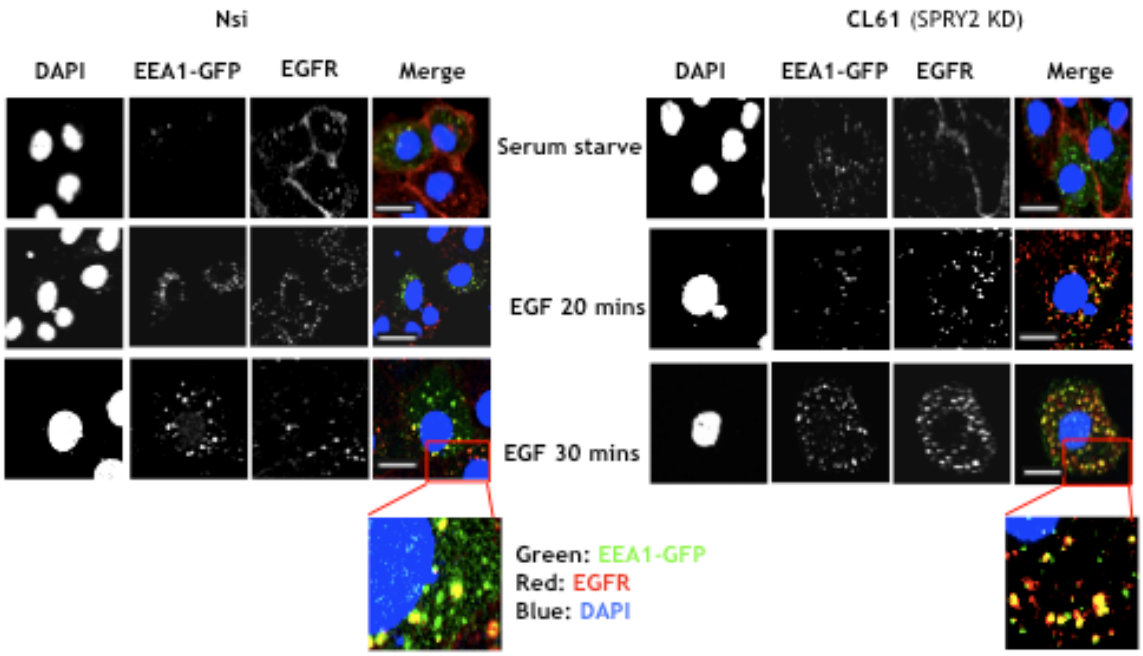

Figure 4.1.1 SPRY2 KD and its effect on the EGFR distribution

Representative confocal images of Du145 Nsi control and SPRY2 KD cells were transfected with EEA1-GFP (green). EGFR (red) and nuclei (DAPI) were detected. Cells were serum starved over night and stimulated with EGF (20ng/ml) for 15 minutes (Scale bar=10 μm). This was representative of 3 independent experiments.

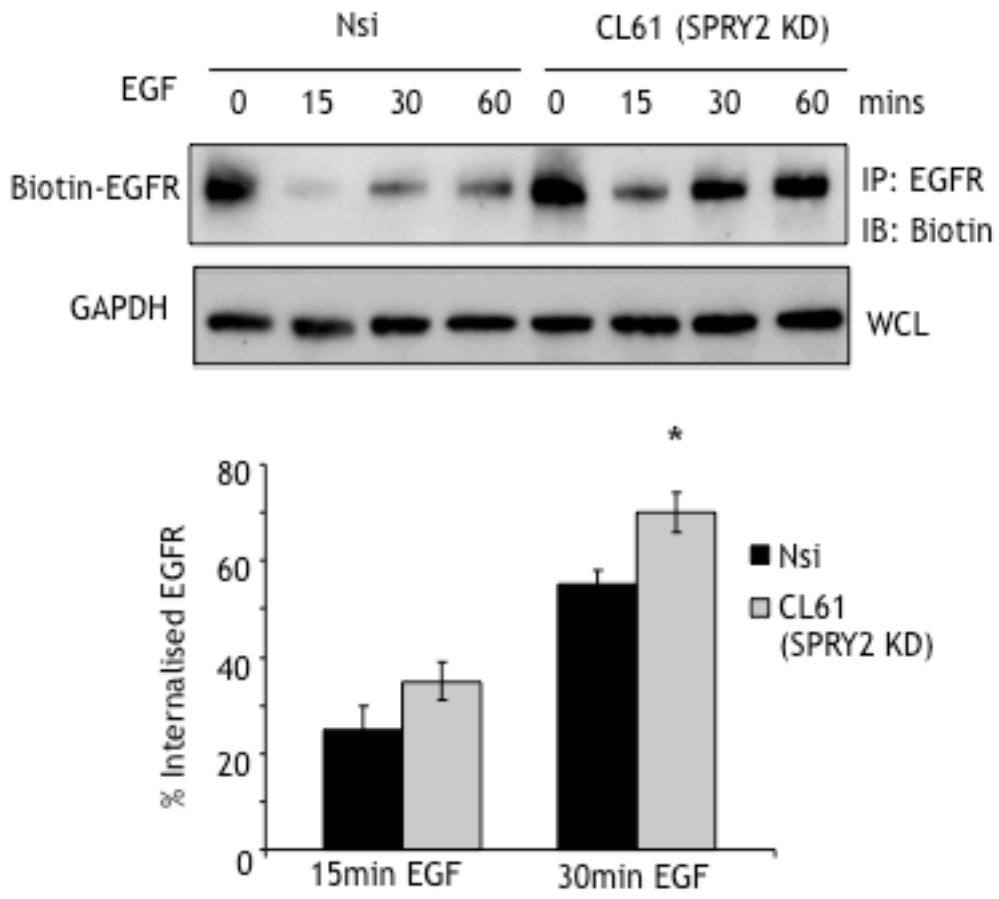

Figure 4.1.2 Loss of SPRY2 promoted internalisation of EGFR

SPRY2 KD and Nsi control DU145 cells were coated with NHS-S-S-biotin, stimulated with EGF to allow EGFR internalisation followed by reduction of surface biotin. Immunoprecipitation for EGFR was performed and internalised biotin-EGFR molecules were detected using HRP-avidin. Data at time 0 min (control) was obtained without surface biotin reduction. Internalised EGFR in SPRY2 KD and Nsi control DU145 cells were quantified in ELISA plates coated with EGFR antibody (*$P<0.01$, n=3).

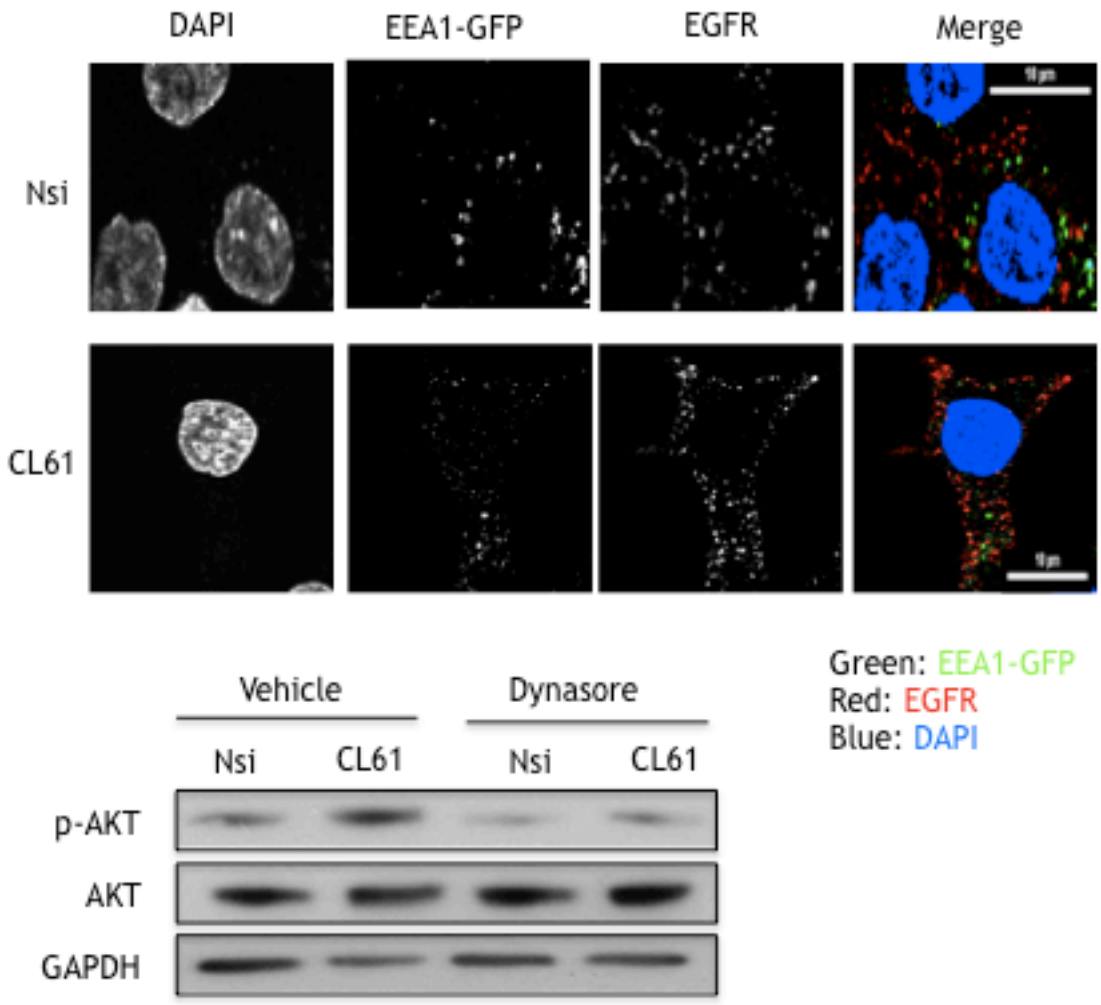

Figure 4.1.3 Rapid internalised EGFR leads to hyperactivation of PI3K/AKT

Cells were treated with dynasore (5 μm) in the presence of EGF. Representative confocal image of Nsi and SPRY2 KD Du145 cells expressing EEA1-GFP (green), and EGFR (red) visualised, and nuclei stained with DAPI (blue) (Scale bar=10 μm). Whole cell lysates were collected and analysed by Western blots, and GAPDH was used as a loading control.

4.2 SPRY2 KD increases EGFR endocytosis via p38 in a PI3K dependent manner

P38 is a key regulator of EGFR and implicated in phosphorylation of EGFR at Ser-1046/1047, which is closely linked to internalisation of the receptor (Nishimura et al., 2009). Furthermore, Zwang and Yarden proposed that chronic activation of p38 facilitates accumulation of EGFR in the endosomal compartments and aids tumour cell survival (Zwang and Yarden, 2006). We also observed an elevated phospho-p38 level in SPRY2 KD cells in the Human Phospho-kinase array in Figure 3.2.1. This was further confirmed by the Western blot analysis in SPRY2 KD DU145 cells. Phosphorylation of EGFR and p38 were increased at both 15 and 30 minutes following stimulation with EGF in SPRY2 KD cells (Figure 4.2.1). In order to examine the role of p38 in terms of EGFR signalling and its downstream signalling in SPRY2 KD cells, cells were treated with p38 inhibitor SB203580, which is a pyridinyl imidazole derivative. The fluorine in the SB203580 compound interacts with ATP binding pocket in p38 MAPK, which inhibits AKT binding (Gum et al., 1998).

First of all, the inhibitory efficacy of SB203580 was examined, Western blot showed a decrease in phosphorylation of ATF2 in both control Nsi and SPRY2 KD cells in the presence of the inhibitor. Transcription factor ATF2 is a direct downstream target of p38. Next, we observed a reduction in phosphorylation levels of EGFR and AKT when treated with the inhibitor in both Nsi and SPRY2 KD cells (Figure 4.2.2). Treatment with SB203580 decreased cell growth by over 30% (from 40% to <10%, or 4 fold reduction), compared with vehicle control sample in SPRY2 KD cells. The Nsi control cells also showed a reduction in proliferation with a fall of just over 10% (or 2 fold) in growth rate following inhibitor treatment (Figure 4.2.3). Furthermore, cells were also transfected with p38 siRNA and Western blot analysis showed lower p38 expression level in both Nsi and SPRY2 KD cells compared to the negative control lanes. The growth rates were reduced to similar level seen with the p38 inhibitor treatment samples (Figure 4.2.4).

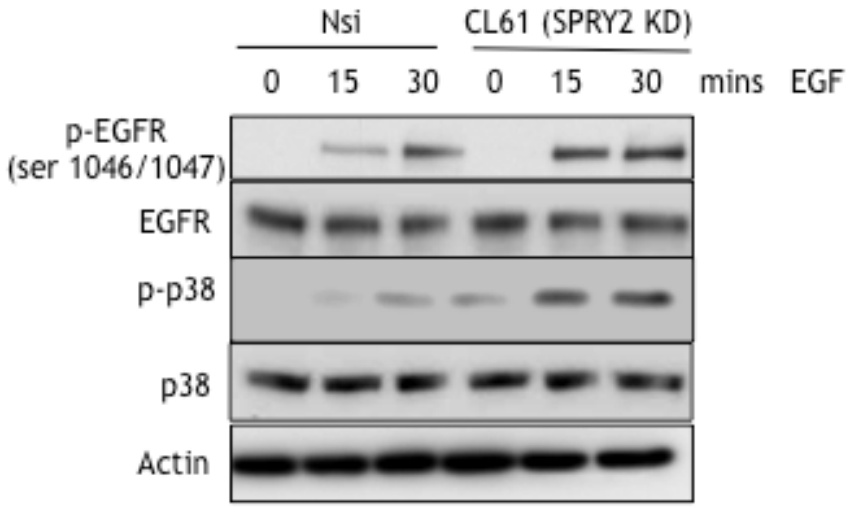

Figure 4.2.1 Loss of SPRY2 enhances the activation of p38 in presence of EGF
Cells were serum starved overnight and stimulated with EGF (20 ng/ml), and whole cell lysates were collected and analysed with western blots. Actin was used as a loading control.

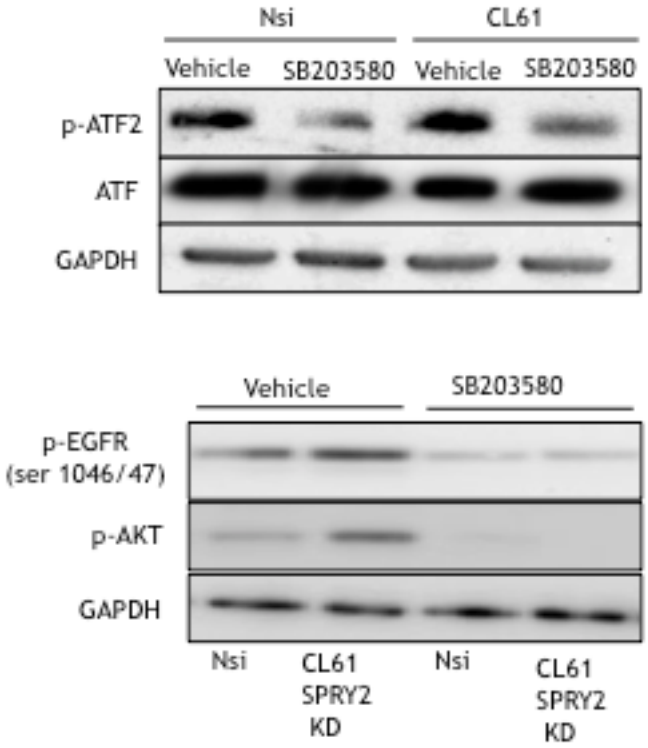

Figure 4.2.2 Inhibition of p38 affects EGFR and its downstream signaling
Cell were pretreated with SB203580 (10 μM) and stimulated with EGF. The whole cell lysates were collected and analysed with western blots, GAPDH was used as a loading control, and DMSO is used as a vehicle control.

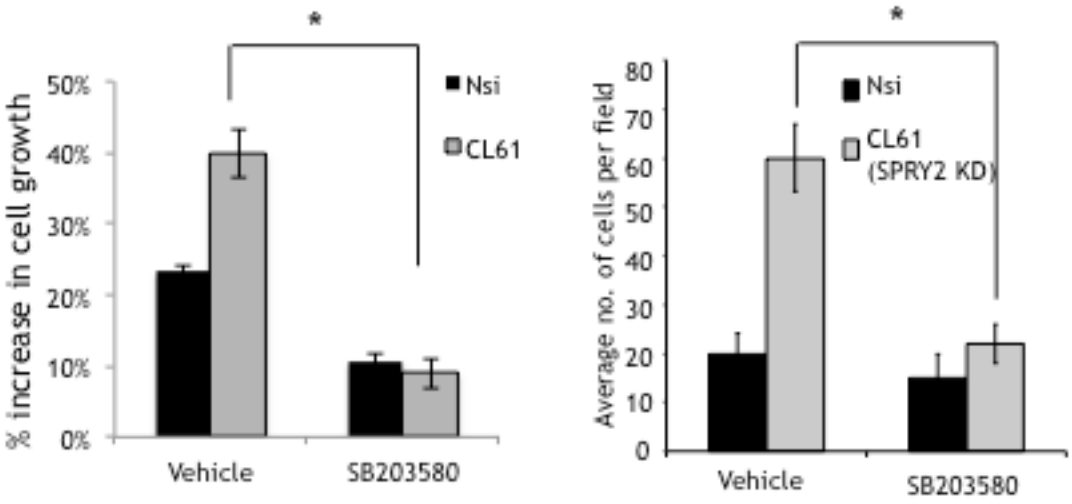

Figure 4.2.3 Inhibition of p38 affects cell growth and invasiveness

Cells were treated with SB203580 (10 μM) and cell proliferation and invasiveness examined and quantified with WST-1 assay and average no of cells per field respectively. DMSO was used in vehicle control samples (*$p<0.01$, $n=3$).

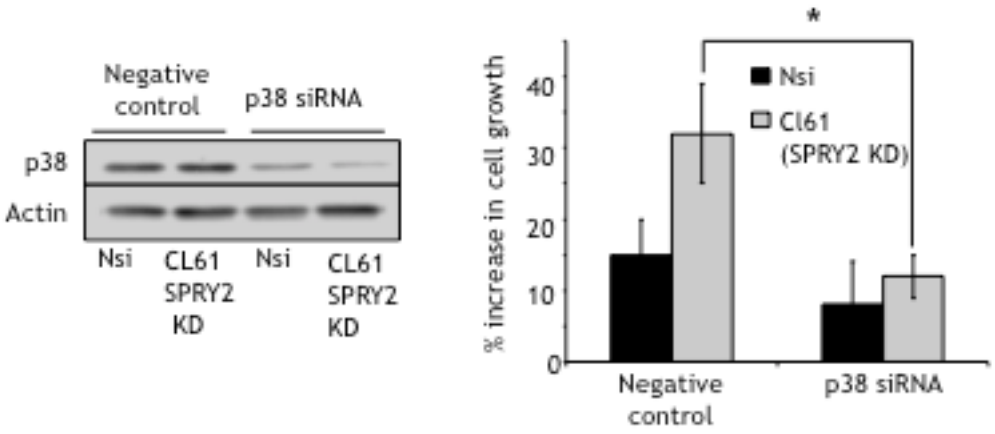

Figure 4.2.4 Loss of p38 inhibits cell proliferation

Cells were transfected with p38 siRNA and anyalysed by Western blotting, and actin was used as a loading control. The effect of p38 siRNA in proliferation was examined using WST-1 assay (*$p<0.01$, $n=3$).

In order to examine the effect of SB203580 in EGFR internalisation, cells were pre-treated with p38 inhibitor and internalisation assay was performed using ELISA assay. The effect of inhibition on EGFR internalisation was observed from 15 minutes in SPRY2 KD cells, but EGFR internalisation was not affected in Nsi control cells at both time points (Figure 4.2.5). It is reasonable that as there was not much active p-p38 detected in the western blot analysis, we may expect that p38 inhibition would not affect the amount of internalised EGFR in Nsi control cells. However, at 30 minutes EGF treatment, there were a 20% reduction of EGFR internalised in SB203580 treated SPRY2 KD cells compared to the vehicle treated cells. In addition, the localisation of EGFR was visualised in cells treated with the p38 inhibitor using confocal microscopy. We transfected cells with EEA1-GFP plasmid to label early endosomes, and cells were treated with vehicle or p38 inhibitors prior to IF analysis. Similarly, there was a notable reduction in endosomal EGFR in inhibitor treated SPRY2 KD cells compared to vehicle treated cells (Figure 4.2.6). These results indicated that cooperation between activated p38 MAPK and loss of SPRY2 in EGFR signalling cascades play a critical role in the trafficking of the receptor and consequently led to uncontrolled PI3K/AKT activation. To understand the crosstalk between PI3K and p38 MAPK, we used PI3K/AKT inhibitor, LY294002, to examine the phosphorylation of EGFR and p38. The PI3K inhibitor abolished both EGFR and p38 phosphorylation in Nsi and SPRY2 KD cells (Figure 4.2.7). Furthermore, loss of SPRY2 in PTEN null PC3 cells results in rapid degradation of EGFR and subsequently no difference in PI3K/AKT activation observed between SPRY2 KD and Nsi control cells (Figure 4.2.8). We concluded that upon ligand binding to EGFR, this leads to enhanced activation of PI3K/AKT in SPRY2 KD cells, which in turn phosphorylates p38 MAPK. Consequently EGFR phosphorylated at serine and threonine sites enhances internalisation and continuous signalling in a positive feedback loop in a PTEN dependent manner.

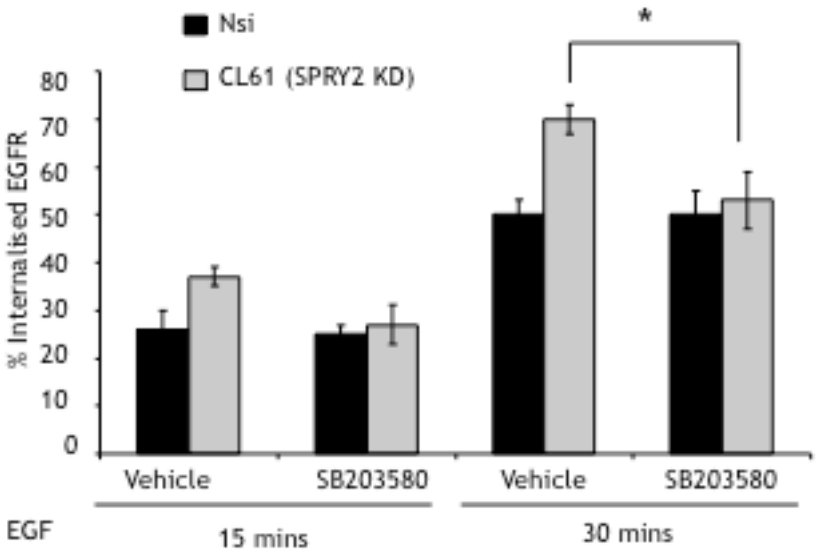

Figure 4.2.5 Inhibition of p38 reduces EGFR internalisation

Cells were pretreated with SB203580 (10 μM) and internalisation assay was carried out as described before. ELISA format was used to detect internalised EGFR using EGFR antibody coated 96-well plates (*$p<0.01$, $n=3$).

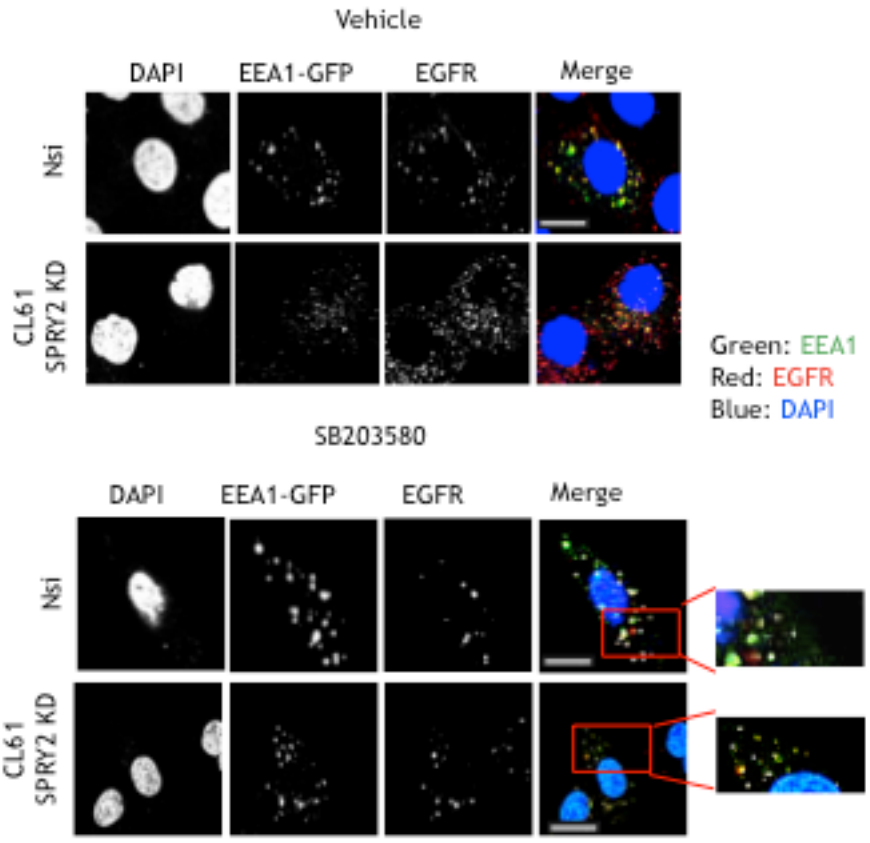

Figure 4.2.6 Inhibition of p38 reduces EGFR internalisation

Representative confocal image of cells were treated with SB203580 (10 μM) and stimulated with EGF. Cells were transfected with EEA1-GFP (green) plasmid, EGFR (red) were detected using IF and nuclei stained with DAPI shown in blue (Scale bar=10 μm).

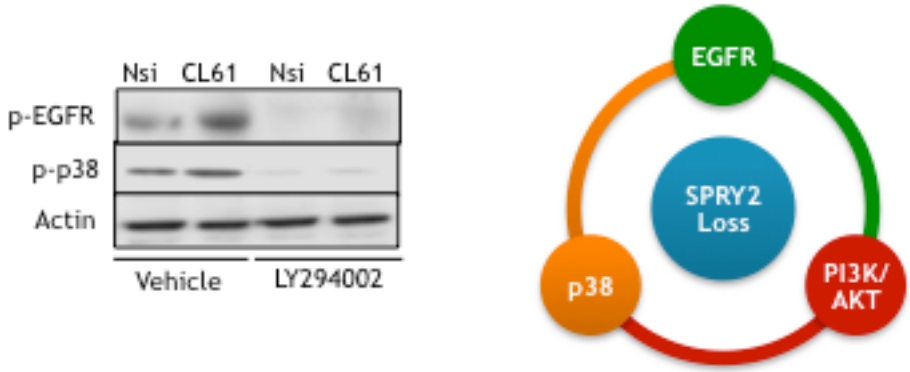

Figure 4.2.7 EGFR, PI3K/AKT and p38 form a positive feedback loop

Cells were treated with LY294002 (10 μM) and the whole cell lysates were collected for western blot analysis. The schematic diagram shows activation of EGFR and downstream PI3K/AKT leads to phosphorylation of p38, which facilitates EGFR internalisation and its signalling amplification and propagation in SPRY2 KD background representing a positive feedback loop.

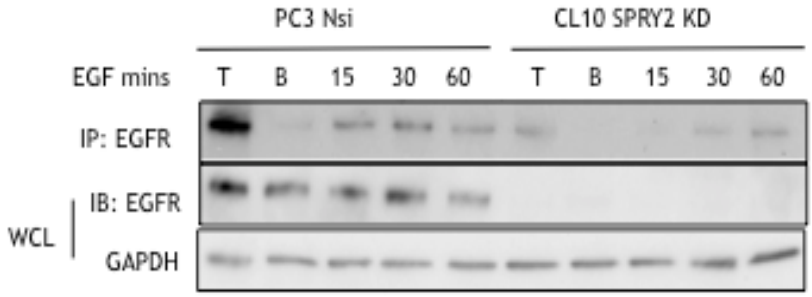

Figure 4.2.8 The positive feedback loop operates in a PTEN-dependent manner

PC3 cells were used to perform internalisation assay and IP as described in Figure 5. The whole cell lysates were collected and immunoblotted EGFR and GAPDH.

4.3 EGFR cooperates HER2 trafficking but not HER3

Abnormal EGFR trafficking and its downstream signalling in SPRY2 KD cells indicated the potential use of EGFR tyrosine kinase inhibitors, such as gefitinib (also known as Iressa). Surprisingly, SPRY2 KD cells showed significant survival advantage over Nsi control cells upon treatment with gefitinib. Hetero-dimer formed by EGFR and other HER family members including HER2 and HER3 may confer a selective growth advantage and can lead to resistance to selective tyrosine kinase inhibitor such as gefitinib (Tomlins et al., 2005). We investigated the involvement of HER2 in EGF stimulated cells. Interestingly, SPRY2 KD cells respond to EGF treatment with enhanced and sustained phospho-HER2 levels (Figure 4.3.1). Hence, lapatinib, a dual inhibitor of both EGFR and HER2, was examined to assess the ability to inhibit SPRY2 KD cell growth more efficiently than gefitinib. Indeed the anti-mitotic effects of lapatinib were very comparable in both control and SPRY2 KD cells. There is over 30% reduction compared to vehicle treated cells, and more than 25% reduction of cell proliferation was observed compared to gefitinib treated cells. Furthermore, heregulin activated both HER3 and HER2 in DU145 cells, but only HER2 activation and cooperation were observed in the presence of EGF not HER3. There were similar levels of AKT phosphorylation in both Nsi and SPRY2 KD cells when stimulated with heregulin. Whereas EGF stimulates more AKT in SPRY2 KD cells, which may be attributed to the trafficking mediated by EGFR and HER2 activation (Figure 4.3.2). This suggests in spite of functional HER3 in DU145 cells, only EGFR and HER2 heterodimers contributed to the enhanced cell growth in the presence of EGF in SPRY2 KD cells.

There are multiple pieces of evidence to suggest a critical role for EGFR and HER2 in PC cell proliferation and invasion, especially castration-resistant disease (Zhan et al., 2006, Mellinghoff et al., 2004). In order to assess the kinetics of HER2 trafficking in EGF stimulated cells, the internalisation assay and Neutravidin immunoprecipitation (IP) were performed to pull down internalised proteins with NHS-S-S-biotin label. The biotinylated proteins were pulled down with NeutrAvidin agarose. The neutravidin beads IP internalised proteins, which were labelled at the cell surface with biotin in the beginning of the experiment. The IP results show clear increase of HER2 accumulation in SPRY2 KD cells

following EGF treatment at 60 minutes. Whereas, there were surface HER3 labelled with the biotin, but no endosomal HER3 detected in Nsi and SPRY2 KD cells (Figure 4.3.3). This supports the observation that HER3 was not significantly activated upon EGF stimulation.

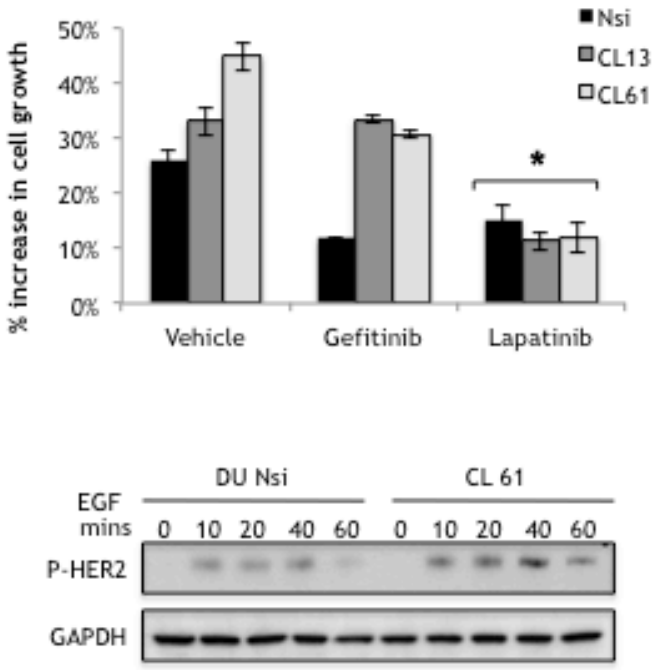

Figure 4.3.1 HER2 cooperates with EGFR to enhance tumorigenesis in SPRY2 KD cells

Du145 Nsi control and SPRY2 KD Cells were incubated with gefitinib (15 μM) and lapatinib (10 μM) , and assessed cell growth assessed using WST-1 assay (*$p<0.01$, n=3). For the western blot analysis, cells were serum starved overnight and stimulated with EGF for the different duration as indicated, whole cell lysates were collected and blotted, and GAPDH is used as a loading control.

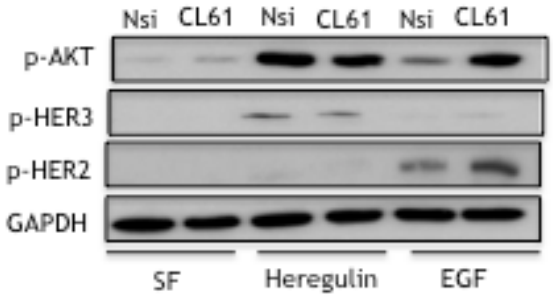

Figure 4.3.2 HER2 cooperates with EGFR signalling in SPRY2 KD cells not HER3

Du145 Nsi control and SPRY2 KD cells were serum starved overnight, and stimulated with heregulin or EGF for 15 minutes. Whole cell lysates were collected and analysed with western blots.

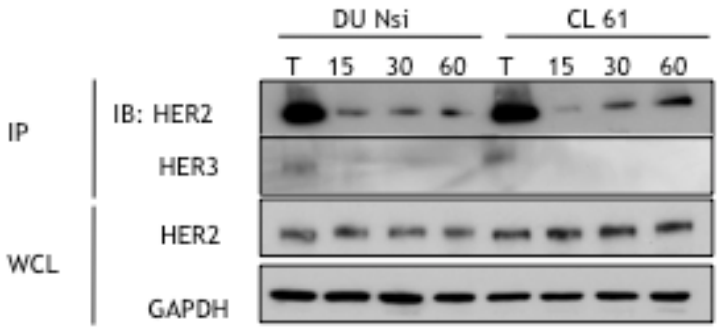

Figure 4.3.3 HER2 trafficking with EGFR in SPRY2 KD cells not HER3

Cells were labelled with the biotin, and internalisation assay was performed as described previously. RTKs were allowed to internalise for the indicated time as shown above, and Neutravidin beads were used to pull down endosomal proteins labelled with the biotin. Proteins were eluted and analysed with western blot. Whole cell lysates prior to IP were collected and detected the total HER2 expression, and GAPDH was used as a loading control.

SPRY2 expression was characterised in two independent PC cohorts in the format of tissue microarray (TMA). The TMA included 202 cases of PC and 107 cases of benign prostatic hyperplasia (BPH) as controls. Patients with reduced SPRY2 expression were stratified according to the HER paralogue expression status: those patients with HER2 positive disease have significantly poorer survival outcomes compared with those with HER2 negative disease (Log rank: p=0.014) (Figure 4.3.4). The IHC staining of human prostate tissue showed membrane and cytoplasmic HER2 immunoreactivity. None of the other members of the ErbB receptors including HER3 and HER4 showed any association with patient outcome. Since the interaction between RTK trafficking and SPRY2 loss occurs in a PTEN dependent manner, we segregated TMA into two groups, moderate and low PTEN expression. Moderate indicates PTEN expression was below median of BPH but above median of the cancer population. Low expression was relatively less PTEN expression than median score in cancer samples, which meant it included a histoscore of zero. The correlation analysis indicated a significant positive association between cytoplasmic HER2 and p-AKT among patients with moderate PTEN expression level, but p-ERK1/2 correlation is not significant (n=110), emphasising the importance of p-AKT in prostate carcinogenesis. Moreover, SPRY2 negatively correlated with both cytoplasmic and membrane HER2 and p-AKT, the association between SPRY2 and p-ERK1/2 was not significant. Interestingly, the association between SPRY2 and p-AKT was lost in the low PTEN expressing PC (p=0.589, n=110) (Table 4.1). These TMA data suggests the in vitro hypothesis that loss of SPRY2 leads to hyperactivation of PI3K/AKT via RTK trafficking in a PTEN dependent manner and promotes PC development.

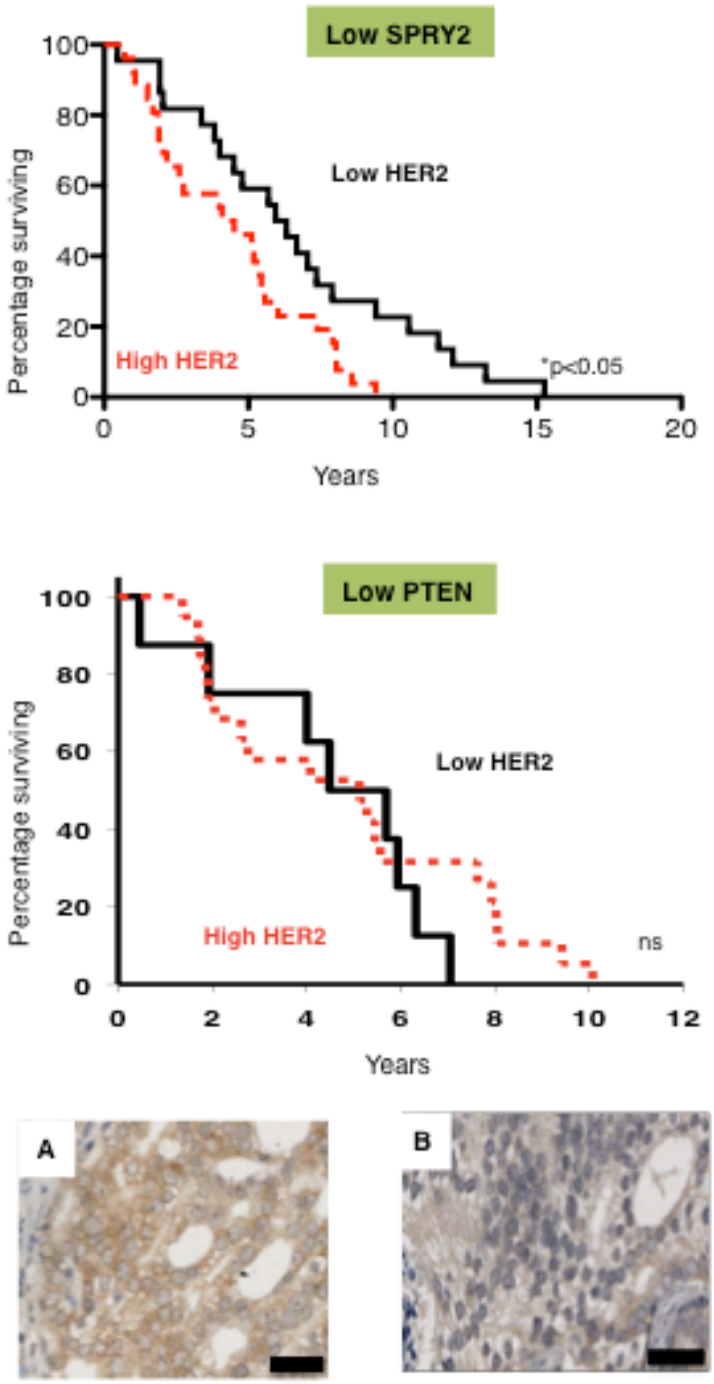

Figure 4.3.4 SPRY2 and HER2 affect survival outcomes in patients

Human TMA2 was stained with SPRY2 and HER2, the samples were segregated according to HER2 expression level in patients with low SPRY2 or reduced PTEN expression. Kaplan-Meier curves of disease free survival was plotted. Representative IHC images show the cytoplasmic staining of high HER2 (A) and low HER2 (B) expression in patient TMA samples.

Pearson's Correlation	HER2(c)	p-AKT	p-ERK
SPRY2	-0.196 p<0.05	-0.410 p<0.0001	0.187 p=0.0674 (ns)
HER2(c)	-	0.281 p<0.01	-0.0997 p=0.344 (ns)

Table 4.1 Correlation analysis in human TMA

Pearson's correlation was performed with TMA samples with moderate PTEN expression level (n=110), HER2(c) indicates cytoplasmic HER2.

4.4 Summary and discussion

The binding of ligands to EGFR leads to homo- and hetero-dimerization with members of the HER kinase family (Voeller et al., 1997). Interestingly, we observed the involvement of HER2, but not HER3, in the flow of EGFR trafficking; further contributing to enhanced RTK mediated intracellular signalling. P38-mediated phosphorylation of EGFR can then evade receptor degradation to produce sustained and enhanced signalling at the endosomes. Consistent with our findings, Zwang and Yarden (Zwang and Yarden, 2006) also postulated that chronic stress induced p38 activation either intrinsically in *in vivo* growth or associated with treatment such as cytotoxic dugs can enhance EGFR localisation to the endosomes with a pro-survival effect. In our PC TMA cohorts, reduced SPRY2 and upregulated p-AKT was significantly associated, but not with ERK activation, suggesting specific oncogenic choice for the cancer with SPRY2 loss. Interestingly, the PTEN status is crucial for such association, since among the PTEN negative tumours (histoscore zero) showed no correlation between low SPRY2 and activation of AKT. In conclusion, complex interactions among RTKs and their downstream effectors exhibit fine regulation of the signalling networks to involve distinct signalling molecules, which may represent important targets for developing treatment in the context of personalised medicine.

Chapter 5. Low SPRY2 and PTEN as biomarkers for PC responsive to PI3K inhibitor therapy

5 Low SPRY2 and PTEN as biomarkers for PC responsive to PI3K inhibitor therapy

Accumulating genetic evidence and cancer research suggest that the PI3K/AKT signalling cascade is pivotal in cancer initiation and growth. In prostate cancer, the main reason for abnormal activation of PI3K/AKT activation is related to the loss of PTEN including haplosufficiency and biallelic loss. Activation of RTKs also accounts for another important mechanism for the activation of PI3K/AKT in cancer. Briefly, activation of the PI3K/AKT signalling pathway often results from RTK (Roche et al., 1998). PI3K is a heterodimer consisting the p85 regulatory subunit and the p110 catalytic subunit. The regulatory domain directs the translocation of PI3K to the plasma membrane, while the catalytic domain phosphorylates PIP_2 (phosphatidylinositol-4,5-bisphospate) at the plasma membrane, which is part of the membrane compartment, to generate the second messenger molecular PIP_3 (phosphatidylinositol-3,4,5-trisphospate). The production of PIP_3 leads to the activation of PI3K and downstream signalling including PDK1 (phosphoinositide-dependent protein kinase1) and AKT through physical interaction (Engelman, 2009). Several small molecules are developed to inhibit PI3K/AKT signalling including dual PI3K/mTOR inhibitor, PI3K inhibitor, AKT inhibitors and mTOR inhibitors. Unlike breast and lung cancer, the amplification of HER2 and mutation of EGFR are rare in prostate tumours. Yet, the tight spatial and temporal regulators of RTKs including SPRY2 are often deregulated in prostate cancer. Loss of SPRY2 in DU145 cells showed hyperactivation of PI3K/AKT in response to EGF stimulation. In addition, reduction of SPRY2 expression in prostate cancer cells exhibited rapid EGFR trafficking along with HER2, which led to the enhanced downstream signalling cascades including PI3K/AKT. In this study, the effect of a dual inhibitor PI103 was investigated in *Nkx CRE* $Spry2^{+/-}$ $Pten^{fl/+}$ mouse model described in Chapter 3.

5.1 PI3K inhibitor reduced SPRY2 KD cell lines growth and invasiveness

As PI3K plays an important role in cancer biology, much interest has been generated to develop inhibitors as potential therapeutic agents. The understanding of the PI3K crystal structure has led to the design of small molecules including well-known compounds LY294002 and wortmannin. LY294002 has been shown to inhibit PI3K more selectively than other protein kinases including EGFR and protein kinase C (Vlahos et al., 1994). In spite of antitumour effects of LY294002 in *in-vitro* and *in-vivo* models, its toxic side effects and poor solubility prevented the compound from entering clinical trials. As a laboratory cell based reagent, LY294002 is a useful tool to understand the function of PI3K in tumorigenesis. Furthermore, MAPK inhibitor PD098059 is also used to study the function of ERK1/2 in SPRY2 KD cells. The compound can inhibit MEK1 direct upstream of ERK1/2.

Our working model is that loss of SPRY2 interacts with abnormal RTK signalling to drive PI3K/AKT hyper-activation mediated prostate carcinogenesis. Therefore, to test the significance of PI3K/AKT signalling, SPRY2 KD DU145 cells were treated with the PI3K inhibitor LY294002 and studied in proliferation and invasion assays. SPRY2 KD DU145 showed significantly reduced growth and invasion in the presence of LY294002. In contrast, the MAPK inhibitor PD098059 did not have any effects (Figure 5.1.1).

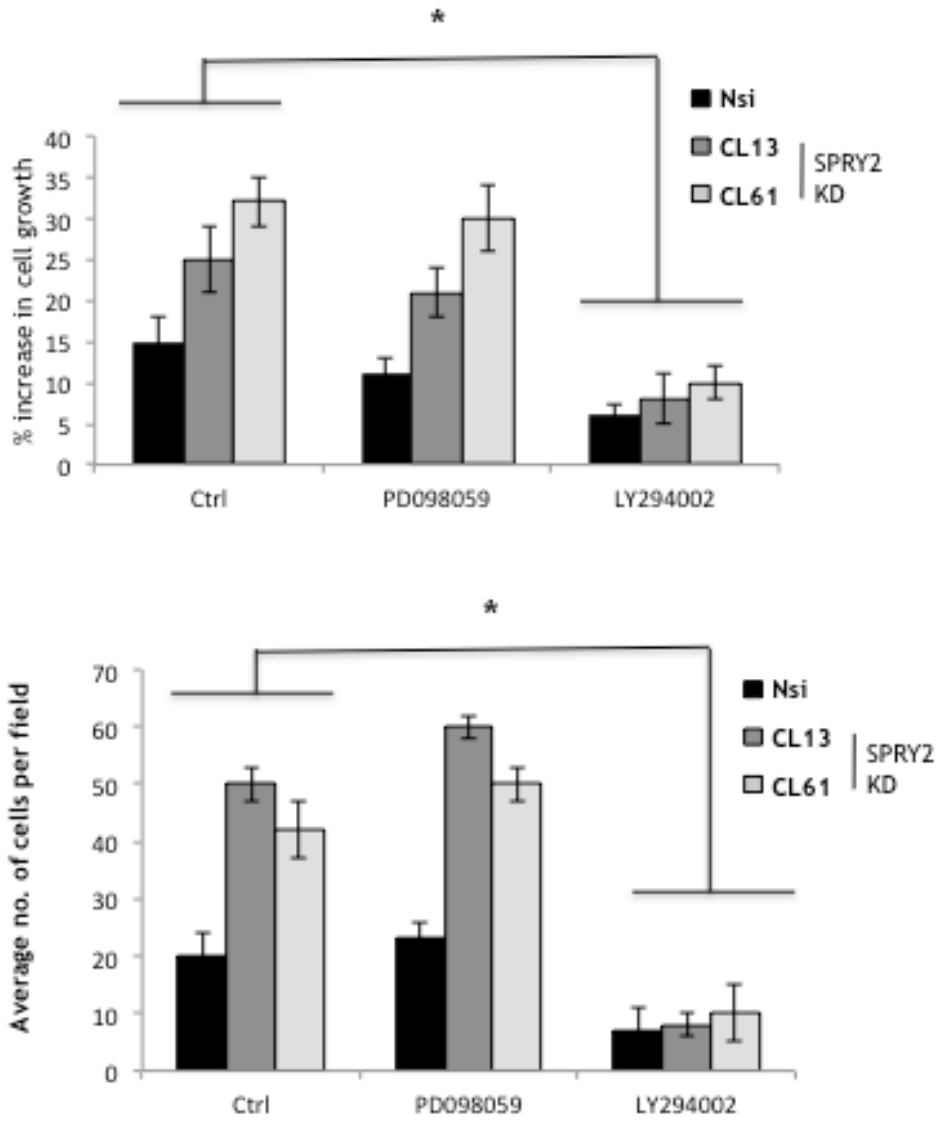

Figure 5.1.1 SPRY2 KD cells respond to PI3K inhibitor but not MAPK inhibition
SPRY2 KD and Nsi control Du145 cells treated with PD098059 (10 µM), LY294004 (10 µM) or DMSO as a vehicle control and analysed for cell proliferation using the WST-1 assay. Invasiveness of SPRY2 KD and Nsi DU145 cells were quantified in the presence of EGF as a chemoattractant after 8 h incubation (*p<0.001, n=3).

5.2 SPRY2 and PTEN mouse model to identify PI3K inhibitor responsive prostate tumours

In the *Nkx CRE Spry2*$^{+/-}$ *Pten*$^{fl/+}$ mouse prostate model, high level of p-AKT, but not phospho-ERK1/2, staining was evident in the prostate of 3 months old animals (Figure 5.2.1). Hence, the *in vivo* significance of SPRY2 loss associated AKT activation was examined using the potent PI3K inhibitor PI103. The compound is a selective class I PI3K inhibitor (IC_{50}=3 nmol/L) and is around 200 fold more potent than LY294002 (IC_{50}= 600 nmol/L). PI103 was also tested for the effect on other tyrosine kinases, a screen against over 70 protein kinases showed little or no inhibitory activity. *In vitro* studies with human cancer cell lines showed inhibitory effects on proliferation of prostate, lung, ovarian and colon cancer cell lines (Carracedo et al., 2011b).

In *Nkx CRE Spry2*$^{+/-}$ *Pten*$^{fl/+}$ mice the prostate tumour was palpated in the mouse model (10-11 months). PI 103 was injected daily 50 mg/kg intra-peritioneal (ip) for 4 weeks, when tumours were apparent. The prostatic epithelium showed significantly fewer Ki67 positive cells (Figure 5.2.2), which is indicative of reduced proliferation. When compared to vehicle control treated mice, using a combination of western blotting and immunohistochemistry (IHC) experiments, p-AKT level was significantly reduced following PI3K inhibition. The H&E staining confirmed the presence of aggressive tumours in the vehicle treated mice (10-12 months). In contrast, PI103 treated animals, the prostate was filled with lymphocytic infiltration and the epithelial cells retained differentiated structure with a glandular architecture (Figure 5.2.3). It is worth noting that, even in the presence of increasing tumour bulk and invasion, these tumours retained their PTEN expression as shown by western blot analysis and IHC staining. PTEN immunoreactivity was observed at high level in lymphocytes (Ly) and at relatively lower level in the epithelial (Ep) cells (Figure 5.2.4), thus excluding the involvement of *de novo* loss of the remaining PTEN allele. Prostatic lesions in these animals following PI 103 treatment were noticeably cystic (Figure 5.2.3) when compared to the solid nature of tumours in control treated animals (n=6). Hence, the lymph node status was used as an endpoint to

test the potential role of PI3K signalling in PC progression. In the cohort of *Spry2*$^{+/-}$ *Pten*$^{fl/+}$ mice studied, 3 of 4 animals treated with vehicle control developed metastatic lymph node lesions with evidence of androgen receptor expression. However, none of the four PI 103 treated animals developed metastatic nodal disease (p=0.025 Figure 5.2.5). Furthermore there was no change observed in phospho-ERK1/2 level in prostates of both treated and untreated animals (Figure 5.2.4). Enhanced apoptosis as illustrated by pyknotic and roughly rounded nuclei on TUNEL assay was also observed in PI 103 treated tumours (Figure 5.2.6). Furthermore, EGFR staining showed cytoplasmic and plasma membrane localisation in the vehicle treated prostate tissue, whereas the PI3K inhibitor treated tissue showed very little or no immunoreactivity of EGFR (Figure 5.2.7). In summary, the potent PI3K inhibitor significantly reduced tumour burden in *Spry2*$^{+/-}$ *Pten*$^{fl/+}$ mice, which suggested enhanced PI3K/AKT signalling plays a key role in PC driven by SPRY2 and PTEN loss.

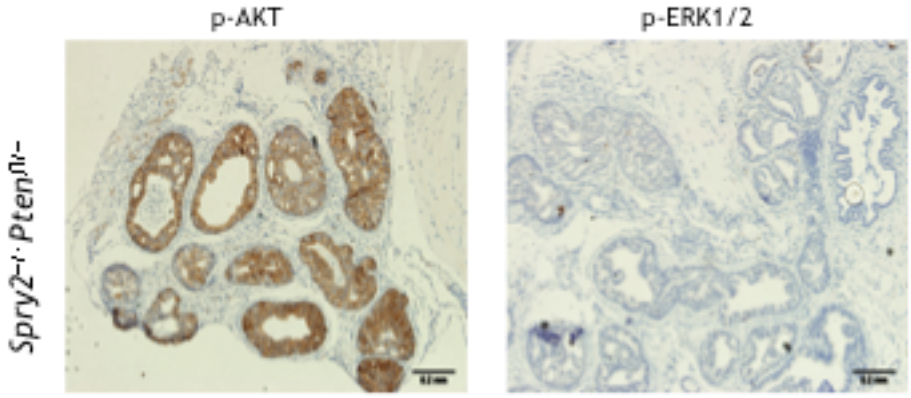

Figure 5.2.1 Activation of PI3K/AKT in *Spry2*$^{+/-}$*Pten*$^{fl/+}$ mouse model
Representative image of IHC staining of p-AKT and p-ERK1/2, the prostate tissue was collected from 3 months old mice (scale bar = 200 μm, n=3 for each genotype).

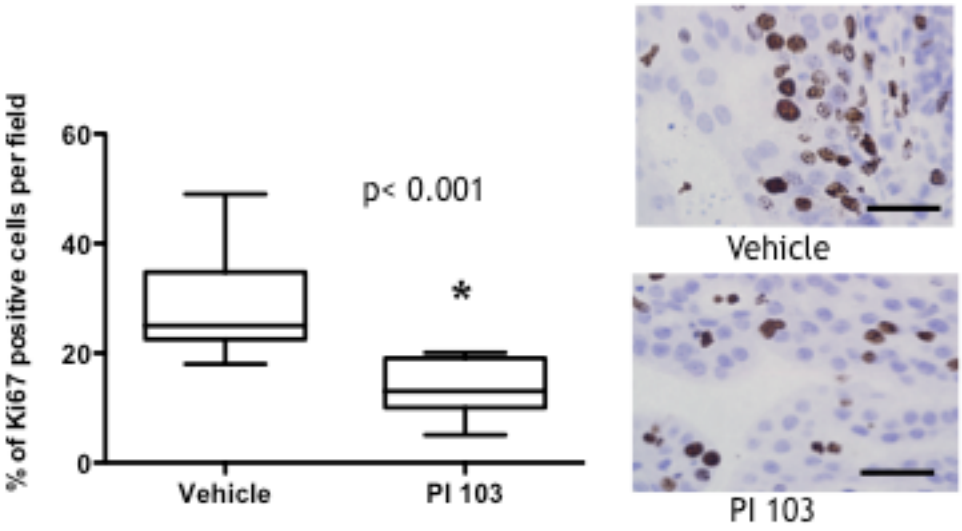

Figure 5.2.2 PI3K inhibitor PI103 inhibits proliferation in vivo

Spry2$^{-/-}$*Pten*$^{+/-}$ mice were treated with PI103 or vehicle for 4 weeks, prostate tissues were collected and fixed. The percentage of ki67 staining positive cells per field was quantified (n=3 for each genotype), and the representative images were shown (scale bar=50μm).

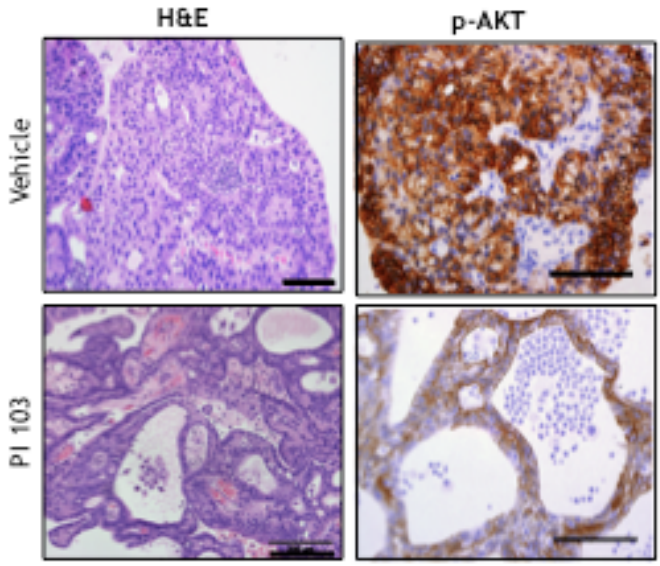

Figure 5.2.3 PI3K reduced prostate tumour burden in *Spry2*$^{+/-}$ *Pten*$^{fl/+}$ mice
Representative tissue sections of H&E and immunostaining of indicated antibodies were shown (Immunostaining scale bar=100 μm, H&E=200 μm, age of animals =12months, n=3 for each genotype).

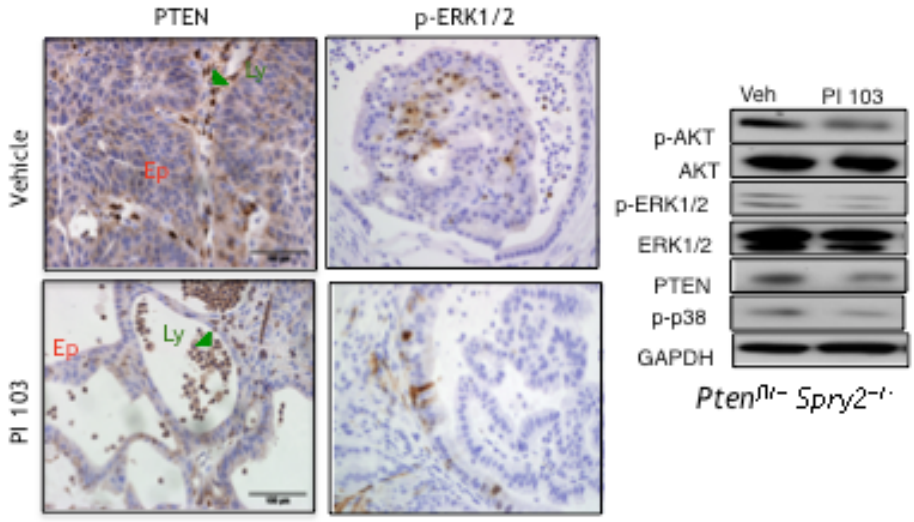

Figure 5.2.4 Prostate tumour from *Spry*$^{+/-}$ *Pten*$^{n/+}$ mice sustains PTEN expression

Representative images of prostate tissue section from animals treated with vehicle or PI103. PTEN staining was stronger in lymphocytes (Ly) than *Spry2*$^{-/-}$ *Pten*$^{n/-}$epithelial cells (Ep) (Scale bar = 100 µm, n=3 for each treatment). Representative images of prostate tissue section with indicated treatment immunostained with p-ERK1/2. Western blots of protein extracts from prostate tissues of *Spry2*$^{-/-}$ *Pten*$^{n/-}$ mice (12 months old) following indicated treatments. GAPDH was used as a loading control.

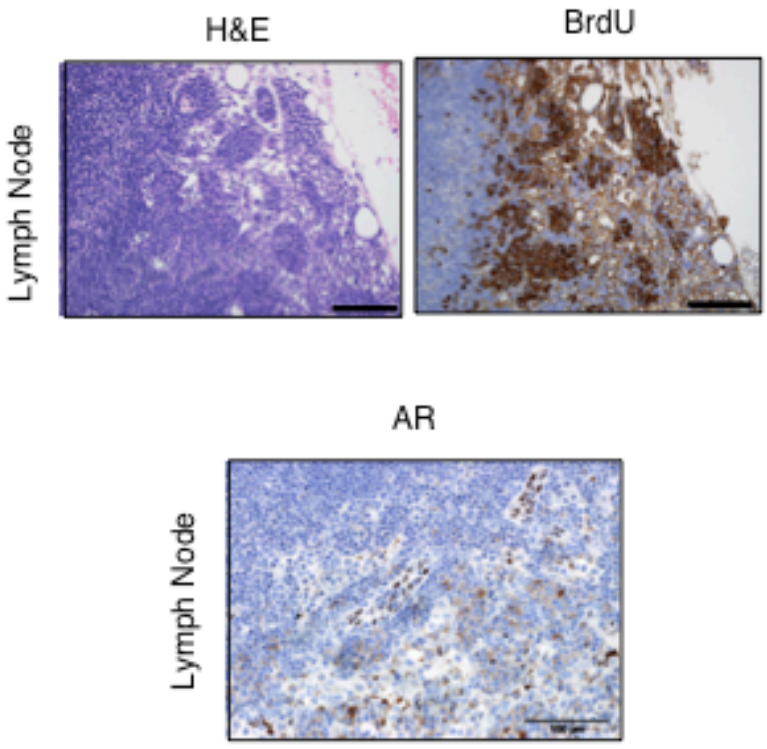

No of Animals with Lymph Node metastatic	Vehicle	PI 103
Spry2$^{+/-}$ *Pten*$^{fl/+}$	3/4	0/4

Figure 5.2.5 *Spry2*$^{+/-}$ *Pten*$^{fl/+}$ mice develop metastatic disease

Representative images of lymph nodes collected from vehicle treated animals. H&E, BrdU and AR staining were performed with fixed lymph nodes (scale bar=200 μm. The number of enlarged lymph nodes were collected and counted.

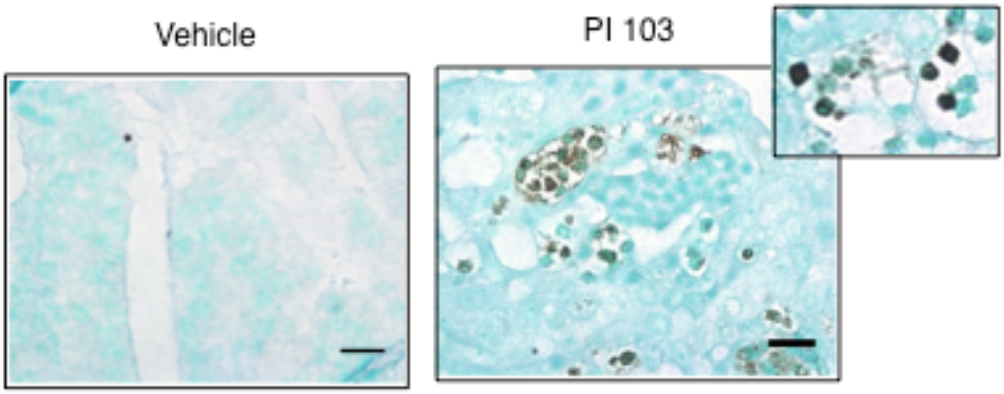

Figure 5.2.6 Apoptotic effect of PI3K inhibitor

Prostate tissue section from control and PI103 treated animals were stained for apoptotic cells using TUNEL assay (scale bar 20 µm, n=6, age=12 months).

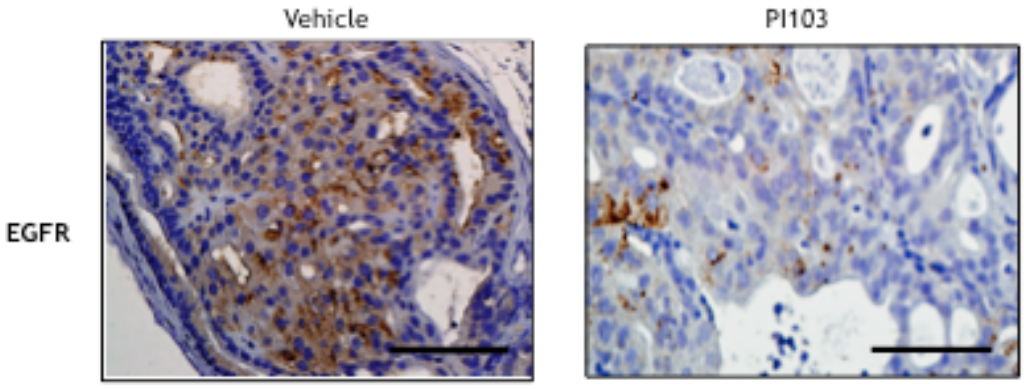

Figure 5.2.7 EGFR localises to cytoplamic and plasma membrane in *Spry2*$^{+/-}$ *Pten*$^{fl/+}$ mice

Representative tissue sections of immunostaining of EGFR shown (Immunostaining scale bar=100 µm, n=6, age=12 months).

5.3 Summary and discussion

Recent evidence suggested combinatory targeted therapies could be more effective. For instance, MAPK and PI3K/AKT are simultaneously and synergistically activated in a $PTEN^{+/-}$ mouse prostate model (Gumerlock et al., 1997). Our genetically modified *(Nkx Cre* $Spry2^{+/-}$ $Pten^{+/-}$*)* mouse model showed evidence of PI3K/AKT hyper-activation, without MAPK activation, in the prostate and enhanced capability to develop metastatic nodal disease by 12 months. Significantly, the PI3K inhibitor PI103 exerted a dramatic inhibitory effect on the growth of nodal metastasis. In addition, the reduction of SPRY2 expression has been associated with high-grade prostate tumour, and patients often are treated with androgen depletion therapy. Combination of PI3K and androgen inhibition strategies may delay the onset of androgen independent disease progression. Hsieh and his colleagues suggested the importance of 4EBP-elF4E in translational components and as a potential target in AKT-mediated lymphoma and rapamycin-resistant tumours (Hsieh et al., 2010). Indeed, as PI3K/AKT are important upstream kinases, there are many downstream targets that may need further assessment for potential therapeutic strategies.

Taken together, the selective activation of PI3K/AKT associated with SPRY2 loss in the context of PTEN insufficiency is important in prostate carcinogenesis: PI3K/AKT function enhances EGFR/HER2 signalling; PI3K/AKT promotes a proliferative and an invasive phenotype *in vitro* and *in vivo*; suppression of PI3K/AKT function reverse the above *in vitro* and *in vivo* phenotype; and finally, upregulated p-AKT expression was closely associated with reduced SPRY2 expression in clinical PC.

Chapter 6. SILAC analysis of SPRY2 interacting partners

6 SILAC analysis of SPRY2 interacting partners

In the last few decades, there has been an explosion of information and understanding in human genetics, which has given biologist a great insight into what we are made of and particularly be able to pinpoint many forms of diseases. No doubt, the genetic information reveals generally mutations, copy number changes and level of mRNA particularly in tumour biology, which has greatly improved prognosis and therapy. There are significant gap in our ability to translate tumour biology information into clinical application aimed for better patient proteome. The majority of enzymatic reactions are carried out by various proteins in the cell, and proteins undergo many post-translational modifications, compartmental trafficking, physical interaction with other partners and degradation. These processes are tightly controlled via many forms of feedback and signalling networks. Recently, many novel technologies have been developed to study the behaviour of proteins in a high throughput manner, namely proteomics. In tumour biology, complementary to genomic knowledge the global profiling of the protein pattern can be studied to compare normal and diseased conditions, in the hope of identifying molecular markers in order to elucidate disease mechanisms, including the initiation and progression of the disease.

At present there are two types of labelling protocols commonly used in mass spectrometry (MS), including biological and chemical incorporation. The biological labelling of the proteins in the cell is achieved by adding stable isotope-containing anabolites to the media for cells to grow in tissue culture and this approach is used in this project. The purpose of using stable isotopes (^{13}C, ^{15}N, ^{2}H) is that the MS quantitative analysis of protein/peptides can distinguish between test samples by comparison of distinct molecular mass peaks of the labelled proteins, which gives a relative ratio of abundance of the different labelled isotopic forms present in the various test samples.

Typical SILAC MS is achieved by culturing two /three groups of cells in culture media containing ‘light’, ‘medium’, and ‘heavy’ labelled amino acids (aa) (often with lysine and arginine). Since these aa are not synthesised by the cells, the labelled aa are incorporated into the cell in approximately 5 doubling

time. The SILAC method is a straightforward and efficient comparison of chemical incorporation, because there is no need to remove additional labels from the media or involve multiple steps for the labelling. In terms of signal-to-noise quantitative analysis still require further development in future MS instrument and methodology. The samples in this project are prepared using the whole cell lysates, which means the quantification of the protein change may not capture the accurate interactions due to the disruption and dilution of the native conditions, particularly for those interactions, which occur in different intracellular compartments. To date there are different methods in quantitative proteomics, which have their advantage and limitations. Inevitably the global MS analysis will provide an enormous volume of quantitative data, although the ability to filter out specific/useful information would be the challenge in the future when the MS becomes a routine technique.

In this project, GFP-tagged SPRY2 is transiently overexpressed in prostate cancer cell lines, and SPRY2 interaction proteome studied following EGF stimulation, which may give an insight into the mechanisms of SPRY2 involvement in RTK signalling and trafficking. Potential interaction partners of SPRY2 may give better understanding of how SPRY2 exerts its inhibitory action, and consequently may help us to identify potential targets involving SPRY2 loss in carcinogenesis. Particularly in the presence of EGF, we have shown that loss of SPRY2 enhances prostate cancer development through EGFR/HER2 activation. An overview of the experimental design is shown in Figure 6.1.1.

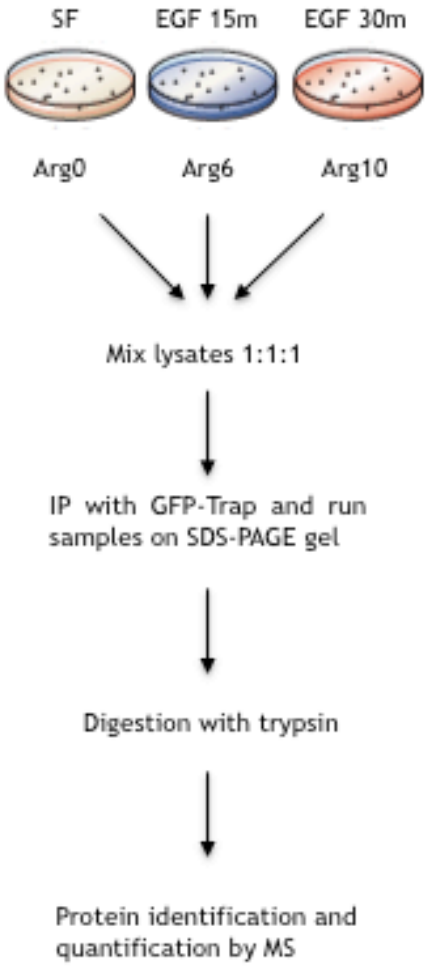

Figure 6.1.1 Overview of SILAC IP experimental strategy

Cells were grown in the medium with various isotopes, and lysed after transfection and EGF treatments. Lysates were collected and protein concentration was determined. Lysates from various experimental conditions were then mixed and IP was performed. The samples were run in the SDS-PAGE gel, and digested with trypsin then analysed with MS.

6.1 Generation of SPRY2 overexpression model

In order to further understand the action of SPRY2 in prostate carcinogenesis, endogenous SPRY2 IP was performed in DU145 cells. Firstly, the SPRY2 antibody was crosslinked to agarose beads and titration experiment was carried out with increasing volume of agarose beads. Western blot analysis with post IP supernatants (S) and IP sample indicated that 3 μl of beads volume is the optimal condition (Figure 6.1.2). Up to 1 μl beads volume, the level of SPRY2 in supernatants was still higher than in the post IP supernatants following incubation with 3-10 μl beads, although the non-specific signals were also weaker. Hence, 3 μl beads per 2 mg of proteins were chosen for the future IP.

For MS analysis, 10^6 cells were seeded and lysed on a 15 cm diameter dish and the protein concentration was determined using BioRad and Bradford assay. Samples were run on a 10% SDS-PAGE gel (Invitrogen), and the protein bands were visualised with Simply Blue™ SafeStain (coomassie blue staining kit) (Figure 6.1.3). Even with optimised beads volume, there are many non-specific bands in beads alone lane, which was IP with beads without primary antibody crosslink. The SPRY2 protein bands were expected to be the most prominent in the IP lane, but this was not observed. Nonetheless, there was a double band at 43 kDa marker, which was identified as SPRY2 with MS. However the list of proteins pulled down were mostly nonspecific or mostly bead specific namely beadome including actin and actin related proteins.

It is reasoned that the amount of SPRY2 in DU145 are limited and the primary antibody may not be as specific as we wished for IP. Next, the flag-tagged SPRY2 plasmid was used to transiently transfect prostate cancer cell lines to increase the amount of SPRY2 expression level, and to overcome the difficulties. The efficiency of the plasmid transfection was assessed using IF, the endogenous SPRY2 showed punctuated staining near perinuclear localisation. In contrast, the flag-tagged SPRY2 localised all over the cytoplasm of the cell, with no specific localisation (Figure 6.1.4). In addition, SPRY2 antibody was not able to recognise the Flag-tagged SPRY2, since the endogenous SPRY2 signal was not overlapping with Flag signal. It may be due to the fact that Flag was tagged on the N-terminus of SPRY2 protein, where SPRY2 antibody recognises the protein.

The Flag IP was performed with caution, since SPRY2 expression seems overwhelming. As expected, the MS identified many Flag-bead specific proteins, with the most abundant protein identified to be SPRY2. In order to overcome such problem, GFP tagged SPRY2 plasmid was generated by inserting SPRY2 sequence into pEGFP-C1 plasmid (Figure 6.1.5). Cells were transfected with pEGFP-C1 as control or GFP-SPRY2 plasmid, and visualised under the microscope. Interestingly, SPRY2-GFP localised to the peri-nuclear region, similar to endogenous SPRY2 (Figure 6.1.6). The transfection rate was only between 20-30%, and the transfection reagent lipofectamine 2000 was toxic. Prior to the MS quantification, the samples were analysed by western blot. GFP and GFP-tagged SPRY2 were detected in whole cell lysates (WCL) samples lane 1 and 2 respectively in Figure 6.1.7. The efficiency of GFP pull down was tested with post IP WCL, which was collected after separation of beads from the lysates. As expected, the GFP-SPRY2 transfected sample (2) had reduced amount of SPRY2 compared to the initial WCL. In the IP sample, the empty vector and GFP-SPRY2 lanes were confirmed to have high levels of GFP and GFP tagged SPRY2 respectively. The endogenous SPRY2 was detected in all lanes except in the negative control IP sample. Furthermore, a positive interaction partner of SPRY2 was assessed. It is reported that both SPRY2 and SPRY4 directly binds to wild type BRAF (not V599E mutant) and interferes with MAPK signalling cascades (Lampugnani and Dejana, 2007). BRAF was detected across all of the cell lysates with weak signal, and the GFP-SPRY2 IP sample showed the strongest band, indicating the interaction between exogenous GFP-SPRY2 and BRAF. These results suggested that GFP-tagged SPRY2 transfection system could be used for SILAC MS/MS analysis.

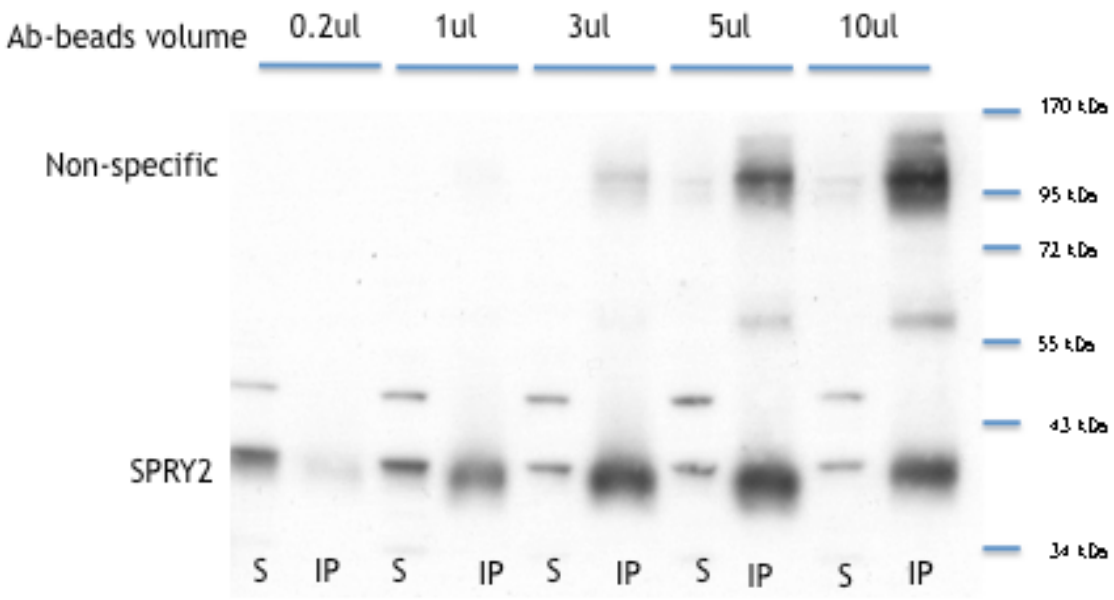

Figure 6.1.2 Optimisation of antibody-beads volume for IP

Du145 cells were lysed and incubated with different volumes of SPRY2 antibody cross-linked to agarose beads, and the whole cell lysates after IP (S) and samples eluted from beads (IP) were analysed with western blots. SPRY2 protein was detected between the molecular marker 43 and 34 kDa.

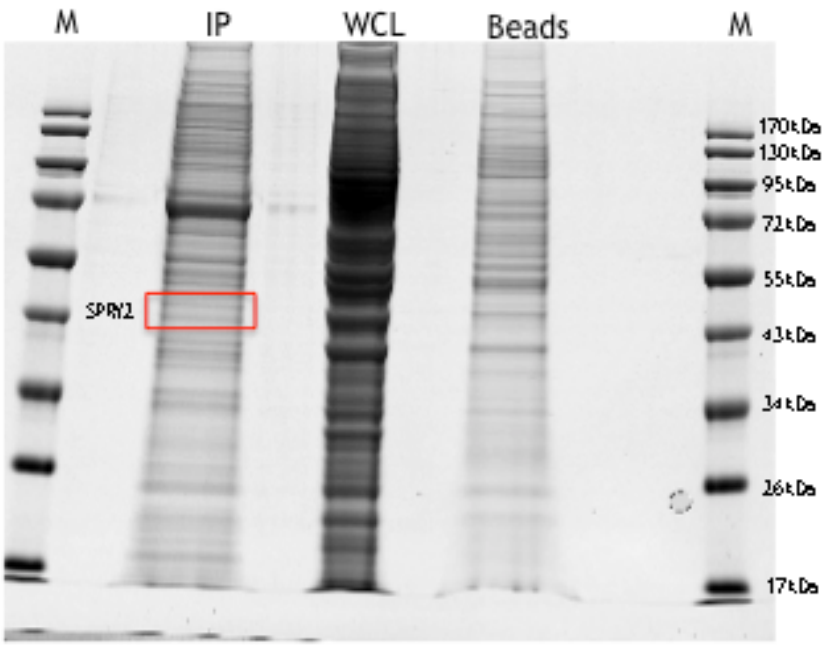

Figure 6.1.3 Endogenous SPRY2 IP using prostate cancer cell line

Du145 cells were lysed and whole cell lysates (WCL) collected . According to the protein concentration, the appropriate amount of agarose beads (20 µl) linked with SPRY2 antibody and performed IP. For the negative control, agarose beads without primary antibody were added to WCL (beads).

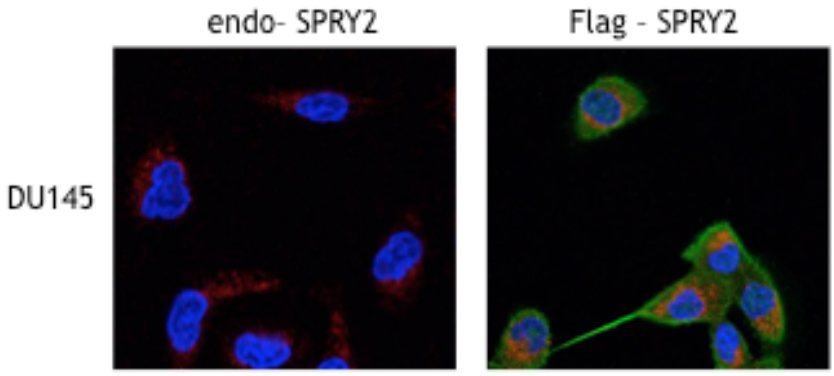

Figure 6.1.4 Overexpression of flag-tagged SPRY2 in prostate cancer cell line
Du145 cells are transiently transfected with PXJ40 plasmid containing flag-tagged SPRY2, and cells were fixed, endogenous SPRY2 (red), flag-SPRY2 (green) and nuclei (blue). Representative confocal images are shown.

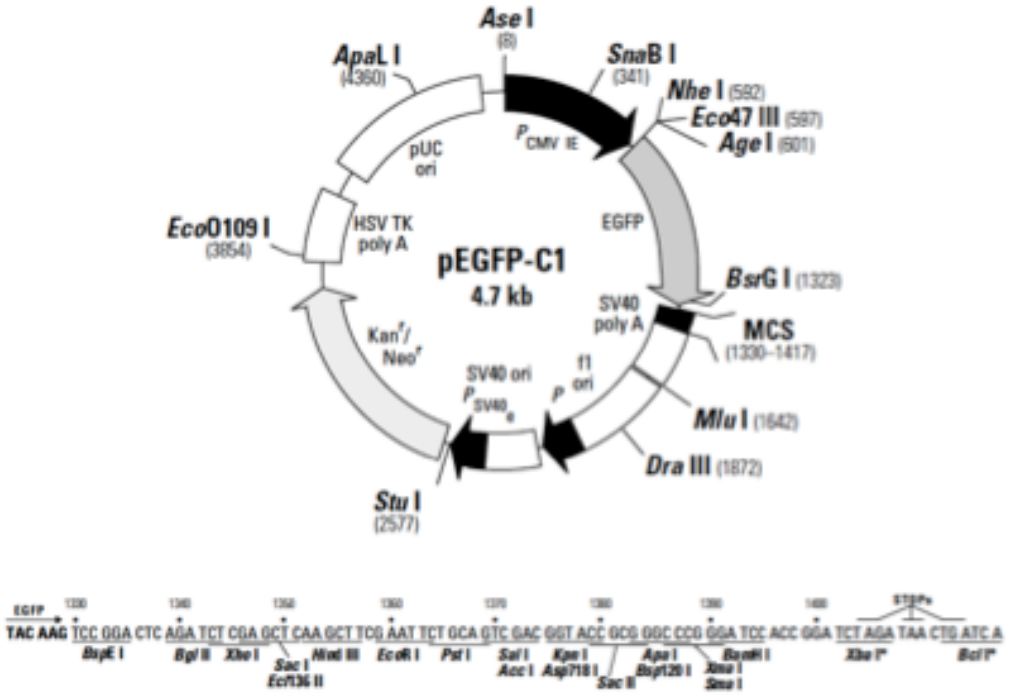

Figure 6.1.5 Map of pEGFP-C1 plasmid

SPRY2 gene is inserted in the pEGFP-C1 plasmid shown.

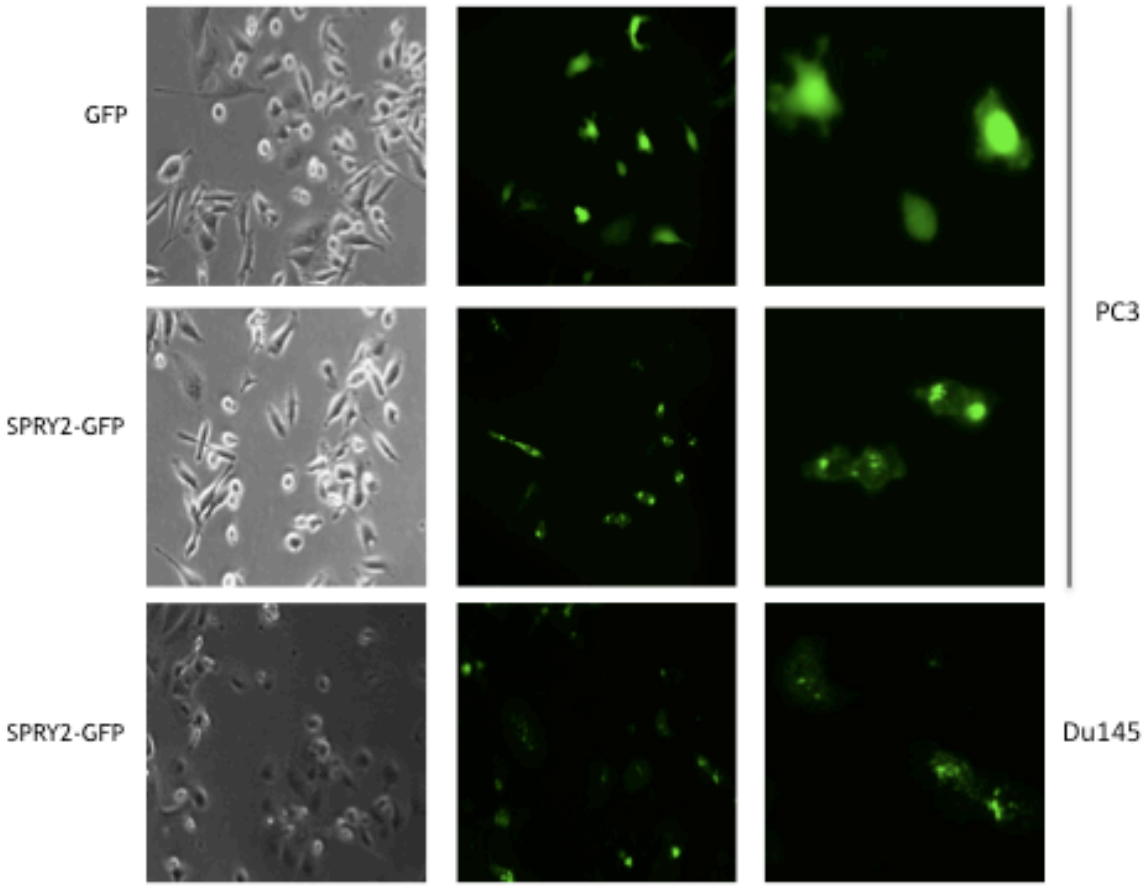

Figure 6.1.6 Overexpression of GFP-tagged SPRY2 in prostate cancer cell lines
Representative images of PC3 and Du145 cells transiently transfected with pEGFP-C1 plamid containing SPRY2 or empty vector.

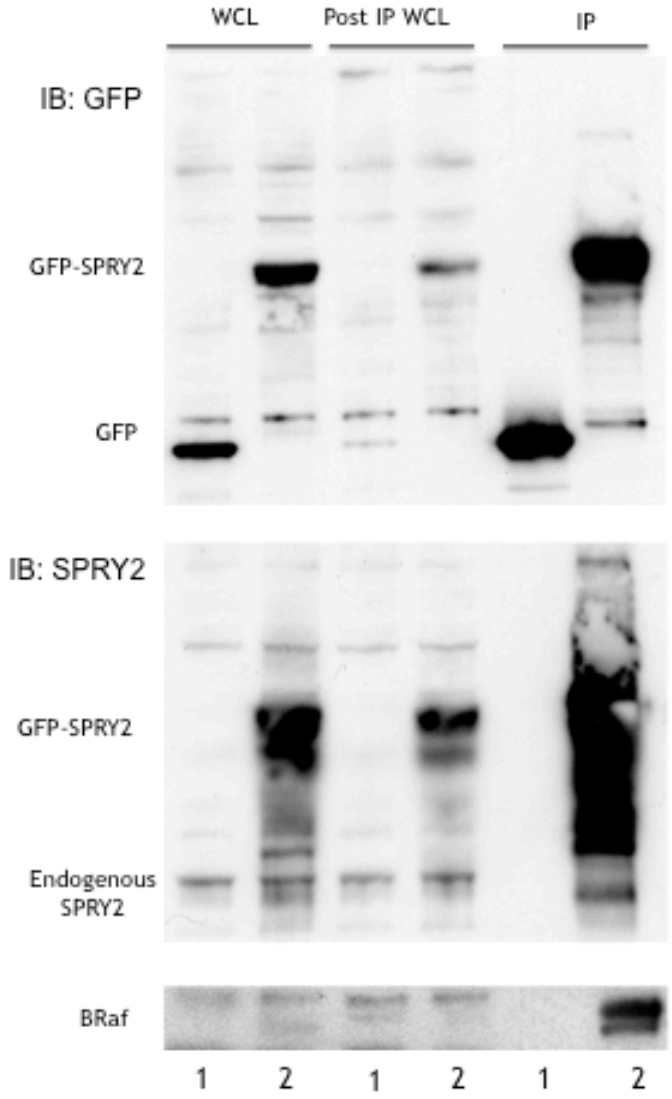

Figure 6.1.7 Western analysis of IP in cells with GFP-tagged SPRY2 overexpression
Cells were transfected with GFP-tagged SPRY2 plasmid, whole cell lysates were collected and GFP was IP using GFP-Trap_A beads. Cell lysates and IP samples were analysed with western blots. Lane 1: Empty vector, Lane 2: GFP-tagged SPRY2

6.2 Analysis of SILAC mass spectrometry

Firstly, PC3 cells were passaged in culture media containing isotope labels shown in Table 2.3. After 5 passages, the whole cell lysates were collected and the incorporation of the isotopes assessed. Such growth media did not show any detrimental effect on cell growth and morphology. The samples were prepared as illustrated in Figure 6.1.1, the protein sequences of the GFP-tagged SPRY2 is shown below (Figure 6.2.1). For the negative control, the empty vector pEGFP-C1 was transfected. Both samples were run on a SDS-PAGE gel and stained with coomassie blue. As expected, GFP-SPRY2 (61 kDa) was the most prominent band was between 72 and 55 kDa. The negative control lane had a strong band around 34 kDa marker, which was the GFP tag alone (Figure 6.2.2). The gel was cut as indicated, digested with trypin, and performed LC MS/MS analysis. The MS analysis identified around 90 different proteins. GFP beadome, and proteins identified in the negative control samples were excluded from the candidate lists. For example, variants of heat shock 70KDa protein, cytokeratin 8 and 18, and ubiquitin are most commonly detected in GFP pull down (Trinkle-Mulcahy et al., 2008). Indeed these proteins were identified in both empty vector and GFP-SPRY2 IP samples. In addition, there are also sepharose bead associated non-specific binders, including cofilin, filamin, vimentin, plectin, actin, myosin, and tubulin, which are cytoskeletal, motility or structural protein families. Also, it is reported that various histones, heat shock proteins, ribosomal proteins, hnRNP proteins and translational factors are mostly pulled down with sepharose beads IP. Considering the non-specific binding proteins, most of proteins identified from PC3 cell line SILAC IP were bead related protein, not SPRY2 interaction partners. It was thought that in vitro findings from Chapter 3 explains non-inclusive results from the SILAC IP, since PTEN null PC3 cells had showed no effect when SPRY2 expression level was reduced. Thus, overexpression of SPRY2 may not be functional in PTEN negative cells.

In contrast to PC3, DU145 (PTEN positive) SILAC IP results revealed a different list of proteins as candidate interaction partners. Although GFP beads related non-specific binding proteins were similar as mentioned above. There were interesting potential authentic interacting partners of SPRY2, including creatin kinase B, serine/threonine-protein phosphatase 2A (PP2A) 65 kDa

regulatory subunit A alpha isoform, and LIM domain only protein 7. Lao and his colleagues reported that SPRY2 co-IP with PP2A and regulates downstream of FGFR signalling cascade (Lao et al., 2007). In addition, there were few candidates identified including creatin kinase B (CKB), LIM domain only protein 7 (LMO7), pyruvate kinase isoenzyme M1/M2 (PKM2), and Ras GTPase-activating protein binding protein 1 (G3BP1) (Table 6.1).

GFP-tagged SPRY2 (GFP - Link - SPRY2)

GFP tag sequence

MVSKGEELFTGVVPILVELDGDVNGHKFSVSGEGEGDATYGKLTLKFICTTGKLPVPWPTLVTTL
TYGVQCFSRYPDHMKQHDFFKSAMPEGYVQERTIFFKDDGNYKTRAEVKFEGDTLVNRIELKGID
FKEDGNILGHKLEYNYNSHNVYIMADKQKNGIKVNFKIRHNIEDGSVQLADHYQQNTPIGDGPVL
LPDNHYLSTQSALSKDPNEKRDHMVLLEFVTAAGITLGMDELYKSGRTQISSSSFEFCSRRYRGPGI
HRI

Link between GFP and SPRY2

K S G R T Q I S S S S F E F T

SPRY2

MEARAQSGNGSQPLLQTPRDGGRQRGEPDPRDALTQQVHVLSLDQIRAIRNTNEYTEGPTVVP
RPGLKPAPRPSTQHKHERLHGLPEHRQPPRLQHSQVHSSARAPLSRSISTVSSGSRSSTRTSTSSSS
SEQRLLGSSFSSGPVADGIIRVQPKSELKPGELKPLSKEDLGLHAYRCEDCGKCKCKECTYPRPLPS
DWICDKQCLCSAQNVIDYGTCVCCVKGLFYHCSNDDEDNCADNPCSCSQSHCCTRWSAMGVMS
LFLPCLWCYLPAKGCLKLCQGCYDRVNRPGCRCKNSNTVCCKVPTVPPRNFEKPT

Figure 6.2.1 The protein sequence of transfected GFP- tagged SPRY2

The plasmid was sequenced, and amino acids sequences are translated from the DNA sequences.

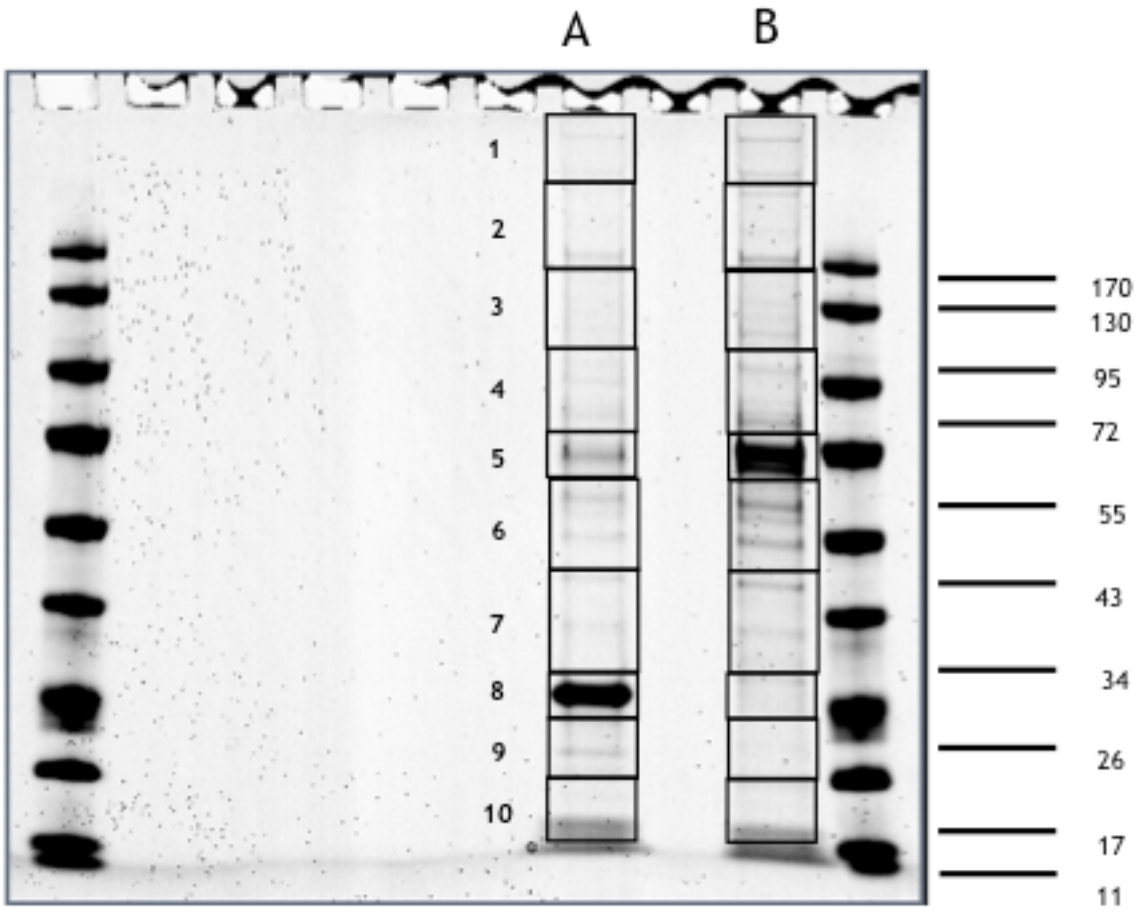

Figure 6.2.2 SiLAC IP samples from Du145 cells on a SDS-PAGE gel

Lane A is the negative control with empty vector, and lane B is the GFP-SPRY2 IP sample. Markers were run at both end, and the molecular weight was shown.

Accession number	Gene	Mass (Da)	# Peptides	SILAC M/L ratio ± SD	SILAC H/L ratio ± SD
O43597	SPRY2	36148	47	0.66 ± 0.06	0.72 ± 0.12
P30153	PPP2R1A	66065	4	0.82 ± 0.11	0.66 ± 0.08
Q8WWI1	LMO7	194016	3	0.86 ± 0.05	0.80 ± 0.16
P12277	CKB	42902	2	0.90 ± 0.19	0.78 ± 0.06
P14618	PKM2	58470	15	0.88 ± 0.18	0.73 ± 0.06
Q13283	G3BP1	52189	2	0.78 ± 0.07	0.74 ± 0.05

Tabel 6.1 Summary of protein interaction SILAC datasets

Cell were transfected with GFP-SPRY2 and IP using GFP-Trap system, the sample is analysed with LC MS/MS. SILAC ratio with SD (standard deviation) was shown, M/L and H/L indicated medium/ Light and Heavy/Light respectively. L-serum free, M-15 mins EGF, H- 30 mins EGF.

6.3 Validation of its interaction partners

In order to validate the candidates identified from the MS analysis, the potential interaction partners were validated with western blots. Whole cell lysates were collected before and post IP, which is shown in the Figure 6.3.1. The possible candidates suggested by the SILAC IP were PP2A (protein phosphatase 2A), PKM2 (pyruvate kinase isoenzyme M1/M2), CKB (creatin kinase brain type) and clathrin heavy chain. There were difficulties to obtain commercially available antibodies, which can be used for western analysis, for some of candidates in the lists. PKM2, CKB and clathrin were detected in WCL and post IP WCL, and also in the negative control lane. The GFP beads strongly bind to the proteins, thus these were considered as non-specific binding, namely beadome. These proteins were detected in the SPRY2-GFP IP sample lane with weaker signal compared to negative control. Interestingly, PP2A is only detected in SPRY2 IP lane and WCL, but not in the negative control lane. This confirms that PP2A is the true binding partner of SPRY2. The peptides were identified in MS/MS are highlighted in the Figure 6.3.2. It has been reported that upon FGF stimulation SPRY2 directly binds to PP2A and the binding sites involving SPRY2 are tyrosine 55 residue (Lao et al., 2007).

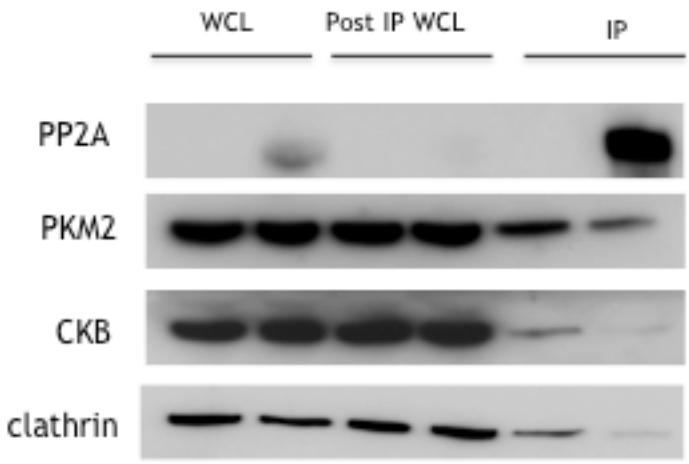

Figure 6.3.1 Validation of SILAC IP interaction candidate

Du145 cells were transfected with pEGFP-C2 or pEGFP-C2-SPRY2 plasmids, and cell lysates were collected before and post IP. GFP-Trap beads were used to IP and analysed with western blots.

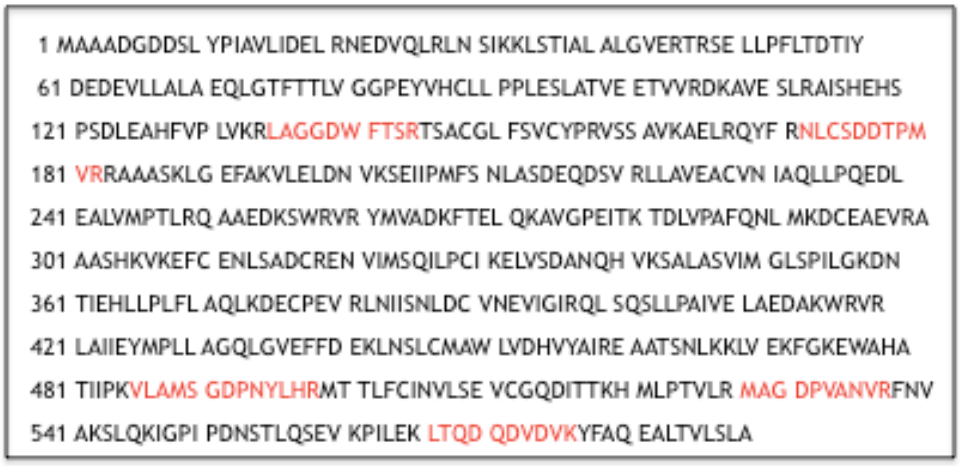

Figure 6.3.2 PP2A aa sequences and peptides identified with MS/MS

PP2A aa sequence was listed and the peptides identified through MS/MS were highlighted.

6.4 Summary and discussion

Various proteomic techonologies particularly SILAC MS and pre-existing cell biology knowledge provide many opportunities and questions to be asked in post genome era. The project involving endogenous SPRY2 IP demonstrated the difficulties underlie in cellular and technical aspects. It was due to the fact that the level of SPRY2 expression is not abundant enough to pull down for MS analysis. Kriegsheim and his colleagues (von Kriegsheim et al., 2009) managed for the first time to IP endogenous ERK, which is often ubiquitously expressed. Also commercially available antibodies for SPRY2, which is an affinity isolated polyclonal antibody (Sigma), may not be as specific and effective as monoclonal antibodies used in ERK IP.

The separation of specific protein interactions from bead proteomes is a major challenge in the field. There are over 30 proteins pulled down as GFP specific binding partners and several hundreds of proteins interact with sepharose beads (Trinkle-Mulcahy et al., 2008). These proteins are mainly cytoskeletal, structural and motility proteins, which are often considered as the most abundant proteins in a cell. In order to increase the amount of protein expression, plasmids are used to express the protein of the interest. As described in Chapter 6, Flag and GFP tagged SPRY2 were overexpressed in prostate cancer cell lines. The GFP-Trap system was more effective compared to Flag pull down. GFP pull down validated BRaf as a positive control but not in Flag-tagged SPRY2 IP. In addition, the localisation of the tagged SPRY2 seemed more specific with GFP tag rather than Flag. Transient transfections system with plasmid should be used with consideration of other side effects including overwhelming the cell with the protein of interests, which is not physiological. Thus the effect and potential interaction candidates could well be non-physiological or non-specific. Furthermore, common tags including GFP and Flag could affect the host protein folding, behaviour or its binding partners.

Chapter 7. Discussion

7 Discussion

Recent advances in global genomic profiling have generated vast amounts of data from cancer patients including prostate tumour, which has provided us with better understanding of carcinogenesis and confirming molecular abnormalities and revealing potential targets for therapy. Loss of PTEN plays a key role in PC progression, and is a hallmark of advanced disease. Indeed, cBio portal indicated that 16% of cases (n=194) either lost both copies or one copy of Pten alleles. As expected, almost half of patients have complete loss of Pten in patients (n=37) with advanced metastatic diseases (Taylor et al., 2010). The rest of metastatic disease still express PTEN, the interesting question is how these cancers become aggressive with PTEN retention. In this project, I examined the significance of regulatory components of the PI3K/AKT signalling particularly focused on SPRY2, which is known as a negative regulator of RTK cascades. Following the discovery of Drosophila SPRY as an antagonist of FGFR signalling pathway, many researchers have uncovered the role of mammalian SPRY family members in various cancer developments (Hacohen et al., 1998). Given the important role of RTK in normal and tumour development, no doubt SPRY proteins regulate various RTK including FGFR, VEGFR and EGFR in a temporal and spatial manner. However, the role of SPRY members particularly SPRY2, remains to be elucidated in cancer biology. In advanced metastatic PC, there are a total of 38% of cases with downregulation of SPRY2 expression. Interestingly, half of the cases have PTEN complete deletion, and the other half are with retention of PTEN expression (Figure 7.1). Considering PTEN is essential for SPRY2's regulatory role, this project focused on the role of SPRY2 in EGFR with PTEN expressing PC.

Firstly, in vitro cell line studies showed that stable KD SPRY2 leads to enhancement in cell proliferation and invasiveness in PTEN positive DU145 cell lines in response to EGF stimulation. Engagement of ligands to EGFR often results in MAPK and PI3K/AKT signalling activation to aid cell growth and movements. Interestingly, the human phospho-kinase array suggested that the exacerbated signalling activation in SPRY2 KD cells was associated with the hperactivation of PI3K/AKT. This project further investigated the potential mechanisms entailing RTK and the regulatory component of PI3K/AKT. Among

RTK family, ErbB family members including EGFR and HER2 involve complex compartment-specific signalling upon ligand binding. Internalisation assay indicated both EGFR and HER2 (not HER3) rapidly trafficking and retention at endosomal compartments resulted in enhanced downstream PI3K/AKT signalling in SPRY2 KD cells. Such trafficking and signal amplification in SPRY2 KD cells required the presence of PTEN expression. Furthermore, dissection of RTK and PI3K/AKT signalling cascades with various inhibitors including LY294002 and SB203580 confirmed the involvement of p38 serine/threonine kinase in protecting RTK from degradation and facilitating internalisation, which forms feedback forward loop described in Chapter 4. Thus PC cells are capable of utilising RTK signalling component without amplification or mutation of the receptors for cell growth unlike common amplification of HER2 in breast cancer.

Secondly, Nkx $Pten^{fl/+}$ $Spry2^{+/-}$mouse model developed aggressive PC around 10-12 months with mestastatic involvement of lymph nodes. Prostate tumour tissue collected from these transgenic mice showed hyperactivation of PI3K/AKT and enhanced cytoplasmic EGFR. This supports the hypothesis drawn from in vitro human cell lines. Reduction of SPRY2 expression was associated with enhanced activation of PI3K/AKT signalling cascades in response to EGF stimulation. EGFR and HER2 heterodimers showed rapid trafficking and amplification of the signalling via p38 and in a PTEN dependent manner (Figure 7.2). In addition, the mouse model provided an experimental platform for testing chemotherapy strategies. In contrast to PTEN or SPRY2, it is much easier to target activated PI3K/AKT signalling pathways for therapy rather than trying to restore the lost tumour suppressor function. One of the major challenges in the clinical use of PI3K inhibitors is to identify patients with PC specifically driven by such molecular abnormalities. However, PC is a heterogeneous disease with complex genetic and epigenetic abnormalities, which are difficult to be fully represented in a single transgenic mouse model. Thus this study provides an important insight into potential strategies for developing future combinatorial therapeutic approaches. Of note, both in vitro cell model and preclinical mouse prostate tumour responded well to the treatment with the PI3K inhibitor PI103 in terms of inhibition of cell proliferation and invasiveness. It is worth considering the particular patient cohort with PC showing SPRY2 and PTEN along with

hyperactivation of PI3K/AKT. These patients may be responsive to targeted therapy to PI3K/AKT signalling.

Thirdly, the human TMA data further confirms the important roles of PTEN, SPRY2 and RTK in PC development. Correlation analysis suggested a strong asscociation between SPRY2, HER2 and AKT. Loss of SPRY2 acts as a negative regulator of HER2 function and results in hyperactivation of AKT in prostate carcinogenesis. Given HER2 has no known intrinsic ability to bind to cognate ligands, its function relies on the formation of heterodimers with EGFR and HER3, and the significant correlation between cytoplasmic HER2 is concomitant with the importance of signal amplication via internalisation of the receptors. For future studies, there are PC patients with both PTEN completely loss and downregulation of SPRY2 (10/194), which may have different profile of abnormal molecular mechanisms contributing PC progression. Further research of *in vivo* models with homozygous deletion of *Spry2* and *Pten* may give insight into other potential therapeutic targets for this particular subset of patient.

Finally, cancer is generally believed to be a multistep genetic disorder (Potente et al., 2007). Either by loss of tumour suppressor gene or hyperactivation of specific oncogene, we have tried to restore, repair or inactivate these abnormal pathways. Abatement of certain oncogenic activity led to regression of tumours, so called tumour with oncogenic addiction. However, relapsed tumour with more aggressive phenotype is often observed within various cancers, which may be attributed to the pressure encouraging cancer cell evolution and adaptation. A recent popular topic is to understand the metabolic signature of tumour cells and find therapeutic targets. Whether the metabolic concept is merely another form of oncogenic addiction remains to be answered. In addition, it is clear that in addition to genetic alteration, there are other components essential for tumour maintenance including microenvironment surrounding cancer cells and cancer stem cells. Thus, there is neither a single model nor magic bullet in cancer biology. Given PC is an age related disease, it is clear that for PC the future goal of research is to delay the onset of the aggressive and metastatic form, which may allow patients to live and manage the disease with ease like diabetes. This may reduce PC related mortality and morbidity.

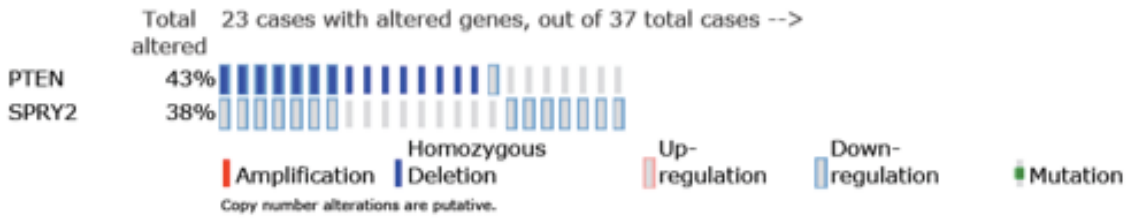

Figure 7.1 PTEN and SPRY2 in metastatic PC patient samples

Patients with both gene alteration accounts for 62% of total cases (n=37). Pten alteration is mostly homozygous deletion labelled with filled blue box, Spry2 is often down-regulated in metastatic diseases.

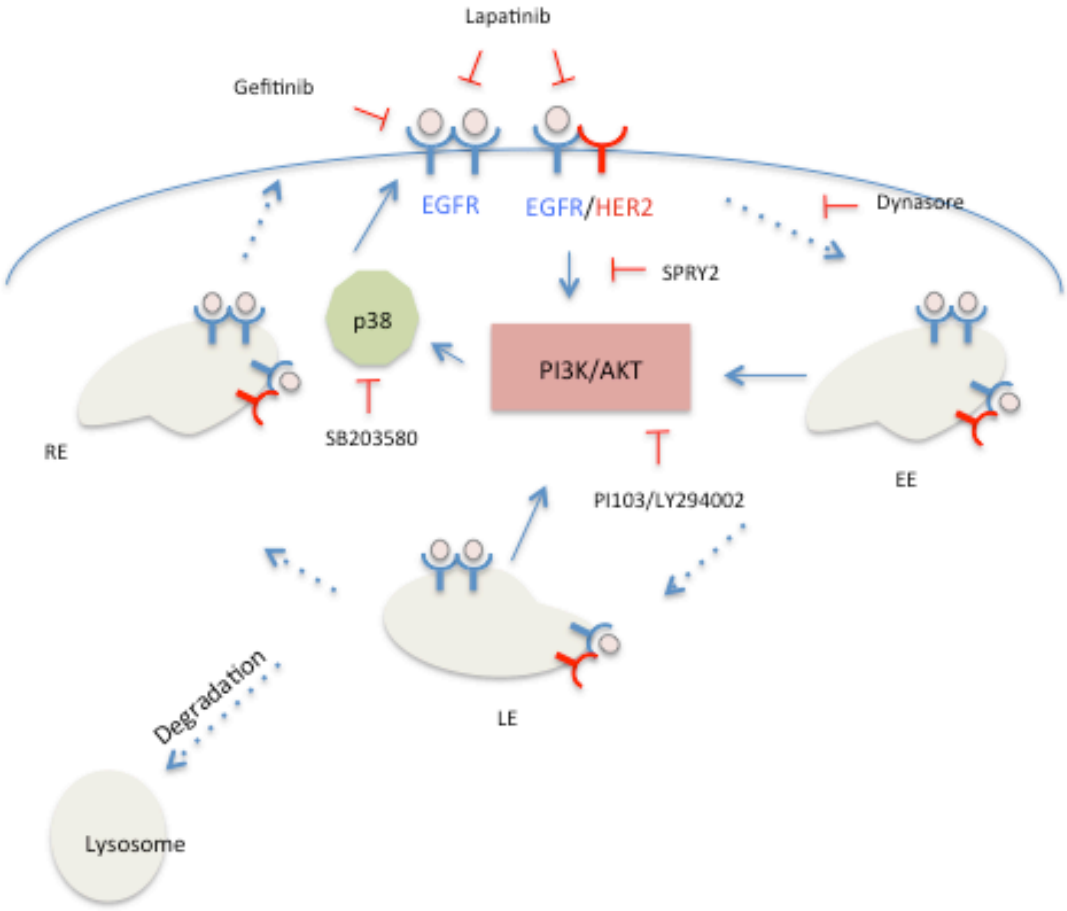

Figure 7.2 Summary schematic model

The graphic abstract illustrates the signalling network of EGFR and HER2, which occur at both plasma membrane and endocytic compartments. The trafficking of the receptors through EE (early endosome), LE (late endosome) and RE (recycling endosome) are critical for the maintenance and amplification of the downstream signalling outcome.

References

ANDRECHEK, E. R., HARDY, W. R., SIEGEL, P. M., RUDNICKI, M. A., CARDIFF, R. D. & MULLER, W. J. 2000. Amplification of the neu/erbB-2 oncogene in a mouse model of mammary tumorigenesis. *Proc.Natl.Acad.Sci.U.S.A,* 97**,** 3444-3449.

ATTARD, G., SWENNENHUIS, J. F., OLMOS, D., REID, A. H., VICKERS, E., A'HERN, R., LEVINK, R., COUMANS, F., MOREIRA, J., RIISNAES, R., OOMMEN, N. B., HAWCHE, G., JAMESON, C., THOMPSON, E., SIPKEMA, R., CARDEN, C. P., PARKER, C., DEARNALEY, D., KAYE, S. B., COOPER, C. S., MOLINA, A., COX, M. E., TERSTAPPEN, L. W. & DE BONO, J. S. 2009. Characterization of ERG, AR and PTEN gene status in circulating tumor cells from patients with castration-resistant prostate cancer. *Cancer Res,* 69**,** 2912-8.

BALUK, P., FUXE, J., HASHIZUME, H., ROMANO, T., LASHNITS, E., BUTZ, S., VESTWEBER, D., CORADA, M., MOLENDINI, C., DEJANA, E. & MCDONALD, D. M. 2007. Functionally specialized junctions between endothelial cells of lymphatic vessels. *The Journal of experimental medicine,* 204**,** 2349-62.

BLOETHNER, S., CHEN, B., HEMMINKI, K., MULLER-BERGHAUS, J., UGUREL, S., SCHADENDORF, D. & KUMAR, R. 2005. Effect of common B-RAF and N-RAS mutations on global gene expression in melanoma cell lines. *Carcinogenesis,* 26**,** 1224-32.

BORDONI, V., ALONZI, T., ZANETTA, L., KHOURI, D., CONTI, A., CORAZZARI, M., BERTOLINI, F., ANTONIOTTI, P., PISANI, G., TOGNOLI, F., DEJANA, E. & TRIPODI, M. 2007. Hepatocyte-conditioned medium sustains endothelial differentiation of human hematopoietic-endothelial progenitors. *Hepatology,* 45**,** 1218-28.

BOSTWICK, D. G. 1989. Prostatic intraepithelial neoplasia (PIN). *Urology,* 34**,** 16-22.

BOSTWICK, D. G. & BRAWER, M. K. 1987. Prostatic intra-epithelial neoplasia and early invasion in prostate cancer. *Cancer,* 59**,** 788-94.

BROOKE, G. N., PARKER, M. G. & BEVAN, C. L. 2008. Mechanisms of androgen receptor activation in advanced prostate cancer: differential co-activator recruitment and gene expression. *Oncogene,* 27**,** 2941-50.

BUBENDORF, L., SCHOPFER, A., WAGNER, U., SAUTER, G., MOCH, H., WILLI, N., GASSER, T. C. & MIHATSCH, M. J. 2000. Metastatic patterns of prostate cancer: an autopsy study of 1,589 patients. *Hum Pathol,* 31**,** 578-83.

CARRACEDO, A., ALIMONTI, A. & PANDOLFI, P. P. 2011a. PTEN level in tumor suppression: how much is too little? *Cancer Res,* 71**,** 629-33.

CARRACEDO, A., ALIMONTI, A. & PANDOLFI, P. P. 2011b. PTEN level in tumor suppression: how much is too little? *Cancer research,* 71**,** 629-33.

CARVER, B. S., TRAN, J., GOPALAN, A., CHEN, Z., SHAIKH, S., CARRACEDO, A., ALIMONTI, A., NARDELLA, C., VARMEH, S., SCARDINO, P. T., CORDON-CARDO, C., GERALD, W. & PANDOLFI, P. P. 2009. Aberrant ERG expression cooperates with loss of PTEN to promote cancer progression in the prostate. *Nat Genet,* 41**,** 619-24.

CASCI, T., VINOS, J. & FREEMAN, M. 1999. Sprouty, an intracellular inhibitor of Ras signaling. *Cell,* 96**,** 655-65.

CHAMBERS, D. & MASON, I. 2000. Expression of sprouty2 during early development of the chick embryo is coincident with known sites of FGF signalling. *Mech Dev,* 91**,** 361-4.

CHAMBERS, D., MEDHURST, A. D., WALSH, F. S., PRICE, J. & MASON, I. 2000. Differential display of genes expressed at the midbrain - hindbrain junction identifies sprouty2: an FGF8-inducible member of a family of intracellular FGF antagonists. *Mol Cell Neurosci,* 15**,** 22-35.

CHEN, Z., TROTMAN, L. C., SHAFFER, D., LIN, H. K., DOTAN, Z. A., NIKI, M., KOUTCHER, J. A., SCHER, H. I., LUDWIG, T., GERALD, W., CORDON-CARDO, C. & PANDOLFI, P. P. 2005. Crucial role of p53-dependent cellular senescence in suppression of Pten-deficient tumorigenesis. *Nature,* 436**,** 725-30.

DANESE, S., DEJANA, E. & FIOCCHI, C. 2007. Immune regulation by microvascular endothelial cells: directing innate and adaptive immunity, coagulation, and inflammation. *Journal of immunology,* 178**,** 6017-22.

DASILVA, J., XU, L., KIM, H. J., MILLER, W. T. & BAR-SAGI, D. 2006. Regulation of sprouty stability by Mnk1-dependent phosphorylation. *Mol Cell Biol,* 26**,** 1898-907.

DEJANA, E., TADDEI, A. & RANDI, A. M. 2007a. Foxs and Ets in the transcriptional regulation of endothelial cell differentiation and angiogenesis. *Biochimica et biophysica acta,* 1775**,** 298-312.

DEJANA, E., TADDEI, A. & RANDI, A. M. 2007b. Foxs and Ets in the transcriptional regulation of endothelial cell differentiation and angiogenesis. *Biochim Biophys Acta,* 1775**,** 298-312.

DEMILLE, M. M., KIMMEL, B. E. & RUBIN, G. M. 1996. A Drosophila gene regulated by rough and glass shows similarity to ena and VASP. *Gene,* 183**,** 103-8.

DI CRISTOFANO, A., PESCE, B., CORDON-CARDO, C. & PANDOLFI, P. P. 1998. Pten is essential for embryonic development and tumour suppression. *Nat Genet,* 19**,** 348-55.

EDWIN, F., SINGH, R., ENDERSBY, R., BAKER, S. J. & PATEL, T. B. 2006. The tumor suppressor PTEN is necessary for human Sprouty 2-mediated inhibition of cell proliferation. *J Biol Chem,* 281**,** 4816-22.

EGAN, J. E., HALL, A. B., YATSULA, B. A. & BAR-SAGI, D. 2002. The bimodal regulation of epidermal growth factor signaling by human Sprouty proteins. *Proc Natl Acad Sci U S A,* 99**,** 6041-6.

EMMERT-BUCK, M. R., VOCKE, C. D., POZZATTI, R. O., DURAY, P. H., JENNINGS, S. B., FLORENCE, C. D., ZHUANG, Z., BOSTWICK, D. G., LIOTTA, L. A. & LINEHAN, W. M. 1995. Allelic loss on chromosome 8p12-21 in microdissected prostatic intraepithelial neoplasia. *Cancer research,* 55**,** 2959-62.

ENGELMAN, J. A. 2009. Targeting PI3K signalling in cancer: opportunities, challenges and limitations. *Nat Rev Cancer,* 9**,** 550-62.

EPSTEIN, J. I. 2010. An update of the Gleason grading system. *J Urol,* 183**,** 433-40.

FALZARANO, S. M. & MAGI-GALLUZZI, C. 2011. Prostate cancer staging and grading at radical prostatectomy over time. *Advances in anatomic pathology,* 18**,** 159-64.

FONG, C. W., CHUA, M. S., MCKIE, A. B., LING, S. H., MASON, V., LI, R., YUSOFF, P., LO, T. L., LEUNG, H. Y., SO, S. K. & GUY, G. R. 2006. Sprouty 2, an inhibitor of mitogen-activated protein kinase signaling, is down-regulated in hepatocellular carcinoma. *Cancer Res,* 66**,** 2048-58.

FONG, C. W., LEONG, H. F., WONG, E. S., LIM, J., YUSOFF, P. & GUY, G. R. 2003. Tyrosine phosphorylation of Sprouty2 enhances its interaction with c-Cbl and is crucial for its function. *J Biol Chem,* 278**,** 33456-64.

FURTHAUER, M., REIFERS, F., BRAND, M., THISSE, B. & THISSE, C. 2001. sprouty4 acts in vivo as a feedback-induced antagonist of FGF signaling in zebrafish. *Development,* 128**,** 2175-86.

GAO, J., ARNOLD, J. T. & ISAACS, J. T. 2001. Conversion from a paracrine to an autocrine mechanism of androgen-stimulated growth during malignant transformation of prostatic epithelial cells. *Cancer Res,* 61**,** 5038-44.

GOLDSTEIN, A. S., HUANG, J., GUO, C., GARRAWAY, I. P. & WITTE, O. N. 2010. Identification of a cell of origin for human prostate cancer. *Science,* 329**,** 568-71.

GREENBERG, N. M., DEMAYO, F., FINEGOLD, M. J., MEDINA, D., TILLEY, W. D., ASPINALL, J. O., CUNHA, G. R., DONJACOUR, A. A., MATUSIK, R. J. & ROSEN, J. M. 1995. Prostate cancer in a transgenic mouse. *Proc Natl Acad Sci U S A,* 92**,** 3439-43.

GROSS, I., BASSIT, B., BENEZRA, M. & LICHT, J. D. 2001. Mammalian sprouty proteins inhibit cell growth and differentiation by preventing ras activation. *J Biol Chem,* 276**,** 46460-8.

GROSS, M., HIGANO, C., PANTUCK, A., CASTELLANOS, O., GREEN, E., NGUYEN, K. & AGUS, D. B. 2007. A phase II trial of docetaxel and erlotinib as first-line therapy for elderly patients with androgen-independent prostate cancer. *BMC Cancer,* 7**,** 142.

GUM, R. J., MCLAUGHLIN, M. M., KUMAR, S., WANG, Z., BOWER, M. J., LEE, J. C., ADAMS, J. L., LIVI, G. P., GOLDSMITH, E. J. & YOUNG, P. R. 1998. Acquisition of sensitivity of stress-activated protein kinases to the p38 inhibitor, SB 203580, by alteration of one or more amino acids within the ATP binding pocket. *J Biol Chem,* 273**,** 15605-10.

GUMERLOCK, P. H., CHI, S. G., SHI, X. B., VOELLER, H. J., JACOBSON, J. W., GELMANN, E. P. & DEVERE WHITE, R. W. 1997. p53 abnormalities in primary prostate cancer: single-strand conformation polymorphism analysis of complementary DNA in comparison with genomic DNA. The Cooperative Prostate Network. *Journal of the National Cancer Institute,* 89**,** 66-71.

GUO, Z., YANG, X., SUN, F., JIANG, R., LINN, D. E., CHEN, H., KONG, X., MELAMED, J., TEPPER, C. G., KUNG, H. J., BRODIE, A. M., EDWARDS, J. & QIU, Y. 2009. A novel androgen receptor splice variant is up-regulated during prostate cancer progression and promotes androgen depletion-resistant growth. *Cancer Res,* 69**,** 2305-13.

HACOHEN, N., KRAMER, S., SUTHERLAND, D., HIROMI, Y. & KRASNOW, M. A. 1998. sprouty encodes a novel antagonist of FGF signaling that patterns apical branching of the Drosophila airways. *Cell,* 92**,** 253-63.

HADARI, Y. R., KOUHARA, H., LAX, I. & SCHLESSINGER, J. 1998. Binding of Shp2 tyrosine phosphatase to FRS2 is essential for fibroblast growth factor-induced PC12 cell differentiation. *Mol Cell Biol,* 18**,** 3966-73.

HAFFNER, M. C., ARYEE, M. J., TOUBAJI, A., ESOPI, D. M., ALBADINE, R., GUREL, B., ISAACS, W. B., BOVA, G. S., LIU, W., XU, J., MEEKER, A. K., NETTO, G., DE MARZO, A. M., NELSON, W. G. & YEGNASUBRAMANIAN, S. 2010. Androgen-induced TOP2B-

mediated double-strand breaks and prostate cancer gene rearrangements. *Nat Genet,* 42**,** 668-75.

HAGLUND, K., SCHMIDT, M. H., WONG, E. S., GUY, G. R. & DIKIC, I. 2005. Sprouty2 acts at the Cbl/CIN85 interface to inhibit epidermal growth factor receptor downregulation. *EMBO Rep,* 6**,** 635-41.

HOLCOMB, I. N., GROVE, D. I., KINNUNEN, M., FRIEDMAN, C. L., GALLAHER, I. S., MORGAN, T. M., SATHER, C. L., DELROW, J. J., NELSON, P. S., LANGE, P. H., ELLIS, W. J., TRUE, L. D., YOUNG, J. M., HSU, L., TRASK, B. J. & VESSELLA, R. L. 2008. Genomic alterations indicate tumor origin and varied metastatic potential of disseminated cells from prostate cancer patients. *Cancer Res,* 68**,** 5599-608.

HOLGREN, C., DOUGHERTY, U., EDWIN, F., CERASI, D., TAYLOR, I., FICHERA, A., JOSEPH, L., BISSONNETTE, M. & KHARE, S. 2010. Sprouty-2 controls c-Met expression and metastatic potential of colon cancer cells: sprouty/c-Met upregulation in human colonic adenocarcinomas. *Oncogene,* 29**,** 5241-53.

HSIEH, A. C., COSTA, M., ZOLLO, O., DAVIS, C., FELDMAN, M. E., TESTA, J. R., MEYUHAS, O., SHOKAT, K. M. & RUGGERO, D. 2010. Genetic dissection of the oncogenic mTOR pathway reveals druggable addiction to translational control via 4EBP-eIF4E. *Cancer cell,* 17**,** 249-61.

HUGGINS, C. 1967. Endocrine-induced regression of cancers. *Cancer Res,* 27**,** 1925-30.

ILJIN, K., WOLF, M., EDGREN, H., GUPTA, S., KILPINEN, S., SKOTHEIM, R. I., PELTOLA, M., SMIT, F., VERHAEGH, G., SCHALKEN, J., NEES, M. & KALLIONIEMI, O. 2006. TMPRSS2 fusions with oncogenic ETS factors in prostate cancer involve unbalanced genomic rearrangements and are associated with HDAC1 and epigenetic reprogramming. *Cancer Res,* 66**,** 10242-6.

IMPAGNATIELLO, M. A., WEITZER, S., GANNON, G., COMPAGNI, A., COTTEN, M. & CHRISTOFORI, G. 2001. Mammalian sprouty-1 and -2 are membrane-anchored phosphoprotein inhibitors of growth factor signaling in endothelial cells. *J Cell Biol,* 152**,** 1087-98.

JATHAL, M. K., CHEN, L., MUDRYJ, M. & GHOSH, P. M. 2011. Targeting ErbB3: the New RTK(id) on the Prostate Cancer Block. *Immunol Endocr Metab Agents Med Chem,* 11**,** 131-149.

KATO, R., NONAMI, A., TAKETOMI, T., WAKIOKA, T., KUROIWA, A., MATSUDA, Y. & YOSHIMURA, A. 2003. Molecular cloning of mammalian Spred-3 which suppresses tyrosine kinase-mediated Erk activation. *Biochem Biophys Res Commun,* 302**,** 767-72.

KAWAKAMI, Y., KUBOTA, N., EKUNI, N., SUZUKI-YAMAMOTO, T., KIMOTO, M., YAMASHITA, H., TSUJI, H., YOSHIMOTO, T., JISAKA, M., TANAKA, J., FUJIMURA, H. F., MIWA, Y. & TAKAHASHI, Y. 2009. Tumor-suppressive lipoxygenases inhibit the expression of c-myc mRNA coding region determinant-binding protein/insulin-like growth factor II mRNA-binding protein 1 in human prostate carcinoma PC-3 cells. *Bioscience, biotechnology, and biochemistry,* 73**,** 1811-7.

KIM, H. J., TAYLOR, L. J. & BAR-SAGI, D. 2007. Spatial regulation of EGFR signaling by Sprouty2. *Curr Biol,* 17**,** 455-61.

KIM, J., ELTOUM, I. E., ROH, M., WANG, J. & ABDULKADIR, S. A. 2009. Interactions between cells with distinct mutations in c-MYC and Pten in prostate cancer. *PLoS genetics,* 5**,** e1000542.

KIM, M. J., BHATIA-GAUR, R., BANACH-PETROSKY, W. A., DESAI, N., WANG, Y., HAYWARD, S. W., CUNHA, G. R., CARDIFF, R. D., SHEN, M. M. & ABATE-SHEN, C. 2002a. Nkx3.1 mutant mice recapitulate early stages of prostate carcinogenesis. *Cancer research,* 62**,** 2999-3004.

KIM, M. J., CARDIFF, R. D., DESAI, N., BANACH-PETROSKY, W. A., PARSONS, R., SHEN, M. M. & ABATE-SHEN, C. 2002b. Cooperativity of Nkx3.1 and Pten loss of function in a mouse model of prostate carcinogenesis. *Proceedings of the National Academy of Sciences of the United States of America,* 99**,** 2884-9.

KING, J. C., XU, J., WONGVIPAT, J., HIERONYMUS, H., CARVER, B. S., LEUNG, D. H., TAYLOR, B. S., SANDER, C., CARDIFF, R. D., COUTO, S. S., GERALD, W. L. & SAWYERS, C. L. 2009a. Cooperativity of TMPRSS2-ERG with PI3-kinase pathway activation in prostate oncogenesis. *Nature genetics,* 41**,** 524-6.

KING, J. C., XU, J., WONGVIPAT, J., HIERONYMUS, H., CARVER, B. S., LEUNG, D. H., TAYLOR, B. S., SANDER, C., CARDIFF, R. D., COUTO, S. S., GERALD, W. L. & SAWYERS, C. L. 2009b. Cooperativity of TMPRSS2-ERG with PI3-kinase pathway activation in prostate oncogenesis. *Nat Genet,* 41**,** 524-6.

KRAMER, S., OKABE, M., HACOHEN, N., KRASNOW, M. A. & HIROMI, Y. 1999. Sprouty: a common antagonist of FGF and EGF signaling pathways in Drosophila. *Development,* 126**,** 2515-25.

KURITA, T., WANG, Y. Z., DONJACOUR, A. A., ZHAO, C., LYDON, J. P., O'MALLEY, B. W., ISAACS, J. T., DAHIYA, R. & CUNHA, G. R. 2001. Paracrine regulation of apoptosis by steroid hormones in the male and female reproductive system. *Cell Death Differ,* 8**,** 192-200.

KWABI-ADDO, B., WANG, J., ERDEM, H., VAID, A., CASTRO, P., AYALA, G. & ITTMANN, M. 2004. The expression of Sprouty1, an inhibitor of fibroblast growth factor signal transduction, is decreased in human prostate cancer. *Cancer Res,* 64**,** 4728-35.

LAMPUGNANI, M. G. & DEJANA, E. 2007. The control of endothelial cell functions by adherens junctions. *Novartis Foundation symposium,* 283**,** 4-13; discussion 13-7, 238-41.

LAO, D. H., CHANDRAMOULI, S., YUSOFF, P., FONG, C. W., SAW, T. Y., TAI, L. P., YU, C. Y., LEONG, H. F. & GUY, G. R. 2006. A Src homology 3-binding sequence on the C terminus of Sprouty2 is necessary for inhibition of the Ras/ERK pathway downstream of fibroblast growth factor receptor stimulation. *J Biol Chem,* 281**,** 29993-30000.

LAO, D. H., YUSOFF, P., CHANDRAMOULI, S., PHILP, R. J., FONG, C. W., JACKSON, R. A., SAW, T. Y., YU, C. Y. & GUY, G. R. 2007. Direct binding of PP2A to Sprouty2 and phosphorylation changes are a prerequisite for ERK inhibition downstream of fibroblast growth factor receptor stimulation. *The Journal of biological chemistry,* 282**,** 9117-26.

LAPIDOT, T., SIRARD, C., VORMOOR, J., MURDOCH, B., HOANG, T., CACERES-CORTES, J., MINDEN, M., PATERSON, B., CALIGIURI, M. A. & DICK, J. E. 1994. A cell initiating human acute myeloid leukaemia after transplantation into SCID mice. *Nature,* 367**,** 645-8.

LAWSON, D. A. & WITTE, O. N. 2007. Stem cells in prostate cancer initiation and progression. *J Clin Invest,* 117**,** 2044-50.

LEE, S. A., HO, C., ROY, R., KOSINSKI, C., PATIL, M. A., TWARD, A. D., FRIDLYAND, J. & CHEN, X. 2008. Integration of genomic analysis and in vivo transfection to identify sprouty 2 as a candidate tumor suppressor in liver cancer. *Hepatology,* 47**,** 1200-10.

LESCHE, R., GROSZER, M., GAO, J., WANG, Y., MESSING, A., SUN, H., LIU, X. & WU, H. 2002. Cre/loxP-mediated inactivation of the murine Pten tumor suppressor gene. *Genesis,* 32**,** 148-9.

LEVERSHA, M. A., HAN, J., ASGARI, Z., DANILA, D. C., LIN, O., GONZALEZ-ESPINOZA, R., ANAND, A., LILJA, H., HELLER, G., FLEISHER, M. & SCHER, H. I. 2009. Fluorescence in situ hybridization analysis of circulating tumor cells in metastatic prostate cancer. *Clin Cancer Res,* 15**,** 2091-7.

LI, J., YEN, C., LIAW, D., PODSYPANINA, K., BOSE, S., WANG, S. I., PUC, J., MILIARESIS, C., RODGERS, L., MCCOMBIE, R., BIGNER, S. H., GIOVANELLA, B. C., ITTMANN, M., TYCKO, B., HIBSHOOSH, H., WIGLER, M. H. & PARSONS, R. 1997. PTEN, a putative protein tyrosine phosphatase gene mutated in human brain, breast, and prostate cancer. *Science,* 275**,** 1943-7.

LINDSAY, Y., MCCOULL, D., DAVIDSON, L., LESLIE, N. R., FAIRSERVICE, A., GRAY, A., LUCOCQ, J. & DOWNES, C. P. 2006. Localization of agonist-sensitive PtdIns(3,4,5)P3 reveals a nuclear pool that is insensitive to PTEN expression. *J Cell Sci,* 119**,** 5160-8.

LINJA, M. J., SAVINAINEN, K. J., SARAMAKI, O. R., TAMMELA, T. L., VESSELLA, R. L. & VISAKORPI, T. 2001. Amplification and overexpression of androgen receptor gene in hormone-refractory prostate cancer. *Cancer Res,* 61**,** 3550-5.

LO, T. L., YUSOFF, P., FONG, C. W., GUO, K., MCCAW, B. J., PHILLIPS, W. A., YANG, H., WONG, E. S., LEONG, H. F., ZENG, Q., PUTTI, T. C. & GUY, G. R. 2004. The ras/mitogen-activated protein kinase pathway inhibitor and likely tumor suppressor proteins, sprouty 1 and sprouty 2 are deregulated in breast cancer. *Cancer Res,* 64**,** 6127-36.

LOGOTHETIS, C. J. & LIN, S. H. 2005. Osteoblasts in prostate cancer metastasis to bone. *Nat Rev Cancer,* 5**,** 21-8.

MARTINEZ, N., GARCIA-DOMINGUEZ, C. A., DOMINGO, B., OLIVA, J. L., ZARICH, N., SANCHEZ, A., GUTIERREZ-EISMAN, S., LLOPIS, J. & ROJAS, J. M. 2007. Sprouty2 binds Grb2 at two different proline-rich regions, and the mechanism of ERK inhibition is independent of this interaction. *Cell Signal,* 19**,** 2277-85.

MASTERS, J. R. & STACEY, G. N. 2007. Changing medium and passaging cell lines. *Nat Protoc,* 2**,** 2276-84.

MCKIE, A. B., DOUGLAS, D. A., OLIJSLAGERS, S., GRAHAM, J., OMAR, M. M., HEER, R., GNANAPRAGASAM, V. J., ROBSON, C. N. & LEUNG, H. Y. 2005. Epigenetic inactivation of the human sprouty2 (hSPRY2) homologue in prostate cancer. *Oncogene,* 24**,** 2166-74.

MELLINGER, G. T., GLEASON, D. & BAILAR, J., 3RD 1967. The histology and prognosis of prostatic cancer. *J Urol,* 97**,** 331-7.

MELLINGHOFF, I. K., VIVANCO, I., KWON, A., TRAN, C., WONGVIPAT, J. & SAWYERS, C. L. 2004. HER2/neu kinase-dependent modulation of androgen receptor function through effects on DNA binding and stability. *Cancer cell,* 6**,** 517-27.

MINOWADA, G., JARVIS, L. A., CHI, C. L., NEUBUSER, A., SUN, X., HACOHEN, N., KRASNOW, M. A. & MARTIN, G. R. 1999. Vertebrate Sprouty genes are induced by FGF signaling and can cause chondrodysplasia when overexpressed. *Development,* 126**,** 4465-75.

MORRIS, M. J., REUTER, V. E., KELLY, W. K., SLOVIN, S. F., KENNESON, K., VERBEL, D., OSMAN, I. & SCHER, H. I. 2002. HER-2 profiling and targeting in prostate carcinoma. *Cancer,* 94**,** 980-6.

MOSESSON, Y., MILLS, G. B. & YARDEN, Y. 2008. Derailed endocytosis: an emerging feature of cancer. *Nat Rev Cancer,* 8**,** 835-50.

NADEAU, R. J., TOHER, J. L., YANG, X., KOVALENKO, D. & FRIESEL, R. 2007. Regulation of Sprouty2 stability by mammalian Seven-in-Absentia homolog 2. *J Cell Biochem,* 100**,** 151-60.

NAGY, A. 2000. Cre recombinase: the universal reagent for genome tailoring. *Genesis,* 26**,** 99-109.

NISHIMURA, M., SHIN, M. S., SINGHIRUNNUSORN, P., SUZUKI, S., KAWANISHI, M., KOIZUMI, K., SAIKI, I. & SAKURAI, H. 2009. TAK1-mediated serine/threonine phosphorylation of epidermal growth factor receptor via p38/extracellular signal-regulated kinase: NF-{kappa}B-independent survival pathways in tumor necrosis factor alpha signaling. *Mol Cell Biol,* 29**,** 5529-39.

OHORI, M., WHEELER, T. M. & SCARDINO, P. T. 1994. The New American Joint Committee on Cancer and International Union Against Cancer TNM classification of prostate cancer. Clinicopathologic correlations. *Cancer,* 74**,** 104-14.

OZAKI, K., KADOMOTO, R., ASATO, K., TANIMURA, S., ITOH, N. & KOHNO, M. 2001. ERK pathway positively regulates the expression of Sprouty genes. *Biochem Biophys Res Commun,* 285**,** 1084-8.

OZAKI, K., MIYAZAKI, S., TANIMURA, S. & KOHNO, M. 2005. Efficient suppression of FGF-2-induced ERK activation by the cooperative interaction among mammalian Sprouty isoforms. *J Cell Sci,* 118**,** 5861-71.

PANTEL, K. & ALIX-PANABIERES, C. 2010. Circulating tumour cells in cancer patients: challenges and perspectives. *Trends in molecular medicine,* 16**,** 398-406.

PERNER, S., DEMICHELIS, F., BEROUKHIM, R., SCHMIDT, F. H., MOSQUERA, J. M., SETLUR, S., TCHINDA, J., TOMLINS, S. A., HOFER, M. D., PIENTA, K. G., KUEFER, R., VESSELLA, R., SUN, X. W., MEYERSON, M., LEE, C., SELLERS, W. R., CHINNAIYAN, A. M. & RUBIN, M. A. 2006. TMPRSS2:ERG fusion-associated deletions provide insight into the heterogeneity of prostate cancer. *Cancer Res,* 66**,** 8337-41.

PETRYLAK, D. 2005. Therapeutic options in androgen-independent prostate cancer: building on docetaxel. *BJU Int,* 96 Suppl 2**,** 41-6.

PIGNON, J. C., KOOPMANSCH, B., NOLENS, G., DELACROIX, L., WALTREGNY, D. & WINKLER, R. 2009. Androgen receptor controls EGFR and ERBB2 gene expression at different levels in prostate cancer cell lines. *Cancer Res,* 69**,** 2941-9.

PODSYPANINA, K., ELLENSON, L. H., NEMES, A., GU, J., TAMURA, M., YAMADA, K. M., CORDON-CARDO, C., CATORETTI, G., FISHER, P. E. & PARSONS, R. 1999. Mutation of Pten/Mmac1 in mice causes neoplasia in multiple organ systems. *Proc Natl Acad Sci U S A,* 96**,** 1563-8.

POTENTE, M., GHAENI, L., BALDESSARI, D., MOSTOSLAVSKY, R., ROSSIG, L., DEQUIEDT, F., HAENDELER, J., MIONE, M., DEJANA, E., ALT, F. W., ZEIHER, A. M. & DIMMELER, S. 2007. SIRT1 controls endothelial angiogenic functions during vascular growth. *Genes & development,* 21**,** 2644-58.

REICH, A., SAPIR, A. & SHILO, B. 1999. Sprouty is a general inhibitor of receptor tyrosine kinase signaling. *Development,* 126**,** 4139-47.

ROCHE, S., DOWNWARD, J., RAYNAL, P. & COURTNEIDGE, S. A. 1998. A function for phosphatidylinositol 3-kinase beta (p85alpha-p110beta) in fibroblasts during mitogenesis: requirement for insulin- and lysophosphatidic acid-mediated signal transduction. *Mol Cell Biol,* 18**,** 7119-29.

RUBIN, C., LITVAK, V., MEDVEDOVSKY, H., ZWANG, Y., LEV, S. & YARDEN, Y. 2003. Sprouty fine-tunes EGF signaling through interlinked positive and negative feedback loops. *Curr Biol,* 13**,** 297-307.

SALZBERG, M., ROCHLITZ, C., MORANT, R., THALMANN, G., PEDRAZZINI, A., ROGGERO, E., SCHONENBERGER, A., KNUTH, A. & BORNER, M. 2007. An open-label, noncomparative phase II trial to evaluate the efficacy and safety of docetaxel in combination with gefitinib in patients with hormone-refractory metastatic prostate cancer. *Onkologie,* 30**,** 355-60.

SARTO, P., BALDUCCI, E., BALCONI, G., FIORDALISO, F., MERLO, L., TUZZATO, G., PAPPAGALLO, G. L., FRIGATO, N., ZANOCCO, A., FORESTIERI, C., AZZARELLO, G., MAZZUCCO, A., VALENTI, M. T., ALBORINO, F., NOVENTA, D., VINANTE, O., PASCOTTO, P., SARTORE, S., DEJANA, E. & LATINI, R. 2007. Effects of exercise

training on endothelial progenitor cells in patients with chronic heart failure. *Journal of cardiac failure,* 13**,** 701-8.

SASAKI, A., TAKETOMI, T., WAKIOKA, T., KATO, R. & YOSHIMURA, A. 2001. Identification of a dominant negative mutant of Sprouty that potentiates fibroblast growth factor- but not epidermal growth factor-induced ERK activation. *J Biol Chem,* 276**,** 36804-8.

SCIAVOLINO, P. J., ABRAMS, E. W., YANG, L., AUSTENBERG, L. P., SHEN, M. M. & ABATE-SHEN, C. 1997. Tissue-specific expression of murine Nkx3.1 in the male urogenital system. *Developmental dynamics : an official publication of the American Association of Anatomists,* 209**,** 127-38.

SHAPPELL, S. B., THOMAS, G. V., ROBERTS, R. L., HERBERT, R., ITTMANN, M. M., RUBIN, M. A., HUMPHREY, P. A., SUNDBERG, J. P., ROZENGURT, N., BARRIOS, R., WARD, J. M. & CARDIFF, R. D. 2004. Prostate pathology of genetically engineered mice: definitions and classification. The consensus report from the Bar Harbor meeting of the Mouse Models of Human Cancer Consortium Prostate Pathology Committee. *Cancer Res,* 64**,** 2270-305.

SHIM, K., MINOWADA, G., COLING, D. E. & MARTIN, G. R. 2005. Sprouty2, a mouse deafness gene, regulates cell fate decisions in the auditory sensory epithelium by antagonizing FGF signaling. *Dev.Cell,* 8**,** 553-564.

SIVAK, J. M., PETERSEN, L. F. & AMAYA, E. 2005. FGF signal interpretation is directed by Sprouty and Spred proteins during mesoderm formation. *Dev Cell,* 8**,** 689-701.

SLACK, A., CHEN, Z., TONELLI, R., PULE, M., HUNT, L., PESSION, A. & SHOHET, J. M. 2005. The p53 regulatory gene MDM2 is a direct transcriptional target of MYCN in neuroblastoma. *Proceedings of the National Academy of Sciences of the United States of America,* 102**,** 731-6.

SONG, M. S., CARRACEDO, A., SALMENA, L., SONG, S. J., EGIA, A., MALUMBRES, M. & PANDOLFI, P. P. 2011. Nuclear PTEN regulates the APC-CDH1 tumor-suppressive complex in a phosphatase-independent manner. *Cell,* 144**,** 187-99.

STECK, P. A., PERSHOUSE, M. A., JASSER, S. A., YUNG, W. K., LIN, H., LIGON, A. H., LANGFORD, L. A., BAUMGARD, M. L., HATTIER, T., DAVIS, T., FRYE, C., HU, R., SWEDLUND, B., TENG, D. H. & TAVTIGIAN, S. V. 1997. Identification of a candidate tumour suppressor gene, MMAC1, at chromosome 10q23.3 that is mutated in multiple advanced cancers. *Nat Genet,* 15**,** 356-62.

STEINKAMP, M. P., O'MAHONY, O. A., BROGLEY, M., REHMAN, H., LAPENSEE, E. W., DHANASEKARAN, S., HOFER, M. D., KUEFER, R., CHINNAIYAN, A., RUBIN, M. A., PIENTA, K. J. & ROBINS, D. M. 2009. Treatment-dependent androgen receptor mutations in prostate cancer exploit multiple mechanisms to evade therapy. *Cancer Res,* 69**,** 4434-42.

SU, A. I., COOKE, M. P., CHING, K. A., HAKAK, Y., WALKER, J. R., WILTSHIRE, T., ORTH, A. P., VEGA, R. G., SAPINOSO, L. M., MOQRICH, A., PATAPOUTIAN, A., HAMPTON, G. M., SCHULTZ, P. G. & HOGENESCH, J. B. 2002. Large-scale analysis of the human and mouse transcriptomes. *Proc Natl Acad Sci U S A,* 99**,** 4465-70.

SUTTERLUTY, H., MAYER, C. E., SETINEK, U., ATTEMS, J., OVTCHAROV, S., MIKULA, M., MIKULITS, W., MICKSCHE, M. & BERGER, W. 2007. Down-regulation of Sprouty2 in non-small cell lung cancer contributes to tumor malignancy via extracellular signal-regulated kinase pathway-dependent and -independent mechanisms. *Mol Cancer Res,* 5**,** 509-20.

TAKAHASHI, T., YAMAGUCHI, S., CHIDA, K. & SHIBUYA, M. 2001. A single autophosphorylation site on KDR/Flk-1 is essential for VEGF-A-dependent activation of PLC-gamma and DNA synthesis in vascular endothelial cells. *EMBO J,* 20**,** 2768-78.

TAYLOR, B. S., SCHULTZ, N., HIERONYMUS, H., GOPALAN, A., XIAO, Y., CARVER, B. S., ARORA, V. K., KAUSHIK, P., CERAMI, E., REVA, B., ANTIPIN, Y., MITSIADES, N., LANDERS, T., DOLGALEV, I., MAJOR, J. E., WILSON, M., SOCCI, N. D., LASH, A. E., HEGUY, A., EASTHAM, J. A., SCHER, H. I., REUTER, V. E., SCARDINO, P. T., SANDER, C., SAWYERS, C. L. & GERALD, W. L. 2010. Integrative genomic profiling of human prostate cancer. *Cancer cell,* 18**,** 11-22.

TEFFT, J. D., LEE, M., SMITH, S., LEINWAND, M., ZHAO, J., BRINGAS, P., JR., CROWE, D. L. & WARBURTON, D. 1999. Conserved function of mSpry-2, a murine homolog of Drosophila sprouty, which negatively modulates respiratory organogenesis. *Curr Biol,* 9**,** 219-22.

THOMAS, G. V., HORVATH, S., SMITH, B. L., CROSBY, K., LEBEL, L. A., SCHRAGE, M., SAID, J., DE KERNION, J., REITER, R. E. & SAWYERS, C. L. 2004. Antibody-based profiling of the phosphoinositide 3-kinase pathway in clinical prostate cancer. *Clin Cancer Res,* 10**,** 8351-6.

THOMSEN, M. K., BUTLER, C. M., SHEN, M. M. & SWAIN, A. 2008. Sox9 is required for prostate development. *Dev Biol,* 316**,** 302-11.

TOMLINS, S. A., LAXMAN, B., DHANASEKARAN, S. M., HELGESON, B. E., CAO, X., MORRIS, D. S., MENON, A., JING, X., CAO, Q., HAN, B., YU, J., WANG, L., MONTIE, J. E., RUBIN,

M. A., PIENTA, K. J., ROULSTON, D., SHAH, R. B., VARAMBALLY, S., MEHRA, R. & CHINNAIYAN, A. M. 2007. Distinct classes of chromosomal rearrangements create oncogenic ETS gene fusions in prostate cancer. *Nature,* 448**,** 595-9.

TOMLINS, S. A., RHODES, D. R., PERNER, S., DHANASEKARAN, S. M., MEHRA, R., SUN, X. W., VARAMBALLY, S., CAO, X., TCHINDA, J., KUEFER, R., LEE, C., MONTIE, J. E., SHAH, R. B., PIENTA, K. J., RUBIN, M. A. & CHINNAIYAN, A. M. 2005. Recurrent fusion of TMPRSS2 and ETS transcription factor genes in prostate cancer. *Science,* 310**,** 644-8.

TRAISH, A. M. & MORGENTALER, A. 2009. Epidermal growth factor receptor expression escapes androgen regulation in prostate cancer: a potential molecular switch for tumour growth. *Br J Cancer,* 101**,** 1949-56.

TRINKLE-MULCAHY, L., BOULON, S., LAM, Y. W., URCIA, R., BOISVERT, F. M., VANDERMOERE, F., MORRICE, N. A., SWIFT, S., ROTHBAUER, U., LEONHARDT, H. & LAMOND, A. 2008. Identifying specific protein interaction partners using quantitative mass spectrometry and bead proteomes. *The Journal of cell biology,* 183**,** 223-39.

TROTMAN, L. C., NIKI, M., DOTAN, Z. A., KOUTCHER, J. A., DI CRISTOFANO, A., XIAO, A., KHOO, A. S., ROY-BURMAN, P., GREENBERG, N. M., VAN DYKE, T., CORDON-CARDO, C. & PANDOLFI, P. P. 2003a. Pten dose dictates cancer progression in the prostate. *PLoS biology,* 1**,** E59.

TROTMAN, L. C., NIKI, M., DOTAN, Z. A., KOUTCHER, J. A., DI CRISTOFANO, A., XIAO, A., KHOO, A. S., ROY-BURMAN, P., GREENBERG, N. M., VAN DYKE, T., CORDON-CARDO, C. & PANDOLFI, P. P. 2003b. Pten dose dictates cancer progression in the prostate. *PLoS Biol,* 1**,** E59.

TSAVACHIDOU, D., COLEMAN, M. L., ATHANASIADIS, G., LI, S., LICHT, J. D., OLSON, M. F. & WEBER, B. L. 2004. SPRY2 is an inhibitor of the ras/extracellular signal-regulated kinase pathway in melanocytes and melanoma cells with wild-type BRAF but not with the V599E mutant. *Cancer Res,* 64**,** 5556-9.

VISVADER, J. E. 2009. Keeping abreast of the mammary epithelial hierarchy and breast tumorigenesis. *Genes Dev,* 23**,** 2563-77.

VLAHOS, C. J., MATTER, W. F., HUI, K. Y. & BROWN, R. F. 1994. A specific inhibitor of phosphatidylinositol 3-kinase, 2-(4-morpholinyl)-8-phenyl-4H-1-benzopyran-4-one (LY294002). *J Biol Chem,* 269**,** 5241-8.

VOELLER, H. J., AUGUSTUS, M., MADIKE, V., BOVA, G. S., CARTER, K. C. & GELMANN, E. P. 1997. Coding region of NKX3.1, a prostate-specific homeobox gene on 8p21, is not mutated in human prostate cancers. *Cancer research,* 57**,** 4455-9.

VON KRIEGSHEIM, A., BAIOCCHI, D., BIRTWISTLE, M., SUMPTON, D., BIENVENUT, W., MORRICE, N., YAMADA, K., LAMOND, A., KALNA, G., ORTON, R., GILBERT, D. & KOLCH, W. 2009. Cell fate decisions are specified by the dynamic ERK interactome. *Nature cell biology,* 11**,** 1458-64.

WAKIOKA, T., SASAKI, A., KATO, R., SHOUDA, T., MATSUMOTO, A., MIYOSHI, K., TSUNEOKA, M., KOMIYA, S., BARON, R. & YOSHIMURA, A. 2001. Spred is a Sprouty-related suppressor of Ras signalling. *Nature,* 412**,** 647-51.

WANG, X., KRUITHOF-DE JULIO, M., ECONOMIDES, K. D., WALKER, D., YU, H., HALILI, M. V., HU, Y. P., PRICE, S. M., ABATE-SHEN, C. & SHEN, M. M. 2009. A luminal epithelial stem cell that is a cell of origin for prostate cancer. *Nature,* 461**,** 495-500.

WEBER, C., FRAEMOHS, L. & DEJANA, E. 2007. The role of junctional adhesion molecules in vascular inflammation. *Nature reviews. Immunology,* 7**,** 467-77.

WOODFIN, A., REICHEL, C. A., KHANDOGA, A., CORADA, M., VOISIN, M. B., SCHEIERMANN, C., HASKARD, D. O., DEJANA, E., KROMBACH, F. & NOURSHARGH, S. 2007. JAM-A mediates neutrophil transmigration in a stimulus-specific manner in vivo: evidence for sequential roles for JAM-A and PECAM-1 in neutrophil transmigration. *Blood,* 110**,** 1848-56.

ZERIAL, M. & MCBRIDE, H. 2001. Rab proteins as membrane organizers. *Nat Rev Mol Cell Biol,* 2**,** 107-17.

ZHAN, L., XIANG, B. & MUTHUSWAMY, S. K. 2006. Controlled activation of ErbB1/ErbB2 heterodimers promote invasion of three-dimensional organized epithelia in an ErbB1-dependent manner: implications for progression of ErbB2-overexpressing tumors. *Cancer Res,* 66**,** 5201-8.

ZHANG, H., HU, G., WANG, H., SCIAVOLINO, P., ILER, N., SHEN, M. M. & ABATE-SHEN, C. 1997. Heterodimerization of Msx and Dlx homeoproteins results in functional antagonism. *Molecular and cellular biology,* 17**,** 2920-32.

ZHANG, Y., ZHANG, J., LIN, Y., LAN, Y., LIN, C., XUAN, J. W., SHEN, M. M., MCKEEHAN, W. L., GREENBERG, N. M. & WANG, F. 2008. Role of epithelial cell fibroblast growth factor receptor substrate 2alpha in prostate development, regeneration and tumorigenesis. *Development,* 135**,** 775-84.

ZWANG, Y. & YARDEN, Y. 2006. p38 MAP kinase mediates stress-induced internalization of EGFR: implications for cancer chemotherapy. *EMBO J,* 25**,** 4195-206.